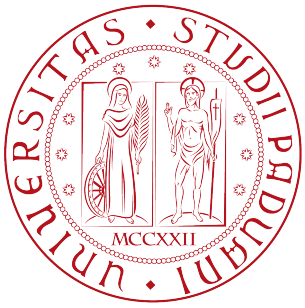


**Università degli Studi di Padova**

DIPARTIMENTO DI FISICA E ASTRONOMIA "GALILEO GALILEI"
Corso di Laurea Magistrale in Fisica Teorica
Curriculum Teorico-Modellistico

Tesi di Laurea Magistrale

# Cosmic Microwave Background (CMB) distortions: a new window into the physics of inflation

Candidato:
**Oreste Ziliani**
**Matricola 1079977**

Relatore:
**Nicola Bartolo**

Correlatori:
**Michele Liguori**
**Benjamin D. Wandelt**

**25 Ottobre 2016**


# *Cosmic Microwave Background (CMB) distortions: a new window into the physics of inflation*

Master Thesis in Physics
by
Oreste Ziliani

Advisors: Nicola Bartolo
Michele Liguori
Foreign advisor: Benjamin D. Wandelt
Referee: Sabino Matarrese

Department of Physics and Astronomy "G. Galilei"
University of Padova
October, 25th 2016

# *Cosmic Microwave Background (CMB) distortions: a new window into the physics of inflation*


## Abstract

The Cosmic Microwave Background (CMB) spectrum in the frequency domain is extremely close to a perfect black-body. However, we know there must be tiny distortions of the CMB spectrum which are within the sensitivity of proposed satellite missions, such as PRISM [1] and PIXIE [2]. These spectral distortions provide a potential powerful source of information about the origin of the primordial density perturbations in the early Universe, i.e. the inflationary paradigm.

In order to achieve a more solid comprehension, we will first introduce our theoretical framework, based on the Cosmological Standard Model, and the Theory of cosmological perturbations, which represents the traditional approach in Cosmology. In particular we will see how primordial density perturbations, of order $10^{-5}$, around a background solution produced the seeds for the Universe we see today.

Thereafter, we will consider various aspects related to CMB spectral distortions: what they consist in, their main properties and why they are so important. Recent works such as [3] proved that a cross correlation between the so-called $\mu$-type (i.e. chemical potential type) distortions and the CMB temperature anisotropy $\Delta T/T$ could constraint the level of primordial non-Gaussianity (NG) via the parameter $f_{NL}^{loc}$ at very small scales so far unexplored, lesser than about a Mpc, and potentially with a precision much higher than the present constraints from CMB anisotropies. The most up-to-date and guaranteed constraints on primordial NG comes from [4] and give $f_{NL}^{loc} = 2.5 \pm 5.7$; however, authors of [3] claimed that a cosmic variance limited experiment could in principle reach $\Delta f_{NL}^{loc} \sim \mathcal{O}(10^{-3})$, which is the typical level predicted by the standard single-field models of slow-roll inflation.

That is a quite bold claim and in this work we will focus on a computation at second-order in the cosmological perturbations to quantify some non-primordial signals that can act as a source of contamination to the measurement of the level of primordial non-Gaussianity. One could be lead to think that a calculation of such kind should in principle follow the same derivation as the bispectrum formula $TTT$, but this idea, although legitimate, is actually incorrect. In fact, we will see that asserting this second-order contamination is an highly non trivial task and we will discover a few crucial subtleties hidden in

the calculation which must be treated very carefully.

The procedure we will follow is surely going to shine a light on the very brief and incomplete derivations and implied assumptions in the research literature. In addition to it, we will develop an analytical formula, initially not intended, which provides the basis for a full numerical calculation once plugged into the Second Order Non Gaussianity (SONG) code [5].

The main goals of this Thesis are therefore to present some remarkable results on recent developments in Cosmology, becoming aware of what we know, and, where possible, to take a step toward what we do not know, clarifying some aspects about CMB spectral distortions that have not been yet explored.

# Contents

# Listing of figures

# Acknowledgments

I want to offer my sincere gratitude to my supervisors Nicola Bartolo and Michele Liguori for giving me the possibility of working with them in the extraordinary field of Cosmology; they have been excellent mentors always willing to help me and their advice has proven very valuable throughout my work.

An heartfelt 'thank you' to Benjamin D. Wandelt, who allowed me to live a once in a lifetime experience. He is truly an exquisite person who, despite the countless commitments and bureaucratic complications, managed to host me in the ILP and granted me some time for meaningful discussions.

I would like to thank also Sébastien Renaux-Petel, Cyril Pitrou and Guillaume Faye for being constant reference point so nice to me, for resolving many doubts of mine with enlightening remarks and for including me in seminars and lectures they organized in the institute; thanks for making my stay in Paris extremely pleasant, for our interesting lunch chat, regardless of the topic, and for the more touristic activities.

Finally, if this work has been pursued all the way to its end, the credit goes partly to Thalia. With her unceasing support, she taught me not to give up, to be bold and believe in myself.

# 1

# The Standard Model of Cosmology

The expansion of the Universe we live in was first discovered by astronomer and astrophysicist Edwin Hubble in 1929, but it was only in the last decades, starting from the 1960's, that Cosmology has increasingly grown becoming a physical science with falsifiable theories. First models were entirely baryonic and involved simple ad hoc initial conditions. In many ways the basic picture has remained the same since then: nearly scale invariant and adiabatic initial conditions, in an almost isotropic and homogeneous Friedmann-Robertson-Walker solution to Einstein's Field Equations. However, Cold Dark Matter was introduced in the 1980's, leading to the *Standard CDM* picture and by the end of the 1980s better fits to the available data were achieved thanks to the addition of a cosmological constant $\Lambda$, soon associated with the concept of Dark Energy. Thus, by the mid-to-late 1990's, the $\Lambda$*CDM model* was established, not without some initial debate among cosmologists, but even now we refer to that as the model that best fits all the present observations.

In the next sections, in order to have a better understanding of our working environment, we are going to present the basic $\Lambda$CDM model assumptions and a brief introduction to the General Theory of Relativity, the very supporting pillar on which all modern Cosmology is based. We will also deal with three great problems that are innate in the Standard Model and we will see that the theory of *Inflation* brilliantly solves all of them and, maybe more surprisingly, does it at the same time.

As starting point, we are now going to introduce some basic concepts (present in any textbook, e.g. [6]) in a qualitative way, but we are going to get back on them in §1.2 et seq with a deeper examination.

## 1.1 The homogeneous and isotropic Universe

Our Universe began in a hot dense state about 14 billions years ago and we have good evidence that it never stopped expanding since then. This depiction falls into the so called *Hot Big Bang model* and, as a matter of fact, the ΛCDM theory is the most updated parametrization of it.

At the heart of this model there is the *Cosmological Principle*, that is the assumption that the universe is homogeneous and isotropic on large scales (for a comoving observer). We are not going to discuss about the implications nor the history behind this basic principle in Cosmology, we just limit ourselves to say that it was originally a mere hypothesis formulated for the sake of simplicity and to reflect the Copernican desire not to occupy a preferred position in the Universe, but, later on, it found its validation in astronomical observations. Talking of observations, what we are going to do instead is introduce some fundamental quantities which will help us along the way.

The expansion process is conveniently described by a *scale factor* $a(t)$, a function of time; its present value is set to 1, as a normalization, and at earlier times $a$ was smaller than it is today. Let us since now highlight that the factor $a$ is crucial to have a proper definition of distance in an expanding Universe. We can imagine space as a grid which expands uniformly with time as in Fig. 1.1.1; the distance between the coordinates of two points is called *comoving distance* and remains constant, whereas the physical distance is proportional to the scale factor and in consequence does evolve with time.

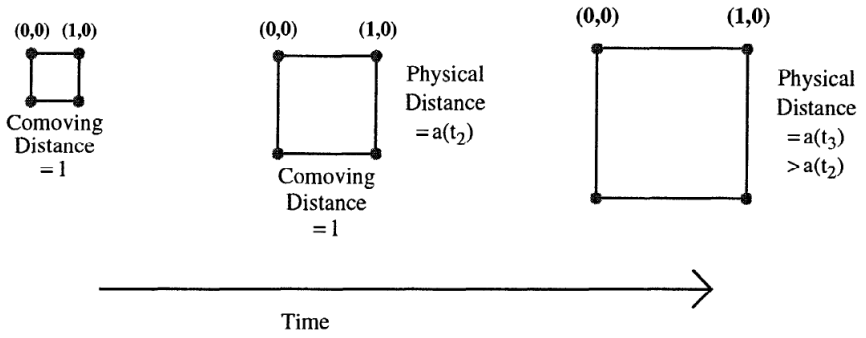


**Figure 1.1.1:** Hypothetical grid representing expansion of the Universe (Picture taken from [6]).

In general, coordinates which are fixed in the frame of the expanding Universe, i. e. that do not change with time, are said to be *comoving*. For instance, if $\lambda$ is a generic coordinate:

$$\lambda_{\text{physical}} = a(t)\lambda_{\text{comoving}}. \tag{1.1}$$

We have implied so far that the scale factor $a$ is a function of time, but we did not specified *what* time: it is the *cosmic time*, which represents the proper time of comoving observers. It is important to notice that the dependence of $a$ on $t$ varies as the Universe evolves, according to what form of energy density $\rho$ is most present in the Universe.

At early times, radiation (meaning all relativistic species) used to dominate while later, after the so-called *matter-radiation equality*, non-relativistic matter came into play. These two different kind of evo-

lution are then

$$a(t) \propto t^{\frac{1}{2}} \quad \text{radiation},$$
$$a(t) \propto t^{\frac{2}{3}} \quad \text{matter}.$$

However, it is now believed that matter-dominated epoch has ended and a new form of energy has come to dominate the cosmological landscape: Dark Energy. This peculiar kind of energy is causing the today's acceleration and the most plausible possibility is that this energy density remains constant with time, acting as a cosmological constant. This possibility was first introduced by Einstein but he started from the wrong hypothesis, as he believed in the Steady State Universe, and he ended up abandoning it defining this idea as the "biggest blunder" of his life.

We said that scale factor $a$ evolves with time, so to quantify its rate of change and its relation to the energy density it is useful to define the *Hubble rate*:

$$H(t) \equiv \frac{1}{a}\frac{\mathrm{d}a}{\mathrm{d}t}.$$

This quantity measures the rate of expansion of the Universe and therefore it allows us to define two reference parameters:

$$H(t)^{-1} \quad \text{Hubble time},$$
$$cH(t)^{-1} \quad \text{Hubble radius}.$$

The latter is also called *horizon* because it provides an estimate of the distance that light can travel while the Universe expands appreciably and reflects the property of causal connection in a time interval $H^{-1}$. That is to say, in a region much smaller than the Hubble distance, during a time interval much less than the Hubble time, i.e. in a region of space-time that is small on the Hubble scale, the expansion of the Universe does not violate the principle of causality in physical processes such as the propagation of waves and the establishment of thermal equilibrium. On larger scales, such processes are no longer causally connected.

The Hubble rate is determined by measuring (at least at the lowest redshifts) the velocity of distant galaxies and dividing by their distance from us, so it is often written in units of velocity per distance. Present measurements are parameterized by $h$:

$$H_0 = 100h \quad \text{km sec}^{-1}\text{Mpc}^{-1},$$

where, here and throughout, the subscript "0" denotes values of quantities *today*. Latest measurements [7] have set

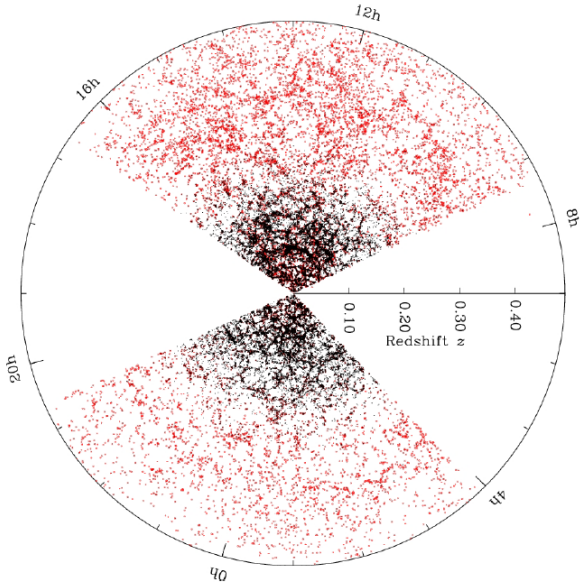


**Figure 1.1.2:** The distribution of galaxies is clumpy on small scales, but becomes more uniform on large scales and early times (Picture taken from [8]).

$$h = 0.6774 \pm 0.0046 \quad \text{at } 68\% \text{ CL.}$$

Notice that, since $H$ depends on time, measuring separately the Hubble rate today $H_0$ and the age of the universe today would represent a powerful test of this cosmological model.

We should now introduce another fundamental quantity in Cosmology: the *redshift* $z$. In the expanding Universe galaxies are moving away from each other, so we see them receding from us. We know from the physics of waves that the wavelength of light or sound emitted by a receding object is stretched out so that the observed wavelength is larger than the emitted one. In this sense, $z$ represents a stretching factor:

$$1 + z \equiv \frac{\lambda_{\text{obs}}}{\lambda_{\text{emit}}} = \frac{a(t_0)}{a(t_1)} = \frac{1}{a(t_1)},$$

where we used the normalization $a(t_0) = 1$; $\lambda$ is the wavelength, and "obs" and "emit" stand respectively for "observed" and "emitted". For low redshifts, the standard Doppler formula applies and we find $z \simeq v/c$.

Redshift $z$, rather than years or Megaparsecs (Mpc) [1], is often used in Cosmology to specify both times and distances as it is very conveniently assimilated in the context of an expanding Universe.

In Fig. 1.1.2 we can see how the cosmological principle is implemented in the practice. According to our definition, the higher the redshift the further we are looking into the Universe. The figure shows that on small scales, close to us, the Universe is everything but homogeneous and isotropic (just think at the Solar System, whose isotropy, for instance, is broken by the presence of orbiting planets); on large

[1] We remind that the *parsec* is the most used unit of length in the astronomical field and 1Mpc $\simeq 3.26 \times 10^6$light years $\simeq 3 \times 10^{22}$metres

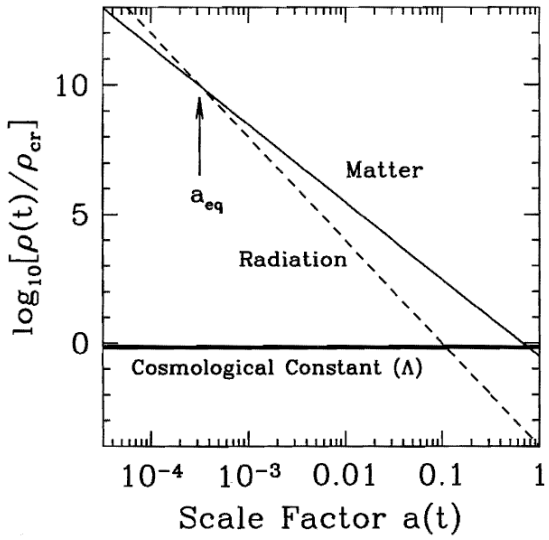


**Figure 1.1.3:** Energy density vs scale factor for different constituents of a flat Universe, in this case: non-relativistic matter, radiation and cosmological constant. All are in logarithmic scale and in units of the critical density today (Picture taken from [6]).

scales, say $\gtrsim$ 10Mpc the distribution of galaxies becomes more and more uniform and we can start to treat them as linear perturbations in the homogeneous and isotropic Universe.

One final remark in this introductory section is about the geometry of our smooth Universe. There are three possible cases and a key role to distinguish among them is played by a critical value of the energy density $\rho_{cr}$. Thus the Universe is said to be

$$\begin{cases} open & \text{if} \quad \rho < \rho_{cr} \\ flat & \text{if} \quad \rho = \rho_{cr} \\ closed & \text{if} \quad \rho > \rho_{cr}. \end{cases}$$

To better understand what this means just consider two freely traveling particles which start their journey moving parallel to each other. A flat Universe is Euclidean, so the particles remain parallel as long as they travel freely. In a closed Universe, gradually the initially parallel particles converge, as all lines of constant longitude meet at the North and South Pole. In the open case, instead, the initially parallel paths diverge, as would two marbles rolling off a saddle.

Our Universe is very close to a flat one and it can be shown that, according to the different epochs, the energy density scales as

$$\rho \propto \begin{cases} a^{-4} & \text{radiation} \\ a^{-3} & \text{matter} \\ a^{0} = const. & \text{dark energy.} \end{cases}$$

These trends are illustrated in Fig. 1.1.3, where $a_{eq}$ is the scale factor evaluated at the time of matter-radiation equivalence.

We will see more about this in the next section, in particular we will learn that the connection be-

tween geometry and energy (density) is made possible by Einstein's Equations in the General Theory of Relativity.

## 1.2 General Relativity

Up to now, we have just presented some phenomenological features of our Universe, namely, that it is homogeneous and isotropic on large scale (Cosmological Principle), that it is subject to an accelerated expansion (conveniently described by the scale factor $a$) and that it is filled with different form of energy density $\rho$ coming from as many different constituents (radiation, non-relativistic matter and, at late times, Dark Energy).

This is all elegantly formulated in the *General Theory of Relativity* (GR) and a proper comprehension of this work would be almost impossible without spending at least a few words on it. On the other hand, most of Cosmology can be learned with only a passing knowledge of GR, such as the concepts of a metric, geodesics and 4-dimensional formalism and indeed we are not going to need anything more than this.

The mathematics employed in the formal construction of the Theory can be quite challenging but the physical idea behind it is as simple as outstanding and it is enclosed in the

> **Equivalence Principle (EP)**, which states the equivalence between gravitational and inertial mass.

This implies that acceleration is independent of the nature of the body, or, in other words, no external static homogeneous gravitational field could be detected in a freely falling elevator since the observers, their test bodies and the elevator itself would respond to the field with the same acceleration. Notice that "freely falling" means that no external forces are acting on the elevator but the gravity itself, thus, the trajectory traced by it is a geodesic, which represents the shortest path between two point in space.

The Principle can be easily applied in a system of N particles subject to some external force that give the system an acceleration $\mathbf{a}$: one just need to write down the equations of motion and perform a non-Galilean space-time coordination transformation

$$\begin{cases} \mathbf{x}' = \mathbf{x} - \frac{1}{2}\mathbf{g}t^2 \\ t' = t. \end{cases} \tag{1.2}$$

to immediately realize that things go along exactly as if the system were within a gravitational field of strength $\mathbf{g} = -\mathbf{a}$ without any external forces.

From what we said, it seems that the Principle holds only in the case of static and homogeneous gravitational field: had $\mathbf{g}$ depended on $\mathbf{x}$ or $t$, we would not have been able to produce an exact cancellation between inertial and gravitational forces with the coordinate transformation 1.2. However, if we restrict our attention to such a small region of space and time that the field changes very little over the region, we can still expect an approximate cancellation and this lead us to state the Equivalence Principle in its final form:

at every space-time point $P$, labeled by a set of coordinates $x^{\mu}_{P}$ in an arbitrary gravitational field, it is possible to choose a *locally inertial coordinate system* $\xi^{a}$ such that, within a sufficient small region of $P$, the laws of nature take the same form as the ones predicted by the Special Relativity (SR) in the absence of gravitation.

The change of coordinates

$$x^{\mu}_{P} \longmapsto \xi^{a}(x)$$

is also called *diffeomorphism* and represents a notion of paramount importance in GR. Just like every other fundamental theory in physics is built on an *invariance principle* which descends directly from simple and basic phenomenological data, one of the main assumptions in GR is that, in the presence of a gravitational field, every physical law has to be invariant under diffeomorphism.

The invoked principle in this case is the one of *General Covariance* and it can be proved to be precisely equivalent to the Equivalence Principle.

It has now come the time to deal with the mathematical aspect of GR we mentioned earlier. We are going to disclose some extremely powerful mathematical tools which will help us to implement the General Covariance Principle in practice.

We have already hinted at the fact that the notion of "distance" in Cosmology is far from trivial by pointing to the expansion of the Universe, but there is actually more than that. As it is nowadays well known, matter in Universe is able to curve the space-time that, consequently, in this view, becomes a specific geometrical structure: a four-dimensional *Differentiable Manifold*. A proper presentation of this subject should be carried out in the context of Differential Geometry, but we are not going to do this at all since we will just need an intuitive idea for our purpose. Specifically, just bear in mind the standard visual analogy in Fig. 1.2.1: matter curves space-time in the same way as a rubber sheet is stretched by something heavy placed on it, for instance a ball.

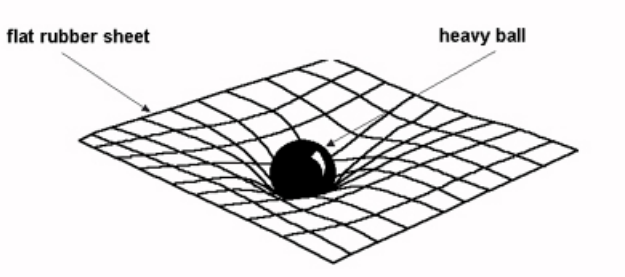


**Figure 1.2.1:** A very simplified view of the differentiable manifold that represents our space-time is offered by the analogy with a rubber sheet stretched by a ball placed on it; the heavier the object, the deeper the resulting gravitational well. The interplay between matter and geometry runs quite deep: matter tells space how to curve and, then, curved space tells matter how to move.

Instead, what is of greatest interest for us are other particular mathematical objects called *tensors*; their importance lies in the fact that they fulfill the General Covariance Principle in a manner that is said to be "covariant by sight" in the four-dimensional formalism framework.

One of the most fundamental tensors is without any doubt the *metric*. We already saw that, in the case of a smooth expanding Universe, the scale factor connects the coordinate distance with physical distance, but, more generally, this task is assigned precisely to the metric which is then an essential tool in order to make quantitative predictions in an expanding Universe.

The metric depends on the space-time point $P$ we are considering and it can be easily derived by defining the interval between $P$ and an infinitesimally nearby point $Q$. They are both events and are labeled by a set of coordinates $x^\mu$, so

$$P \equiv x^\mu \qquad ; \qquad Q \equiv x^\mu + \mathrm{d}x^\mu.$$

According to the EP, there exist a locally inertial frame $\xi^\mu(x)$ in $P$ so that

$$\begin{cases} x^\mu \longmapsto \xi^\mu(x) \\ x^\mu + \mathrm{d}x^\mu \longmapsto \xi^\mu(x + \mathrm{d}x) = \xi^\mu(x) + \partial_\alpha \xi^\mu \mathrm{d}x^\alpha \end{cases}$$

$$\Downarrow$$

$$\mathrm{d}\xi^\mu \equiv \xi^\mu(x + \mathrm{d}x) - \xi^\mu(x) = \mathrm{d}x^\alpha \partial_\alpha \xi^\mu,$$

where we made use of the notation $\partial_\mu \equiv \partial/\partial x^\mu$.

In the $\xi^\mu(x)$ coordinate system we can use results coming from Special Relativity. In particular, the distance between $P$ and $Q$ is defined by the line element

$$\mathrm{d}s^2 = \mathrm{d}\xi^\alpha \mathrm{d}\xi^\beta \eta_{\alpha\beta},$$

with $\eta_{\alpha\beta} = \mathrm{diag}(-1, 1, 1, 1)$ the Minkoskian metric.

Going back in the coordinates $x^\mu$ we finally obtain

$$\mathrm{d}s^2 = \mathrm{d}x^\mu \partial_\mu \xi^\alpha \mathrm{d}x^\nu \partial_\nu \xi^\beta \eta_{\alpha\beta} = \mathrm{d}x^\mu \mathrm{d}x^\nu g_{\mu\nu}(x),$$

where $g_{\mu\nu}(x) \equiv \partial_\mu \xi^\alpha \partial_\nu \xi^\beta \eta_{\alpha\beta}$ is the metric in $x$. Notice that $g_{\mu\nu}$ is symmetric in the two indexes, it admits an inverse $g^{\mu\nu}$ such that $g^{\mu\alpha} g_{\alpha\nu} = \delta^\mu_\nu$ and it is independent from the chosen locally inertial frame.

If we perform a diffeomorphism $x^\mu \longmapsto x'^\mu(x)$:

$g_{\mu\nu}$ transforms exactly as a second rank covariant tensor

$$g'_{\mu\nu}(x') = \frac{\partial x^\alpha}{\partial x'^\mu} \frac{\partial x^\beta}{\partial x'^\nu} g_{\alpha\beta}(x),$$

$\mathrm{d}s^2$ is invariant by construction

$$\mathrm{d}s^2 = \mathrm{d}x^\mu \mathrm{d}x^\nu g_{\mu\nu}(x) = \mathrm{d}x'^\mu \mathrm{d}x'^\nu g'_{\mu\nu}(x').$$

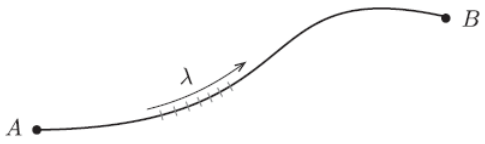


**Figure 1.2.2:** Parameterization of an arbitrary path in spacetime $x^\mu(\lambda)$ (Picture taken from [8]).

It can be seen that on certain manifolds a metric would be unnecessary or inconvenient for whichever problem is being considered. But in our case the metric is absolutely fundamental, since it will carry the information about the rates at which clocks run and the distances between points, just as it does in SR. A differentiable manifold on which a symmetric covariant tensor field $g_{\mu\nu}$ has been singled out to act as the metric at each point is called a Riemannian manifold. [2] It is important to understand that in picking out a metric we add structure to the manifold; we shall see that the metric completely defines the curvature of the manifold. Thus, by our choosing one metric $g_{\mu\nu}$ the manifold gets a certain curvature (perhaps that of a sphere), while a different $\tilde{g}_{\mu\nu}$ would give it a different curvature (perhaps an ellipsoid of revolution). The differentiable manifold itself is "primitive": an amorphous collection of points, arranged locally like the points of Euclidean space, but not having any distance relation or shape specified; giving the metric $g_{\mu\nu}$ gives it a specific shape.

This specific shape is precisely what cause particles to follow complicated paths in general spacetimes. The notion of straight line gets generalized to a *geodesic*, the path followed by a particle in the absence of any forces, i. e. when only gravity acts. If we consider the world line of a particle parametrized by $\lambda$ $x^\mu(\lambda)$ (Fig. 1.2.2), it can be shown that the geodesic equation takes the form

$$\frac{\mathrm{d}u^\alpha}{\mathrm{d}\lambda} + u^\mu u^\nu \Gamma^\alpha_{\mu\nu}(x) = 0,$$

where $u^\alpha \equiv \frac{\mathrm{d}x^\alpha}{\mathrm{d}\lambda}$ is the 4-velocity while $\Gamma^\alpha_{\mu\nu}(x) = \partial_\mu \partial_\nu \xi^\rho \frac{\partial x^\alpha}{\partial \xi^\rho}$ is a very peculiar object called *Affine Connection*, but also known as *Christoffel Symbols*. Like the metric, it is symmetric in the two subscripts and depends on the point $x$, but, surprisingly, despite its appearance, it is not a tensor. This is to be read in the sense that, under a change of coordinates $x^\mu \longmapsto x'^\mu(x)$, $\Gamma^\alpha_{\mu\nu}(x)$ does not transform following the general formula

$$(T')^{\alpha_1\alpha_2\ldots\alpha_n}_{\beta_1\beta_2\ldots\beta_m}(x') = \frac{\partial x'^{\alpha_1}}{\partial x^{\mu_1}} \frac{\partial x'^{\alpha_2}}{\partial x^{\mu_2}} \cdots \frac{\partial x'^{\alpha_n}}{\partial x^{\mu_n}} \frac{\partial x^{\nu_1}}{\partial x'^{\beta_1}} \frac{\partial x^{\nu_2}}{\partial x'^{\beta_2}} \cdots \frac{\partial x^{\nu_m}}{\partial x'^{\beta_m}} (T)^{\mu_1\mu_2\ldots\mu_n}_{\nu_1\nu_2\ldots\nu_m}(x). \tag{1.3}$$

Notice that this transformation formula implies that a tensor is null in a certain coordinate system if and only if it is null in every coordinate system (pointwise).

However, the affine connection proves itself to be an extremely convenient quantity in Differential Geometry and, therefore, in GR.

First of all, one can see that it is intimately related to the metric $g_{\mu\nu}$ and its derivatives:

[2] Strictly speaking, only if the metric is positive-definite - that is, $V^\mu V^\nu g_{\mu\nu} = V^\mu V_\mu > 0$ for all vectors $V^\mu \neq 0$ - is it called Riemannian; indefinite metrics, like SR and GR, are called pseudo-Riemannian.

$$\Gamma^{\mu}_{a\beta}(x) = \frac{1}{2} g^{\mu\nu}(x) \left( \partial_{\beta} g_{a\nu}(x) + \partial_{a} g_{\beta\nu}(x) - \partial_{\nu} g_{a\beta}(x) \right) .$$

Secondly, it exactly compensates for the fact that not even the standard derivative of a vector $\partial_{\mu} V^{\nu}$ is a tensor since from $\Gamma^{\mu}_{a\beta}$ we can define the *covariant derivative operator* $D_{\mu}$; this is the only intrinsic, coordinate-independent derivative operator on a general manifold, and its action on scalars, contravariant vectors and covariant vectors is given by:

$$\begin{aligned} D_{\mu}\varphi &\equiv \partial_{\mu}\varphi && \text{for a scalar field,} \\ D_{\mu}V^{\nu} &\equiv \partial_{\mu}V^{\nu} + \Gamma^{\nu}_{a\mu}V^{a} && \text{for a contravariant vector,} \\ D_{\mu}V_{\nu} &\equiv \partial_{\mu}V_{\nu} - \Gamma^{a}_{\mu\nu}V_{a} && \text{for a covariant vector.} \end{aligned}$$

For general tensors the covariant derivative is the same, with one positive $\Gamma$ - term for each upper index and one negative $\Gamma$ - term for each lower one.

We can now specify that the General Covariance Principle not only contains the concept of invariance under diffeomorphism, but also the idea that physics laws, in presence of a gravitational field $g_{\mu\nu}(x)$, reduce themselves to the corresponding laws of Special Relativity if one puts

a) $g_{\mu\nu} = \eta_{\mu\nu}$,

b) $\Gamma^{\mu}_{a\beta} = 0 \quad \longleftrightarrow \quad \partial_{\rho} g_{a\beta} = 0$.

These two conditions define what we already called the locally inertial coordinate system and it can be proved that such coordinate system exists for every point $P$ of the manifold.

We shall now introduce the most standard way to express curvature of Riemannian manifolds, i.e. the *Riemann curvature tensor*. Very intuitively, it is a tensor field that measures the extent to which the metric is not locally isometric to a Euclidean space. Its components are expressed in terms of the Christoffel symbols:

$$R^{\mu}_{\nu a\beta} = \partial_{\beta}\Gamma^{\mu}_{\nu a} - \partial_{a}\Gamma^{\mu}_{\nu\beta} + \Gamma^{\gamma}_{\nu a}\Gamma^{\mu}_{\beta\gamma} - \Gamma^{\gamma}_{\nu\beta}\Gamma^{\mu}_{a\gamma}.$$

It is important to notice that

$$\Gamma \sim g \cdot \partial g \quad \Longrightarrow \quad R \sim \partial\Gamma + \Gamma\Gamma \sim \partial\partial g + (\partial g)^{2}.$$

The presence of second derivatives of the metric in the Riemann curvature tensor is crucial. We saw that for every space-time point it always possible to move ourselves into a locally inertial coordinate system where the metric is constant and its first derivatives cancel. Unfortunately, this process stops here: we cannot cancel second derivatives of the metric just by changing coordinate system as they represent a much more intrinsic property of the manifold. Therefore, metric and Christoffel symbols are deceptive in order to measure the degree of curvature of the manifold they are defined on and we shall trust only the Riemann tensor, in the sense that

a manifold endowed with a metric tensor $g_{\mu\nu}(x)$ is flat

$$\Updownarrow$$

$$R^{\mu}_{\nu\alpha\beta}(x) = 0 \quad \forall x.$$

Moreover, there are two more standard geometrical objects descending from the precedents:

*Ricci tensor* $R_{\mu\nu} = R^{\alpha}_{\mu\alpha\nu} = R_{\nu\mu}$,

*Curvature Scalar* $R = g^{\mu\nu}R_{\mu\nu}$.

Eventually, we can give the prescription to implement the General Covariance Principle in the General Relativity context; it is also known as *Minimal Coupling* and it is founded on four fundamental substitutions:

1. $\eta_{\mu\nu} \quad \longrightarrow \quad g_{\mu\nu}$,
2. $\partial_{\mu} \quad \longrightarrow \quad D_{\mu}$,
3. $\int \mathrm{d}^4x \quad \longrightarrow \quad \int \sqrt{g}\mathrm{d}^4x$,
4. $\delta^4(x-y) \quad \longrightarrow \quad \frac{\delta^4(x-y)}{\sqrt{g}}$,

where $g \equiv -\det g_{\mu\nu} > 0$.

### Robertson-Walker (RW) metric

We just stressed the fundamental role played by a metric tensor on a differentiable manifold, of dimension four in our case. Thus, let us specify what this metric looks like in the Universe we live in; it is usually expressed in terms of the line element we defined in the previous paragraph, as it is an invariant quantity in GR.

The metric has to reflect all the most important properties of the Universe, i.e. that it is expanding and appears homogeneous and isotropic on large scales. Having this clear in mind, one can find

$$\mathrm{d}s^2 \equiv g_{\mu\nu}(x)\mathrm{d}x^{\mu}\mathrm{d}x^{\nu} = -\mathrm{d}t^2 + a(t)^2\left[\frac{\mathrm{d}r^2}{1-kr^2} + r^2\mathrm{d}\Omega^2\right], \tag{1.4}$$

where

- $\mathrm{d}\Omega^2 = \sin^2\theta\mathrm{d}\varphi^2 + \mathrm{d}\theta^2$ is the solid angle element;
- $t$ is the proper time of an observer comoving with the Universe expansion;
- $(r, \theta, \varphi)$ are spherical comoving coordinates;
- $a(t)$ is the scale factor;

- $k$ parametrizes the spatial curvature of the Universe so that

$$\begin{cases} k = -1 & \text{for an open universe} \\ k = 0 & \text{for a flat universe} \\ k = +1 & \text{for a closed universe.} \end{cases}$$

Notice that, being $(r, \theta, \varphi)$ a set of comoving coordinates, they can be dimensionless and so the parameter $k$; this means that the dimension is carried by the scale factor $a(t)$ which in particular has units of a length. To better understand this, just think back at relation 1.1.

A very interesting property of the Robertson-Walker metric is that, if we perform the particular change of coordinates

$$t \longrightarrow \eta \quad ; \quad d\eta = \frac{dt}{a} \quad \text{(conformal time)},$$

$$r^2 = S_k(\chi^2) = \begin{cases} \sin^2\chi & \text{if} \quad k = +1 \\ \chi^2 & \text{if} \quad k = 0 \\ \sinh^2\chi & \text{if} \quad k = -1, \end{cases}$$

we get

$$ds^2 = a(\eta)^2 \left[ -d\eta^2 + d\chi^2 + S_k(\chi^2) d\Omega^2 \right],$$

which is the so-called *conformal metric*. If we forget about the angular part for a moment, the metric we obtained is proportional to the Minkowskian one by a factor $a(\eta)$. As a matter of fact, it is therefore evident that the causal structure of the RW metric in the coordinates $\eta$ and $\chi$ will appear as in Minkowski space.

### Einstein Equations

We are starting to give structure to the Universe. As we anticipated, Einsteins Equations provide an extremely deep connection between geometry, in particular spatial curvature, and energy (density) $\rho$ of the species that populate the Universe. These constituents, both relativistic and non relativistic, are conveniently described by an *Energy-Momentum Tensor* $T^{\mu\nu}$.

The equations can then be derived through a variational principle starting from the total action $I[\varphi, g]$

$$I[\varphi, g] = I_M[\varphi, g] + I_{E.H.}[g],$$

which is a sum of the action for the matter component $I_M$ and the action accounting for the geometry of the spacetime $I_{E.H.}$, called *Einstein-Hilbert action*. In square brackets we indicated that these actions are functionals that may depend on the metric $g$, a generic scalar, vectorial or tensorial physical field $\varphi$ (and possibly its first and second derivatives), or both. It can be seen that, introducing the concept of functional derivative, the object defined by

$$T^{\mu\nu}(x) \equiv -\frac{2}{\sqrt{g(x)}}\frac{\delta I_M}{\delta g_{\mu\nu}(x)}$$

can be regarded as the Energy-Momentum tensor of our system; in fact, $T^{\mu\nu}(x) = T^{\nu\mu}(x)$ and $D_\mu T^{\mu\nu}(x) = 0$. Then, enforcing the variational principle $\delta I = 0$ and using the explicit expression for the Einstein-Hilbert action

$$I_{E.H.}[g] = \frac{1}{16\pi G}\int \mathrm{d}^4x\sqrt{g}R,$$

with $G$ being the gravitational constant, we finally obtain the Einstein Equations

$$G_{\mu\nu} \equiv R_{\mu\nu} - \frac{1}{2}g_{\mu\nu}R = 8\pi G T_{\mu\nu}. \tag{1.5}$$

$G_{\mu\nu}$ is called *Einstein Tensor* and is symmetrical in the two indices by construction.

As we know, (1.5) stresses the very deep connection between geometry and physics that we mentioned earlier: the left-hand side of the Einstein Equations contains the geometry of our Universe whereas the right-hand side describes the physical properties of its constituent.

In the model involving a cosmological constant $\Lambda \neq 0$, the Einstein-Hilbert action must be corrected as

$$I_{E.H.}[g] = \frac{1}{16\pi G}\int \mathrm{d}^4x\sqrt{g}(R + 2\Lambda),$$

so that (1.5) becomes

$$\begin{gathered} R_{\mu\nu} - \frac{1}{2}g_{\mu\nu}R - \Lambda g_{\mu\nu} = 8\pi G T_{\mu\nu} \\ \Updownarrow \\ R_{\mu\nu} - \frac{1}{2}g_{\mu\nu}R = 8\pi G\left(T_{\mu\nu} + \frac{\Lambda}{8\pi G}g_{\mu\nu}\right) \equiv 8\pi G\tilde{T}_{\mu\nu}. \end{gathered} \tag{1.6}$$

Notice that the addition of this term does not invalidate the initial assumptions we started from to derive the Einstein Equations, since it is a term proportional to the metric.

The two ways of writing the Einstein Equation reflect the two corresponding way of interpreting $\Lambda$: we can leave it left of the equal sign and look at it as a fundamental constant of nature, or we can take it to the right of the equal sign and consider it as a source. Anyway, the value of $\Lambda$ represents one of the biggest discrepancy in modern physics; if $\Lambda$ comes from quantum effects, the theoretical value is $\Lambda_{\text{theo}} = L_p^{-2} \simeq 10^{66}\text{cm}^{-2}$ where $L_p = \sqrt{\hbar G/c^3} = 10^{-33}\text{cm}$ is the Planck length against the observed experimental value $\Lambda_{\text{obs}} \simeq 10^{-56}\text{cm}^{-2}$. This leads to the following strong discrepancy

$$\frac{\Lambda_{\text{theo}}}{\Lambda_{\text{obs}}} \sim 10^{120}.$$

As regards the sign of the cosmological constant, it can be shown that $\Lambda > 0$ implies a negative pres-

sure $P < 0$. Notice that this makes completely sense as an energy density mimicking a repulsive effect which at the same time prevents the Universe gravitational collapse and allows the cosmic accelerated expansion.

### Filling the Universe

In the previous paragraph we introduced the Energy-Momentum tensor $T^{\mu\nu}$ as a quantity able to carry most of the information about the physical properties of the matter in the Universe, both relativistic and non relativistic.

For instance, if we consider the Energy-Momentum tensor of a *relativistic perfect fluid*, then the conditions that, in the coordinate system comoving with the fluid, make it 'perfect' are

- no heat ($\equiv$ energy) conduction;
- no shear stresses, i.e. complete absence of viscosity.

Thus, for a general metric $g_{\mu\nu}$, the explicit expression is

$$T^{\mu\nu} = (p + \rho)u^{\mu}u^{\nu} - pg^{\mu\nu}, \tag{1.7}$$

where $u^{\mu} = (1, \vec{v})/\sqrt{1 - v^2} \overset{\vec{v}=0}{=} (1, 0, 0, 0)$ is the 4-velocity of a particle in the fluid while $\rho$ and $p$ are respectively the proper energy density and the isotropic pressure and are both relativistic scalars. These two quantities are tied by the *equation of state*

$$\frac{p_i}{\rho_i} = w_i,$$

where the subscript $i$ stands for a particular species in the Universe.

If we impose $D_{\mu}T^{\mu\nu} = 0$ we get the energy conservation equation from the temporal component and the Navier-Stokes equation from the spatial one.

When considering a $T^{\mu\nu}$ written as in (1.7) in the cosmological field, there may be some ambiguity about the significance of $u^{\mu}$, so we specify that it refers to the velocity of a 'model' galaxy that is in a free fall motion as the only force acting on it is the gravitational field. Galaxies and particles form the so-called *ordinary matter* for which the Energy-Momentum tensor takes the particular form

$$T^{\mu\nu} = \sum_{r=1}^{N} m_r \int u_r^{\mu} u_r^{\nu} \frac{\delta^{(4)}(x - y_r(s_r))}{\sqrt{g}} \mathrm{d}s_r,$$

where $N$ is the total number of particles (or galaxies) and $s_r$ parametrizes the world line of particle $r$. For ordinary matter it can also be proven that

$$0 \leqslant p \leqslant \frac{1}{3}\rho$$

and the upper and lower limit are given by

ultra-relativistic particles: $v_r \approx 1 \longrightarrow p = \frac{1}{3}\rho$,

non relativistic particles: $v_r \ll 1 \longrightarrow p \ll \rho$.

Notice that $\rho$ is an energy density so it is necessarily positive defined; this means that if in some cases a negative pressure is needed, it is clear that we are no longer considering ordinary matter. This is exactly the case of the cosmological constant $\Lambda$: in the previous paragraph we showed that we can look at $\Lambda$ as a source for the gravitational field when placed at the right-hand side of Einstein equation. As a matter of fact, all we were saying was that we could define a particular Energy-Momentum tensor

$$T^{\mu\nu}_{\Lambda} = (p_\Lambda + \rho_\Lambda)u^\mu u^\nu - p_\Lambda g^{\mu\nu},$$

so that in (1.6) $\tilde{T}^{\mu\nu} = T^{\mu\nu} + T^{\mu\nu}_{\Lambda}$. Now, since

$$T^{\mu\nu}_{\Lambda} = \frac{\Lambda}{8\pi G}$$

and recalling that $\Lambda > 0$, we can make the identification

$$\begin{cases} p_\Lambda = -\frac{\Lambda}{8\pi G} < 0 \\ \rho_\Lambda = -p_\Lambda = \frac{\Lambda}{8\pi G} > 0. \end{cases}$$

Therefore, the Dark Energy sourced by the cosmological constant has an equation of state is characterized by $w_\Lambda = -1$.

### Friedmann equations

We have already said that Einstein Equations represent an extremely powerful tool in Cosmology and now we want to provide one of the most important examples. In 1922, physicist and mathematician Alexander A. Friedmann derived a set of equations governing the expansion of space in homogeneous and isotropic models of the Universe. He started from (1.5) plugging the Robertson-Walker metric (1.4) and the Energy-Momentum tensor of a perfect fluid (1.7).

The complete procedure that leads to the equations can be found in any textbook, such as [9], so we present here just the final result, usually known as *Friedmann Equations*:

$$\begin{cases} H^2 = \left(\frac{\dot{a}}{a}\right)^2 = \frac{8\pi G}{3}\rho - \frac{k}{a^2} \\ \frac{\ddot{a}}{a} = -\frac{4\pi G}{3}\left(\rho + 3p\right). \end{cases} \tag{1.8}$$

The overdot indicates the (cosmic) time derivative and we remind that we are in natural units where $c = 1$.

Notice (1.8) is a set of 2 equations but the starting point, the Einstein equations, is a set of 10 equations (remember $g_{\mu\nu}$ is symmetric); this simplification is made possible precisely by the properties of homogeneity and isotropy of the Universe.

Now, a careful eye may have spotted that Friedmann equations are 2, but there are 3 variables to be determined, namely $p$, $\rho$ and $a$. Actually, we have already introduced the additional condition given by the equation of state $p = w\rho$ and then, thanks to it, the system can be solved.

It is customary to introduce also a third Friedmann equation, better known as *Continuity Equation*:

$$\dot{\rho} + 3H(\rho + p) = 0.$$

It can be obtained from the first two equations with some basic algebraic manipulations and the profound reason is that it comes directly from the *Bianchi Identity* $D_\mu G^{\mu\nu} = 0 = D_\mu T^{\mu\nu}$.

One last remarkable feature of the equations concerns the issue of cosmic acceleration. We know that our Universe is experiencing an accelerated expansion, that is $\ddot{a} > 0$; in order to achieve it, since $a$ and $\rho$ are positive defined, the only possibility is that $p < 0$. As we already mentioned a possibility is provided by the cosmological constant, which, in (1.8), would give

$$\begin{cases} \rho = \rho_m + \rho_\Lambda = \rho_m + \frac{\Lambda}{8\pi G} \\ p = p_m + p_\Lambda = p_m - \frac{\Lambda}{8\pi G}, \end{cases}$$

where the subscript $m$ stands for 'ordinary matter'. If in the future $\rho_m$ and $p_m$ will become always more negligible, we will be left with

$$\rho_m, p_m \xrightarrow{t\to\infty} 0 \quad \Longrightarrow \quad \begin{cases} \frac{\Lambda}{3} - \frac{k}{a^2} = \frac{\dot{a}^2}{a^2} \\ \frac{\ddot{a}}{a} = \frac{\Lambda}{3}. \end{cases}$$

In this hypothetical limit, the evolution of the scale factor with time would be $a(t) \propto e^{Ht}$, with $H = \sqrt{\frac{\Lambda}{3}} = \text{const.}$

In general, models of universes where the scale factor $a(t)$ grows exponentially and that are characterized by an equation of state with $w = -1$ are called *de-Sitter Universes*.

## 1.3 The Cosmic Microwave Background

So far, we have been given a particular structure to the Universe, focusing on its geometrical properties, but it has now come the time to introduce what, for us and for the purposes of this work, is of most interest: the *Cosmic Microwave Background Radiation (CMBR)*.

Be aware that the cosmic inventory is extremely wide and varied as it includes, for instance, photons, baryons, cold dark matter, neutrinos and dark energy. However, we will skip an appropriate description of them with the exception of the photons, which compose the CMBR.

A curious note before going into details is that this radiation was found by chance by American scientists Penzias and Wilson in 1965. They were conducting some experiments about radio astronomy and satellite communications when they noticed that their antennas had an excess in temperature of $\sim 4$K which they could not account for. After some initial discussions with other scientists, they eventually realized that the antenna temperature was indeed due to the microwave background. This accidental

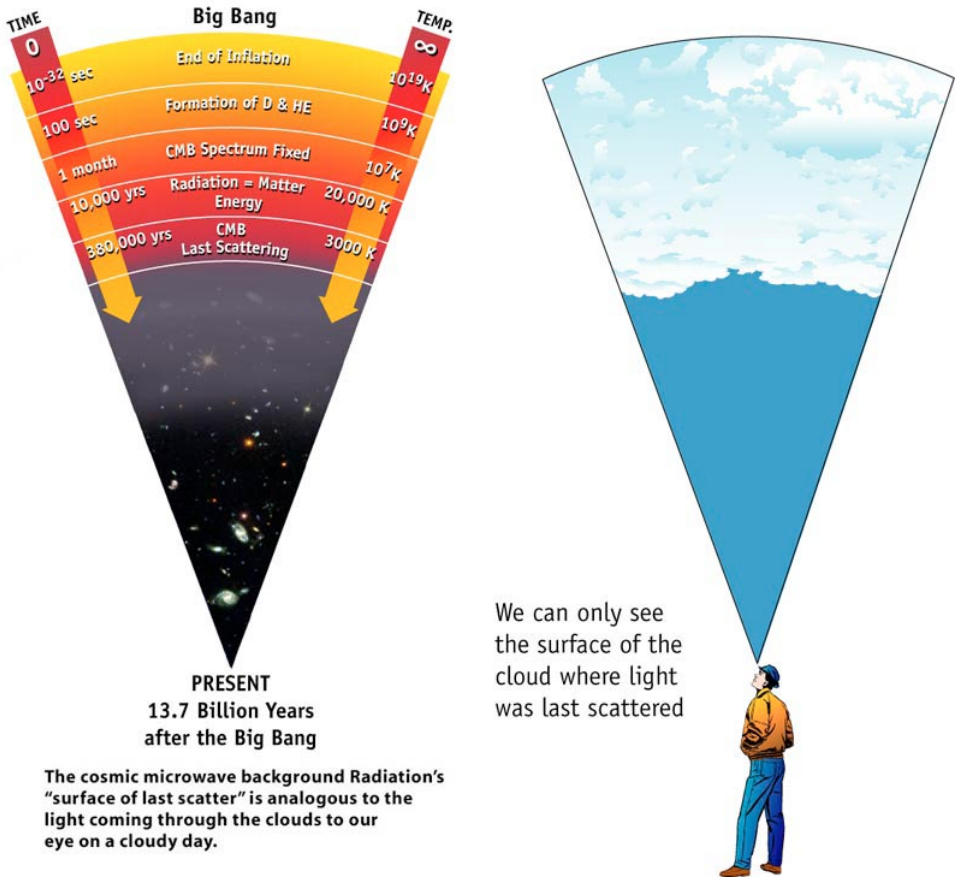


**Figure 1.3.1:** On a cloudy day, we can look out through the air and water vapor to the water droplets in the clouds which obscure our view beyond them (Picture taken from the WMAP official website).

discovery, which was later rewarded with a Nobel prize to both the American scientists, definitely increased the scientists interest in this field as the origins and evolution of the Universe became a physical science with scientific data to collect and analyze.

Right after the Big Bang, a photon-baryon plasma pervaded the Universe and all present particles interacted with each other, for example protons and electrons interacted via the Coulomb force while electrons, in turn, interacted with photons via Compton scattering. When the Universe was about 380000 years old, at redshift $z_* \sim 1000$, the space expansion rate became larger than the interaction rate, so electrons and protons started combining to form neutral Hydrogen during an epoch called *recombination*. Hydrogen is almost completely transparent to the cosmic background radiation, thus photons decoupled from ordinary matter in the sense that could propagate freely through the Universe.

The appearance of the sky on cloudy days is a good analogy to the appearance of the Cosmic Microwave Background Radiation. Water droplets scatter optical light, much like the free electrons scatter the photons of CMB; nevertheless, water vapor is nearly transparent to optical light, just as neutral Hydrogen is nearly transparent to photons.

This cosmic background "cloud surface" is called the *Last Scattering Surface (LSS)* - Fig. (1.3.1). Pho-

tons coming from the LSS literally come from the earliest moment of time, if there were any features imprinted in this surface of last scatter (i.e. regions that were brighter or dimmer than average) they will remain imprinted to this day because emitted light travels across the Universe largely unimpeded. Therefore, observations of the cosmic background radiation is the most powerful probe for the early Universe.

Notice that the LSS has a thickness because the time of last scattering is modeled by a visibility function which measure the probability that a particular photon last scattered in a redshift interval $dz$. Conveniently, this is well approximated by a Gaussian at mean redshift $z_* = 1100$ with width $\Delta z \simeq 80$, pretty much independent of all cosmological parameters.[3]

In 1990, the FIRAS instrument on the COBE satellite revealed in the CMB an almost perfect black-body spectrum of temperature $T_0 = 2.725 \pm 0.001\,\mathrm{K}$ (95% CL):

$$I_\nu = \frac{2h\nu^3}{c^2} \frac{1}{e^{\frac{h\nu}{k_B T_0}} - 1}, \tag{1.9}$$

with possible deviation from black-body limited to $\Delta I_\nu / I_\nu \lesssim 10^{-5}$; we defer an accurate discussion on this subject to §3.1. Later on, in 1992, the COBE DMR experiment reported the first detection of cosmological anisotropy in the CMB temperature field, aside from the dipole induced by the motion of our galaxy of about 3.5 mK, at an rms level of $\Delta T/T = \mathcal{O}(10^{-5})$. These fluctuations, detected on scales larger than the $7^\circ$ resolution of the COBE DRM instrument, represent the direct imprint of initial gravitational potential perturbations through their redshifting effect on the CMB photons, called the *Sachs-Wolfe effect*, and are of the right amplitude to explain the large-scale structure of the Universe. From 1992 onwards, lots of experiments detected a rise and fall in the level of anisotropy from degree scales to arcminute scales (see Fig. 1.3.2).

These observations contributed to build a working cosmological model for our Universe: namely, that the universe is spatially flat, consists mainly of dark matter and dark energy, with the small amount of ordinary matter necessary to explain the light element abundances, and all the rich structure in it formed through gravitational instability from quantum mechanical fluctuations when the Universe was a fraction of a second old.

One of the most important fact about CMB anisotropies is that the photon distribution is quite uniform with very small perturbations and this is in stark contrast to the matter in the Universe, which on scales less than about 10 Mpc is organized in very non-linear structures like galaxies and clusters, following on from gravitational instability. This disparity is due to radiation pressure that prevents photons from clumping. Thus, even though both inhomogeneities in the matter in the Universe and anisotropies in the CMB apparently originated from the same source, these appear very different today. Note that, thanks to the smoothness of the photon distribution we can use linear response theory and predictions

[3] This assumes that there is no very early reionization of the intergalactic medium by ultraviolet photons emitted by the earliest generations of stars and quasars, which could create free electrons that can scatter the microwave photons. However, in inflation-based models, which we will see soon, it is thought that reionization happens at $z \sim 6$, clearly not early enough to rescatter all of the microwave background photons to create a new LSS.

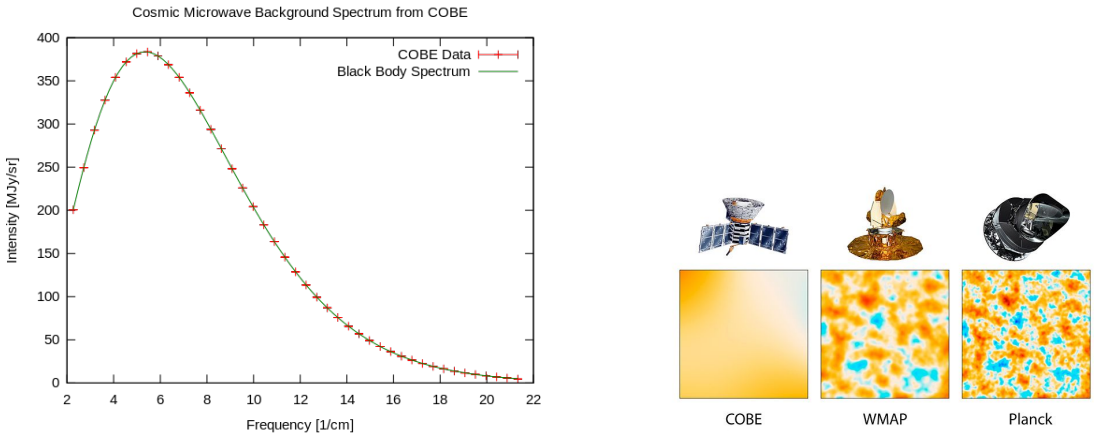


(a) FIRAS spectral measurement

(b) Temperature anisotropies

**Figure 1.3.2:** (a)The almost perfect black-body spectrum of the CMB; error bars too small to be displayed. (b)Resolution enhancement in the CMB temperature anisotropies detection (Pictures taken from the JPL-Caltech official website).

can be made as precisely as their sources are specified; besides, if the sources of the anisotropies are also linear fluctuations, anisotropy formation falls in the domain of linear perturbation theory.

### Temperature Field

As we said before, the CMB spectrum is an extremely good black-body with a nearly constant temperature across the sky $T_o$, so we generally describe its intensity as a function of frequency and direction on the sky $\hat{\mathbf{n}}$ in terms of a temperature fluctuation $\Theta(\hat{\mathbf{n}}) = \Delta T(\hat{\mathbf{n}})/T_o$.

The CMB temperature is a two-dimensional field measured everywhere on the sky, i.e. with two angular coordinates. Thus, instead of Fourier transforming (as in the case, for example, of the galaxy distribution) the CMB temperature, one typically expands it in spherical harmonics, a basis more appropriate for a 2D field on the LSS:

$$\Theta(\hat{\mathbf{n}}) = \frac{\Delta T(\hat{\mathbf{n}})}{T_o} = \sum_{\ell=o}^{\infty} \sum_{m=-\ell}^{\ell} a_{\ell m} Y_{\ell m}(\hat{\mathbf{n}}),$$

where we introduced the multipole moments:

$$a_{\ell m} = \int d\hat{\mathbf{n}} Y^*_{\ell m}(\hat{\mathbf{n}}) \Theta(\hat{\mathbf{n}}).$$

Expanding in multipoles is also useful because it makes it easier to separate large from small scales, since, roughly speaking:

$$\theta \sim \frac{\pi}{\ell},$$

where $\ell$ represents the "angular frequency"; see Fig 1.3.3. In particular, large multipole moments

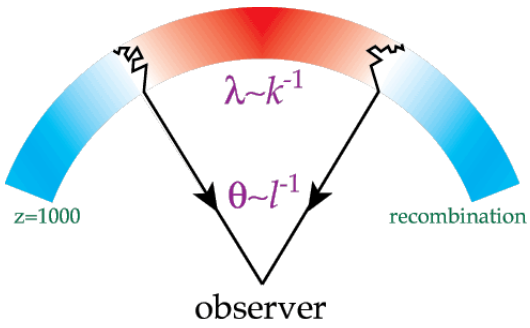


**Figure 1.3.3:** Angular projection of the temperature anisotropies on the LSS.

corresponds to small angular scales with $\ell \sim 10^2$ representing degree scale separations.

For example, recalling Fig. 1.3.2b), COBE had an angular resolution of $7^\circ$ allowing a measurement up to $\ell = 180/7 = 26$, WMAP had resolution $0.23^\circ$ reaching to $\ell = 180/0.23 = 783$, and the Planck satellite has resolution $5'$, which allow us an enhancement up to $\ell = 2160$.

These fluctuations must be analyzed statistically; if they are Gaussian, then the statistical content is encapsulated in the *two point temperature correlation function* since every correlation of an odd number of points is zero and every correlation of an even number of points can be connected to the case with only two points.[4]

When written in the spherical harmonics basis, this two point function is more frequently called *angular Power Spectrum (PS)*:

$$\langle a^*_{\ell m} a_{\ell' m'} \rangle = \delta^{\ell'}_{\ell} \delta^{m'}_{m} C_\ell .$$

Note that the amplitude of the fluctuations is isotropic, that is it depends only on $\ell$ and not on $m$.

It has become customary to plot the angular power spectrum as $\ell(\ell+1)C_\ell/2\pi$ in order to better highlight some of its properties; so, defining the quantity

$$\Delta T^2 \equiv \frac{\ell(\ell+1)}{2\pi} C_\ell T^2,$$

the observations of $\Delta T$ along with the prediction of the working cosmological model gives the spectrum in Fig. 1.3.4.

From the plot we can clearly see that the first two multipoles are not depicted:

- $\ell = 0$: it is a constant, an offset, and if we wanted to know it we would need to average on the ensemble represented by all possible universes, but unfortunately we can see only one of them;
- $\ell = 1$: it is the dipole effect dominated by the peculiar velocity of our galaxy; the earth we live in is indeed not fixed in the CMB frame, this means we are not comoving observers so we see the CMB redshifted in the direction we are moving toward and blueshifted behind.

[4] This descends directly from the Wick Theorem and we are going to use it often later on.

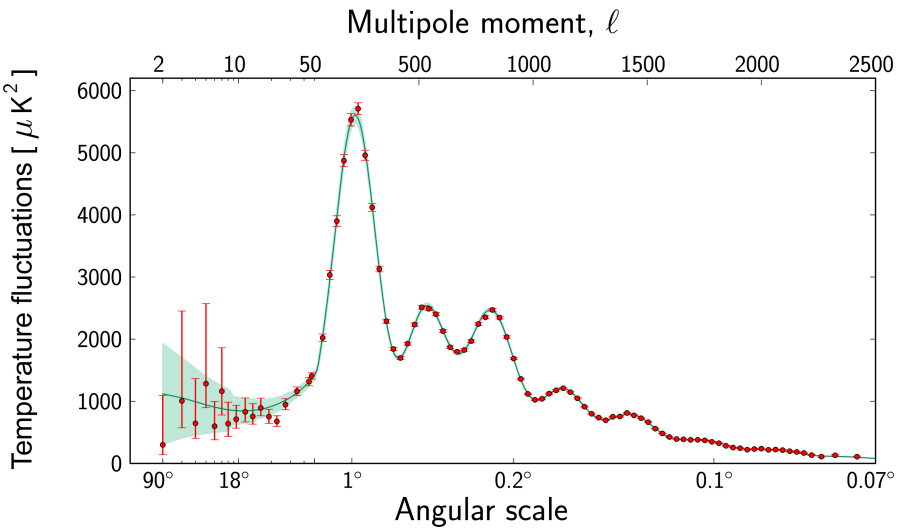


**Figure 1.3.4:** Temperature fluctuations in the Cosmic Microwave Background detected by *Planck* at different angular scales on the sky. Error bars on the measurements, indicated by red dot, account for measurement errors as well as for an estimate of the uncertainty that is due to the limited number of points in the sky at which it is possible to perform measurements. The green curve represents the best fit of the Standard Model of Cosmology' to the *Planck* data; the pale green area around the curve shows the predictions of all the variations of the Standard Model that best agree with the data (Picture taken from ESA official website).

We neglect these two points also because the Power Spectrum exhibits large errors at low multipoles and the reason is that the predicted PS is the average power in the multipole moment $\ell$ an observer would see in an ensemble of universes. However we only observe one realization of this ensemble and thus $C_\ell$ must be estimated with $2\ell + 1$ measurements for each $\ell$ (since $m$ runs from $-\ell$ to $+\ell$); this is particularly problematic for the monopole and dipole ($\ell = 0, 1$).

In fact, while the observations on small and intermediate angular scales agree extremely well with the model predictions, the fluctuations detected on large angular scales on the sky – between $90^\circ$ and $6^\circ$ degrees – are about 10% weaker than the best fit of the standard model to *Planck* data. At angular scales larger than $6^\circ$, there is one data point that falls well outside the range of allowed models. These anomalies in the Cosmic Microwave Background pattern might challenge the very foundations of Cosmology, suggesting that some aspects of the Standard Model of Cosmology may need a rethink.

We can then say that at low $\ell$ there is a fundamental limitations set by a *cosmic variance* which leads to an inevitable error of

$$\Delta C_\ell = \sqrt{\frac{2}{2\ell + 1}} C_\ell .$$

Considering bands of $\Delta\ell \approx \ell$, we see that the precision in the PS determination scales as $\ell^{-1}$, i.e. $\sim 1\%$ at $\ell = 100$ and $\sim 0.1\%$ at $\ell = 1000$. The cosmic variance therefore limits the accuracy of comparison of CMB observations with theory, especially for large scales (low $\ell$).

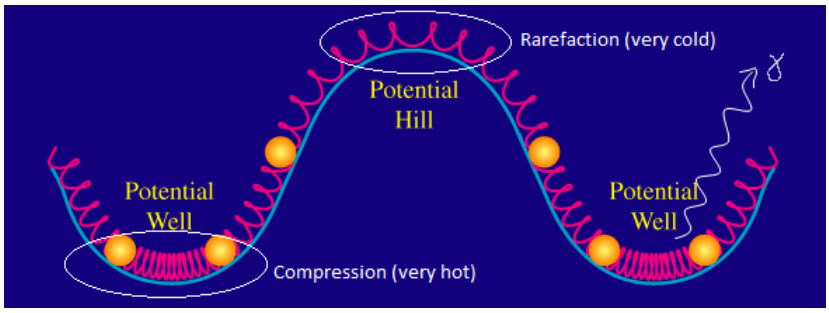


**Figure 1.3.5:** Compressing a gas heats it up. Letting it expand cools it down. The CMB is locally hotter in regions where the acoustic wave causes compression and cooler where it causes rarefaction (Picture adapted from [11]).

### Anisotropies in the CMB

Employing analytic and numerical results, anisotropies formation process has been constructed in a critical, open, close, and cosmological constant Universe with adiabatic or isocurvature initial conditions allowing for possible early reionization. Anisotropy formation is a simple process and it is governed by the Compton scattering of photons off electrons and their gravitational coupling to the other particle species in the Universe (see, for example, [10]).

Fluctuations in the total matter density, which includes decoupled species such as the neutrinos and possibly collisionless dark matter, interact with the photons through the gravitational potentials they create. These primordial perturbations were produced during the very first moments after the Big Bang (we weill see the inflation epoch in the next section) and began to grow when the Universe became dominated by matter. This growth was led by gravitational attraction, i.e. infall into fluctuations' own potential wells, to eventually form large scale structure in the universe becoming the non-linear structure we see today. The presence of fluctuations in the early universe is also responsible for anisotropy formation. Before redshift $z_* \sim 1000$, the CMB was hot enough to ionize hydrogen. Compton scattering off electrons, which are in turn linked to the protons via Coulomb interactions, strongly couples the photons to the baryons and establishes the photon-baryon fluid we mentioned earlier. Photon pressure resists compression of the fluid by gravitational infall and sets up *acoustic oscillations*. At $z_*$, recombination produced neutral hydrogen and the photons last scattering.

Regions of compression and rarefaction at this epoch represent hot and cold spots respectively. Photons also suffer gravitational redshifts from climbing out of the potentials on the last scattering surface; see Fig. 1.3.5. The resultant fluctuations appear to the observer today as anisotropies on the sky.

The little spheres in the figure represent an effective mass of the fluid, which is increased by the presence of baryons. This changes the balance between pressure and gravity in the fluid. Gravitational infall now leads to greater compression of the fluid in the potential well. Just like a mass on a spring, gravity shifts the zero point of the oscillator. Compressions are enhanced over rarefactions of the fluid inside potential wells. Thus the relative heights of the peaks provide one way of measuring the baryon content of the universe. In the scale-invariant adiabatic model, this is how the anisotropy depends on the baryon content.

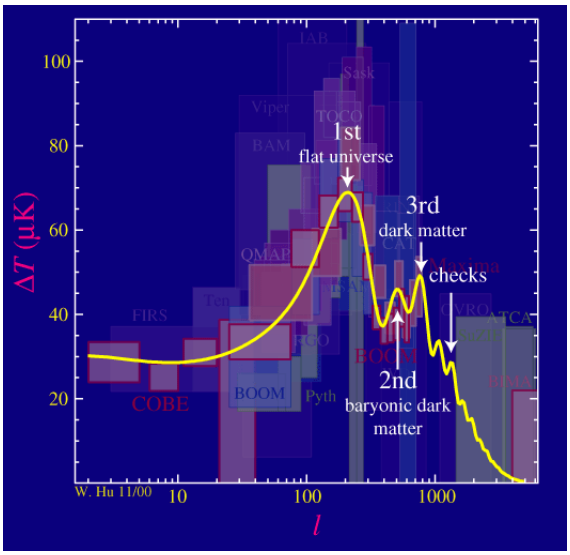


**Figure 1.3.6:** First peak shows the universe is close to spatially flat; constraints on the second peak indicate substantial amounts of dark baryons; third peak will measure the physical density of the dark matter; damping tail will provide consistency checks of underlying assumptions (Picture taken from [11]).

Positions and relative heights of the acoustic peaks give us important information about some of the fundamental cosmological parameters, for example see Fig. 1.3.6.

Odd peaks represent the compression phase (temperature crests), whereas even peaks represent the rarefaction phase (temperature troughs), inside the potential wells.

Theory of Baryon acoustic oscillations and its peaks represents one of the main branches in the cosmological field; unfortunately, it does not fall within the major topic of this work so we will not examine it more.

## 1.4 Problems in the Standard Model and Inflation

In the previous sections we have been giving some hints about the evolution of our Universe and the fact that there have been some initial fluctuations which lead to the formation of structures. It is then right and proper to introduce now the process that most of all is responsible of how we see the Universe today: *inflation*.

Just to be clear, inflation is actually a theory but it wonderfully fits the data we have, that there is really no reason to search an alternative to it as it would be an utterly overwhelming challenge.

In the modern view, without the shadow of a doubt the most important property of inflation is that it can account for the origin of perturbations in the Universe; this allows the possibility of testing various aspects of the inflationary scenario. However, the historical motivation for inflation was rather different and arose largely from the question of whether the initial conditions required for the Hot Big Bang seem likely or not. In particular, inflation was introduced as a mechanism able to solve three notable problems in the Standard Model.

### Horizon Problem

*How can the Universe be homogeneous and isotropic if not all its region have always been in causal contact?*

Let us start by defining the *particle horizon*, which is the distance that light could have traveled since the beginning of the Universe at $t = 0$:

$$d_H(t) = a(t) \int_0^t \frac{\mathrm{d}t'}{a(t')}.$$

It gives the causal connetion properties between two point in the Universe since we can imagine that inside the sphere with radius $d_H(t)$ there are all those points that could have communicated with the observer in the center of the sphere itself.

Another useful quantity is the *comoving Hubble radius*

$$r_H(t) = \frac{H(t)^{-1}}{a(t)} = \frac{1}{\dot{a}(t)},$$

which is the comoving scale of causal correlation and grows with time.

Considering the comoving particle horizon we can see that it is related to the comoving Hubble radius by

$$\frac{d_H(t)}{a(t)} = \int_0^a \frac{\mathrm{d}a'}{a'} r_H(a').$$

These quantities may look similar but there is a conceptual distinction: if particles are separated by distances grater than $d_H/a$, they *never* could have communicated with one another; if they are separated by distances greater than $r_H$, they cannot talk to each other *now*.

Now, the comoving distance on the LSS defined by $r_H(t_{\mathrm{dec}})$ subtends an angle $\theta \sim 2^\circ$ but we observe photons with comoving angular distances $\theta > 2^\circ$ with almost the same temperature ($\Delta T/T \sim 10^{-5}$); this means that microwaves coming from regions separated by more than the horizon scale at last scattering cannot have interacted before decoupling.

The horizon problem is then a problem about causal connection and can be visualized in Fig. 1.4.1.

### Flatness Problem

*How can the Universe be so old and yet so flat?*

There is another fundamental quantity in Cosmology which we have not introduced yet, the *density parameter* $\Omega$

$$\Omega_i(t) = \frac{\rho_i(t)}{\rho_{cr}(t)},$$

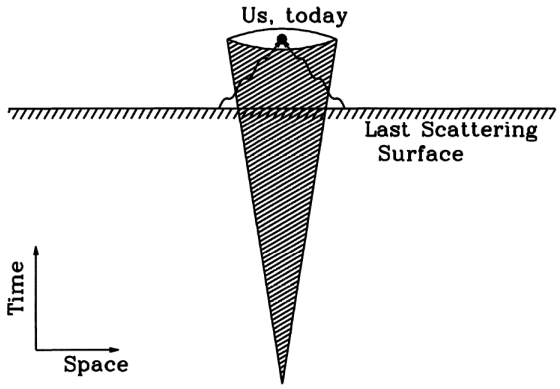


**Figure 1.4.1:** Horizon problem: the region inside the cone at any time is causally connected to us. Photons emitted from the LSS started outside this region and, although they were not in causal contact with us nor with each other, their temepratures are almost identical (Picture taken from [6]).

where $\rho_{cr}(t) = 3H^2/8\pi G$ and $i$ corresponds to different constituents. Recalling the meaning of the critical density we can say that the space is closed ($k = 1$), flat ($k = 0$) or open ($k = -1$) according to whether the density parameter is greater than, equal to, or less than unity.

Now, from the first Friedmann equation, with some algebra and including the cosmological constant $\Lambda$ in the density parameter, we get

$$H^2 = \left(\frac{\dot{a}}{a}\right)^2 = \frac{8\pi G}{3}\rho - \frac{k}{a^2} \qquad \longrightarrow \qquad \Omega(t) - 1 = k r_H^2(t).$$

As we said, $r_H(t)$ grows with time and this causes $\Omega(t)$ departing more and more from 1. However, we know from observations that $\Omega_0$, i.e. the density parameter at present times, is very close to unity and this means that at much earlier times it must have been extremely close to one. To be quantitative, if we take the Planck time $t_P \simeq 10^{-43}$ as a reference epoch when the Universe was dominated by radiation, it can be easily seen that [9]

$$\Omega(t_P) \simeq 1 + (\Omega_0 - 1)10^{-60}.$$

This means that, since current constraints [7] give $\Omega_0 = 1.0023^{+0.0056}_{-0.0054}$ at 68% CL, the kinetic term in the Friedmann equation at $t_P$ must have differed from the gravitational term by about one part in $10^{60}$.

The flatness problem is then a fine-tuning problem: almost all initial conditions lead either to a closed Universe that recollapses almost immediately, or to an open Universe that very quickly enters the curvature-dominated regime and cools below 3 K within the first second of its existence. Nevertheless, the Universe has survived for $10^{10}$ years and our presence here witnesses that. In Fig. 1.4.2 we can see how $\Omega$ goes with cosmic time, in particular how rapidly it diverges from 1. Each curve represents a possible universe. The blue curve is a universe similar to our own, which at the present time has a $|\Omega_0 - 1| \lesssim 10^{-3}$ and therefore must have begun with $\Omega$ very close to 1 indeed. The red curve is a hypothetical different universe in which the initial value of $\Omega$ is not enough close to 1: by the present

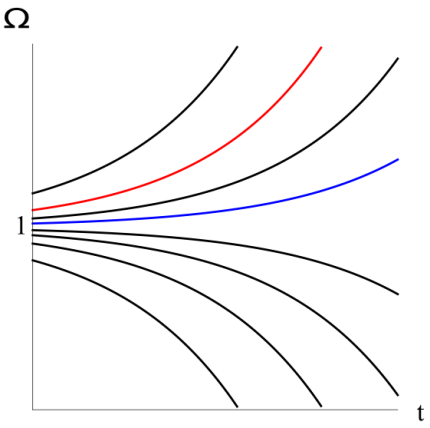


**Figure 1.4.2:** Density parameter Ω as a function of cosmic time $t$. Neither axis to scale.

day it would have diverged extremely and would not be able to support galaxies, stars or planets.

### Unwanted Relics

*How can we get rid of cosmic relics, forbidden by observation but that may survive to the present?*

If the Hot Big Bang begins at a very high temperature, it may have originated some so-called topological defects and very massive particles $X$ which, with $\Omega_X \gg 1$, would tend to close the Universe, but this is not what we observe.

Some examples of these relics are:

- topological defects like magnetic monopoles (point-like defects), cosmic strings (one dimensional), domain walls (two dimensional) and textures (three dimensional); they are likely to emerge when the symmetry of a Grand Unified Theory is broken spontaneously;
- gravitino: a spin-3/2 particle which occurs in supergravity and has only gravitational-strength interactions;
- moduli: they occurs in superstring theory and are spin-0 particles corresponding to the fields that parameterize the vacuum in the absence of supersymmetry breaking.

Historically, the main issue was represented by magnetic monopoles as other topological defects were indeed problematic, but more model dependent; from the modern viewpoint, instead, perhaps the most problematic relic is the gravitino.

### The inflationary scenario

Initially, such problems (the horizon, the flatness and the relics problems) were dealt with just by assuming some particular initial conditions. Of course this was only a temporary relief and cosmologist

investigated more in details where those initial conditions came from. Soon after, starting by the beginning of the 80's, first models of inflation were introduce as a mechanism able to draw the Universe into these extremely peculiar and unlikely initial conditions.

According to the inflationary theory, the Universe experience an exponential expansion from $10^{-36}$ seconds after the Big Bang to sometime between $10^{-33}$ and $10^{-32}$ seconds. It is convenient to label these initial and final times respectively as $t_I$ and $t_F$. After this period the expansion kept going, but at a less rapid rate.

Notice that the inflationary cosmology (Guth 1981, Albrecht and Steinhardt 1982, Linde 1982-1983) is not a replacement for the Hot Big Bang model, but rather an add-on that occurs at very early times without disturbing any of its successes. On a basic ground, the definition of inflation is simply any epoch during which the scale factor $a(t)$ of the Universe is accelerating:

$$\text{INFLATION} \iff \ddot{a} > 0.$$

The problems we listed above are indeed present in standard models of Friedmann-Robertson-Walker (FRW) dominated by radiation or matter where, in particular, the expansion of space is not accelerated, i.e. $\ddot{a} < 0$. Interestingly, there is an analogy between the de-Sitter universes we mentioned in the previous section and inflation since such universes can be considered as reference points for all inflationary models, which (considering the present constraints) are based on small deviations from $w_{\text{inf}} = -1$; we gave an example of de-Sitter universe when we described how the cosmological constant $\Lambda$ will affect the Friedmann equations. Actually, it is easy to see from the Friedmann equations (1.8) that the condition for inflation can be rewritten as

$$\rho + 3p < 0,$$

$\rho$ being positive defined, so one would need

$$w_{\text{inf}} < -\frac{1}{3}.$$

If we recall the concept of Dark Energy (DE) for a moment, it is interesting to notice that latest analysis in [7], combining *Planck* data with other astrophysical data (including Type Ia supernovae), constrained the equation of state of DE to $w_{\text{DE}} = -1.006 \pm 0.045$ at 95% CL, which is consistent with the expected value for a cosmological constant and allows inflation.

Now, let us see how inflation can easily solve all the Standard Model problems at the same time.

First of all, it is quite immediate to see that

$$\ddot{a} > 0 \implies \dot{r_H}(t) < 0.$$

This means that during inflation the comoving Hubble radius decreased with time whereas we saw that if we limit ourselves to FRW models $r_H(t)$ can only increase as time passes. In Fig. 1.4.3 is then easy

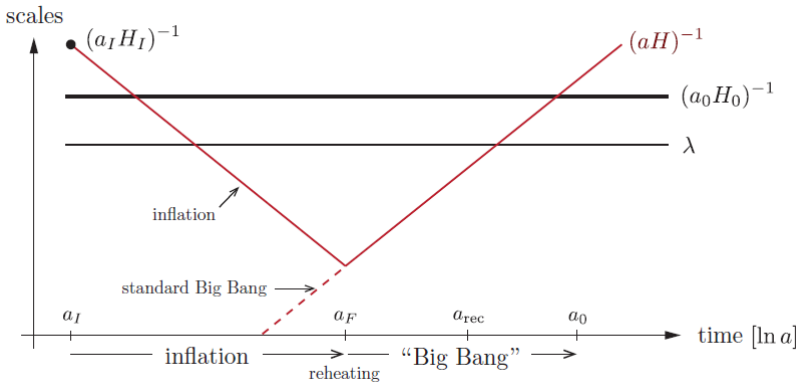


**Figure 1.4.3:** Scales of cosmological interest were larger than the Hubble radius until $a \approx 10^{-5}$ (where today is at $a(t_0) = a_0 = 1$). However, at very early times, during inflation, all scales of interest were smaller than the Hubble radius and therefore susceptible to microphysical processing. Similarly, at very late times, the scales of cosmological interest are back within the Hubble radius. $a_I = a(t_I)$ and $a_F = a(t_F)$ (Picture taken from [8]).

to see how the horizon problem is solved.

The shrinking Hubble sphere means that particles which were initially in causal contact with another, i.e. separated by a distance $\lambda < (a_I H_I)^{-1}$ can no longer communicate after a sufficiently long period of inflation: $\lambda > (aH)^{-1}$. However, at any moment before horizon exit [5] the particles could still talk to each other and establish similar conditions. Everything within the Hubble sphere at the beginning of inflation, $(a_I H_I)^{-1}$, was causally connected. Since the comoving Hubble radius is easier to calculate than the comoving particle horizon (which is an integral) it is common to use the Hubble radius as a means of judging the horizon problem.

Looking at Fig. 1.4.3 it is easy to understand that the solution is guaranteed only if inflation lasts a sufficiently long period of time; the natural unit used for such measure is the *number of e-folds* $N$:

$$N \equiv \ln\left(\frac{a(t_F)}{a(t_I)}\right) = \ln\left(\frac{a_F}{a_I}\right) = \int_{t_I}^{t_F} H(t)\mathrm{d}t.$$

The condition to impose in order to find the minimal value for $N$ is

$$r_H(t_0) \leqslant r_H(t_I)$$

and it can be shown [9] that this condition requires $N \geqslant 60$.

This is quite the same value found to solve also the flatness problem. In Fig. 1.4.4 we can see that during inflation the density parameter $\Omega$ is driven toward 1 and, regardless of the conditions before inflation, at the end of the accelerated expansion $\Omega$ is extremely close to 1, by about one part in $10^{60}$ as we said we needed.

Indicating with $\Omega_I$ and $\Omega_0$ respectively the density parameter at the beginning of inflation and today, the condition to impose is

[5] Careful here: we used 'horizon exit' and we may use it again but we actually mean exit of the Hubble radius, as depicted in Fig. 1.4.3.

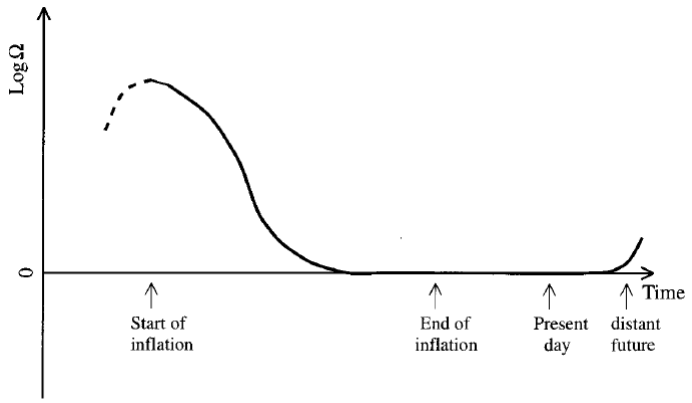


**Figure 1.4.4:** Schematic of the inflationary solution to the flatness problem. By definition, during inflation $\Omega$ is driven toward 1 and it will finish so close that in all the subsequent evolution up to now it remains extremely close to 1, for one part in $10^3$ . Only in the distant future it will move away again. Axis are not in scale (Picture taken from [12]).

$$\frac{1-\Omega_I^{-1}}{1-\Omega_0^{-1}} \geq 1,$$

and $\Omega_I$ can be both $\gg 1$ or $\ll 1$. From this condition, a straightforward calculation [9] leads to $N \gtrsim 70$, even though today's numerical values [7] are for the range $50 \leqslant N \leqslant 60$.

Therefore, by choosing this value for $N$ in order to solve the flatness problem, we automatically solve also the horizon problem, and vice-versa; this is one of the greatest outcome of inflation. On the contrary, inflationary models that do not reach such values for $N$, are rejected.

Finally, the unwanted cosmic relics problem is also taken care of because thanks to the inflationary accelerated expansion, any topological defects formed (like the monopole) during inflation will be drastically diluted as the Universe expands so that their present density will be negligible.

### Dynamics of a scalar field

In order to obtain inflation, we need a form of matter with the unusual property of a negative pressure. The easiest case is that of a scalar field $\varphi$, describing scalar (spin-0) particles. In particular, inflation is based upon the idea that the vacuum energy $\rho_\varphi \simeq V(\varphi)$ of a scalar quantum field, dubbed the *inflaton*, dominates over other forms of energy, hence giving rise to a quasi-exponential (de-Sitter) expansion, with $V(\varphi) \simeq$ const. and scale factor $a(t) \approx e^{Ht}$.

Quantum vacuum oscillations of the inflaton give rise to fluctuations in the energy density, which provide the seeds for Cosmic Microwave Background radiation temperature anisotropies and polarization, as well as for the formation of Large Scale Structures in the present Universe. All the matter and radiation which we see today must have been generated after inflation, during the so-called *reheating* phase, since all previous forms of matter and radiation have been tremendously diluted by the accelerated expansion (Cosmic no-hair conjecture).

The standard way to specify a particle theory is via its Lagrangian, from which the equations of motion

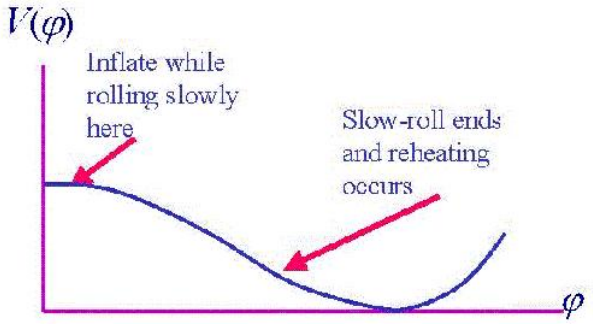


**Figure 1.4.5:** Slow roll phase of a scalar field. We can think at the inflaton as a particle moving under a force induced by the potential $V$.

ca be derived. So, e.g., let us consider the simplest possibility

$$\mathcal{L}_\varphi[\varphi, g_{\mu\nu}] = \frac{1}{2} g^{\mu\nu} D_\mu \varphi D_\nu \varphi - V(\varphi).$$

This Lagrangian is composed by a standard kinetic term and the inflaton potential term describing the self-interactions of the inflation field (and eventually its interactions with the rest of the world). In Cosmology, the scalar field is usually split as

$$\varphi = \varphi(\mathbf{x}, t) = \varphi_0(t) + \delta\varphi(\mathbf{x}, t), \tag{1.10}$$

where, in a FRW context, $\varphi_0(t) = \langle 0|\varphi(\mathbf{x}, t)|0\rangle$ is the classical background value of the field and $\delta\varphi(\mathbf{x}, t)$ represent its quantum fluctuations; also, we have $\langle 0|\delta\varphi(\mathbf{x}, t)|0\rangle = \langle\delta\varphi\rangle = 0$. Notice that the splitting (1.10) is possible if it holds the condition $\langle\delta\varphi^2\rangle \ll \varphi_0^2(t)$.

The vacuum expectation value $\varphi_0(t)$ of the inflaton scalar field behaves like a perfect fluid, but, unlike standard fluids, can be characterized by a negative pressure:

$$\begin{cases} \rho_\varphi = -T^0_0 = \frac{1}{2}\dot{\varphi}_0^2 + V(\varphi_0) \\ p_\varphi = T^i_i = \frac{1}{2}\dot{\varphi}_0^2 - V(\varphi_0). \end{cases}$$

At this point it is customary to make the assumption that the kinetic term is smaller than the potential term, i.e. (dropping the subscript 0) $\frac{1}{2}\dot{\varphi}^2 \ll V(\varphi)$. The equation of state that pressure and energy density must obey becomes then

$$w_\varphi = \frac{p_\varphi}{\rho_\varphi} = \frac{\frac{1}{2}\dot{\varphi}^2 - V(\varphi)}{\frac{1}{2}\dot{\varphi}^2 + V(\varphi)} \simeq -1.$$

As we already saw, $w_\varphi \simeq -1$ corresponds to a quasi de-Sitter phase and therefore this scalar field can drive inflation. In particular, a field with this properties is said to be in a *slow-roll* phase where the inflaton potential is very flat; Fig. 1.4.5 shows it quite clearly.

The equation of motion for such field can be then obtained by applying the Klein-Gordon equation

in the FRW background with $k = 0$; after a few steps one finds

$$\Box\varphi = \frac{\partial V}{\partial \varphi} \quad \Longrightarrow \quad \ddot{\varphi} + 3H\dot{\varphi} - \frac{1}{a^2}\nabla^2\varphi = -\frac{\partial V}{\partial \varphi}. \tag{1.11}$$

Notice that in GR the Minimal Coupling acts on the operator $\Box$ with the substitution $\Box = \partial_\mu \partial^\mu \longrightarrow \Box = D_\mu D^\mu$.

This type of dynamics is conveniently described by the two *slow-roll parameters* $\varepsilon$ and $\eta$ which descend from the two slow-roll conditions

1) $\frac{1}{2}\dot{\varphi}^2 \ll V(\varphi) \quad \Longrightarrow \quad \varepsilon \equiv -\frac{\dot{H}}{H^2} \simeq \frac{1}{16\pi G}\left(\frac{V'}{V}\right)^2$,

2) $\ddot{\varphi} \ll 3H\dot{\varphi} \quad \Longrightarrow \quad \eta \equiv \frac{1}{3}\frac{V''}{H^2}$,

where prime indexes stand for derivatives with respect to the field $\varphi$.

The meaning of these parameters is that inflation takes place precisely if $\varepsilon, |\eta| \ll 1$. Moreover, they are usually introduce also because they provide information about the shape of the potential, as they depend on $V'$ and $V''$, and this shape is essentially what characterizes the different models of inflation. In principle, other parameters of next orders related to $V'''$ and $V''''$ can be introduced, but they would result in a higher order than the ones we are interested in.

Another important remark is that, regardless of the model, the second derivative of the potential is directly related to the mass of the scalar field that drives the inflation, so that

$$m_\varphi^2 = V''(\varphi = 0).$$

Before ending this paragraph, some final remarks are due. There exist many different versions of the inflationary universe. The first was formulated by Guth (1981) [13], although some of his ideas had been presented previously by Starobinsky (1979) [14]. In Guth's model inflation was assumed to occur while the Universe is trapped in a false vacuum with $\varphi = 0$ corresponding to the first-order phase transition which characterizes the breaking of an SU(5) symmetry into SU(4)xU(1). This model, dubbed *old*, was subsequently abandoned for reasons which, for the sake of brevity, we shall not mention. The next generation of inflationary models shared the characteristics of a model called the *new inflationary Universe*, which was suggested independently by Linde (1982) [15] and Albrecht and Steinhardt (1982) [16]. In models of this type, inflation occurs during a phase in which the region which grows to include our observable patch evolves slowly from a false vacuum with $\varphi = 0$ towards a true vacuum with $\varphi = \bar{\varphi}$, as it is indeed displayed in Fig. 1.4.5. In fact, it was later seen that this kind of inflation could also be achieved in many different contexts, not necessarily requiring the existence of a phase transition or a spontaneous symmetry breaking.

In 1983 Linde [17] considered the variant version of the slow-roll inflation called *chaotic inflation*, in which initial conditions of scalar fields are chaotic. According to this model, our homogeneous and isotropic Universe may be produced in the regions where inflation occurs sufficiently. While old and new inflation models are based on the assumption that the Universe was in a state of thermal equilibrium

from the beginning, chaotic inflation can occur even without such an assumption. In addition chaotic inflation can start out in the regime close to Planck density, thereby solving the problem of initial conditions.

Anyway, from an explanatory point of view, the *new* inflationary model appears to be one of the clearest. It is based on a certain choice of parameters for an SU(5) theory which, in the absence of any experimental constraints, appears a little arbitrary. This problem is common also to other inflationary models based on theories like supersymmetry, superstrings or supergravity which have not yet received any experimental confirmation (see, for instance, [18] for a review in such a direction).

Even though no particular version of the inflationary model has received any strong physical support from particle physics theories, it is fair to say that such model has become a sort of paradigm for resolving some of the difficulties with the Standard Model and providing the primordial density fluctuations, as we will better see in the next Chapter.

Four our purposes, we can stop here the discussion about the variety of the inflationary scenario and we refer to textbooks such as [12] and [9] for a more complete description, or to [19] for a more recent review. We will come back to inflation later in §3.2 when we will be interested in the Non-Gaussianity property that may arise from different models.

# 2

# Cosmological Perturbation Theory

In the first Chapter we have hinted at some basic assumptions in Cosmology and we are now going to say something more about them.

So far, we have treated the Universe as perfectly homogeneous. To understand the formation and evolution of large-scale structures, we have to introduce inhomogeneities. As long as these perturbations remain relatively small, we can treat them in perturbation theory. Just think at objects like galaxies and clusters, which have a typical distance of $\sim 1$ Mpc and represent non - linearities; they must be taken into account on scale below the 10 Mpc threshold but can be treated as linear perturbations in the homogeneous and isotropic Universe. These structures arose from initial tiny density perturbation with $10^{-5}$ order of magnitude and grew via the process of *gravitational instability* [9]. Notice that such tiny amplitudes point out that perturbative approach is really legitimate when doing large scale Cosmology.

Moreover, we will see that it is the vacuum quantum fluctuation $\delta\varphi$ of the scalar field driving the inflationary process that provided the seeds for the first primordial energy density perturbations [20]; subsequently, they led to the structure formation and, above all, our major interest, CMB anisotropies. In the inflationary picture, the primordial cosmological perturbations are created from these quantum fluctuations that have remained constant after they exited the horizon during an early period of accelerated expansion of the Universe (inflation). Today, they are observable as temperature anisotropies in the CMB.

At the end of the Chapter, when we will have defined some of the most important physical quantities in Cosmology, we will briefly present the current constraints on the cosmological parameters. They are largely used to parameterize the $\Lambda$CDM fiducial model and, during years, have been lowered to a key number of six. The exact values are not predicted by theory but several estimates have been carried out

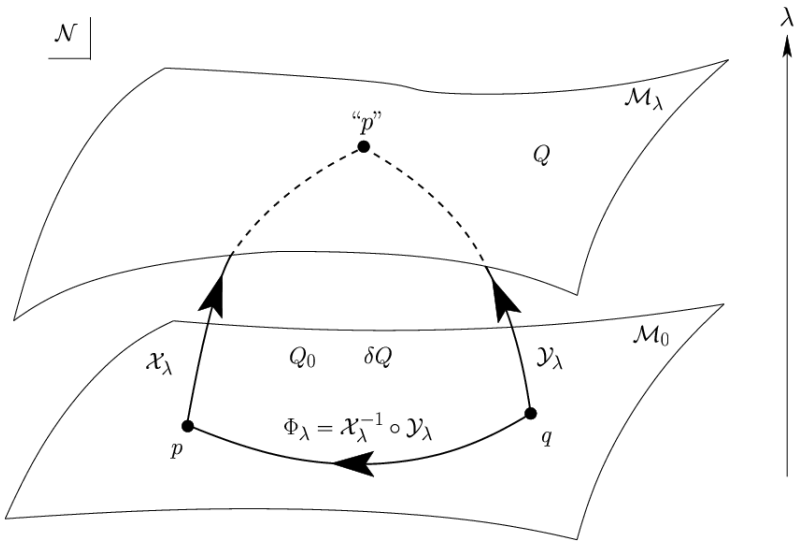


**Figure 2.1.1:** Gauge problem: a point on the background manifold $M_\circ$ does not have unique correspondence to a point on the physical spacetime $M$.

with increasingly sensitivity.

## 2.1 Perturbation theory in General Relativity

Before we start, we have to address an important subtlety that comes up when using the perturbation approach in GR. This is because we perturb not only fields, but also geometry itself. In particular, Einstein Equations are built on the invariance under diffeomorphisms and this implies that the definition of perturbation itself will necessarily present some ambiguities.

Recalling that our space-time is a differentiable manifold as explained in the first chapter, the perturbation method in Cosmology is enforced by imaging that the physical space-time $M$ we live in is a perturbation of an FRW background space-time $M_\circ$. As a matter of fact, the Universe is homogeneous and isotropic on large scales but every piece of information we have about it comes from galaxies, clusters, anisotropies in the CMB and other inhomogeneities.

If we consider a generic tensor $T$ representing a certain geometrical or physical quantity, the perturbation to $T$ is given by

$$\delta T = T - T_\circ,$$

where $T$ is the value of the tensor assumed in the physical space $M$ and $T_\circ$ is the value in the background space $M_\circ$; for example, $T$ can be the metric tensor $g_{\mu\nu}$ or the energy-momentum tensor $T_{\mu\nu}$ of a fluid or a scalar field (inflaton).

Here is where the crucial aspect arises, also known as the *gauge problem*. $M$ and $M_\circ$ are two different manifolds so if we want to confront $T$ and $T_\circ$ in order to estimate $\delta T$, we need a prescription that allow us to map a point in $M_\circ$ to a point in $M$ and viceversa. This prescription is provided by a choice of a so-called *gauge*, a one-to-one map identifying points of $M$ with points of $M_\circ$. However, diffeomorphisms

in GR give us the liberty to change coordinates without changing the physics and this, in turn, creates arbitrariness in the choice of the map since the same point in $M$ can correspond to two different points in $M_\circ$ as depicted in Fig. 2.1.1. $X_\lambda$ and $Y_\lambda$ are two different gauge choices and the diffeomorphism $\Phi_\lambda = X_\lambda^{-1} \circ Y_\lambda$ is exactly what gives the gauge transformation $X_\lambda \to Y_\lambda$. But be aware that a gauge transformation is not a coordinates transformation (in GR), in fact a gauge transformation is a change of the map between points in $M_\circ$ and points in $M$ while the coordinate system $x^\mu$ chosen in the background is fixed. Actually, we can see a gauge transformation as a change of coordinates in the physical space and at the same time a change of the point in $M_\circ$ corresponding to a certain point in $M$.

This can be all summed up in two opposite approaches:

- *active* approach: the transformation $q \to p$ maps every point of $M_\circ$ into another one, keeping coordinates system fixed;
- *passive* approach: the transformation $q \to p$ can be seen as a change of coordinates in the physical space;

and the approach we generally use the passive one since we already know the transformation law of a tensor under a change of coordinates.

We are not going to enter the conceptual difference between the two different approaches, but we want to conclude this section by introducing a mathematical tool which plays a prominent role in the gauge problem.

First of all, notice that choosing a coordinate system $x^\mu$ means choosing a threading in lines of the space-time (keeping spatial coordinates fixed) and a slicing in spatial hyper-surfaces (keeping the time fixed). The choice of coordinates is arbitrary to first-order and the definitions of the first-order metric and matter perturbations are thus gauge-dependent. Let us now consider the diffeomorphism (i.e. a change of coordinates)

$$x^\mu \longmapsto x'^\mu = x^\mu - \xi^\mu(x).$$

Using the General Covariance Principle and the linearity of Einstein Equations, one can see that if $g_{\mu\nu}(x)$ is a solution of (1.5), then

$$g'_{\mu\nu}(x) = g_{\mu\nu}(x) + \mathcal{L}_\xi g_{\mu\nu}$$

is also a solution. $\mathcal{L}_\xi g_{\mu\nu}$ is the *Lie derivative of* $g_{\mu\nu}$ *along* $\xi$ and it can be seen as a 'transport law' allowing us to compare two tensors, one the evolution of the other, along the same curve which is a solution of an appropriate vector field. The proper definition of $\mathcal{L}_\xi$ requires some mathematical insight but since we are not going to need it, we just give here some remarkable results:

$$
\begin{aligned}
\mathcal{L}_\xi S &= S_{;\lambda}\xi^\lambda && \text{for a scalar field,}\\
\mathcal{L}_\xi V_\mu &= V_{\mu;\lambda}\xi^\lambda + V_\lambda \xi^\lambda_{;\mu} && \text{for a covariant vector,}\\
\mathcal{L}_\xi V^\mu &= V^\mu_{;\lambda}\xi^\lambda - V^\lambda \xi^\mu_{;\lambda} && \text{for a contravariant vector,}\\
\mathcal{L}_\xi T^{\mu\nu} &= T^{\mu\nu}_{;\lambda}\xi^\lambda - T^{\lambda\nu}\xi^\mu_{;\lambda} - T^{\mu\lambda}\xi^\nu_{;\lambda} && \text{for a contravariant tensor,}\\
\mathcal{L}_\xi T^\mu_\nu &= T^\mu_{\nu;\lambda}\xi^\lambda - T^\lambda_\nu \xi^\mu_{;\lambda} + T^\mu_\lambda \xi^\lambda_{;\nu} && \text{for a mixed tensor,}
\end{aligned}
$$

where '$_{;a}$' is the very short notation for $D_a$. We wrote these Lie derivatives with the covariant derivatives to make them covariant by sight, but it can be proved that if we open all the $D_a$, the $\Gamma$ coefficients cancel each other out and we are left with standard derivatives $\partial_\mu$.

Basically, going back to the issue of perturbations, since they are gauge-dependent we have that $T = T_0 + \delta T$ becomes, in another gauge, $\widetilde{T} = T_0 + \widetilde{\delta T}$ and we will use the rule:

$$
\widetilde{\delta T} = \delta T + \mathcal{L}_\xi T_0, \tag{2.1}
$$

which holds at linear order, as the 'Lie-dragged' tensor is the one in the background space.

## 2.2 Cosmological Perturbations

In cosmological context, the study of fluctuations around a well known background solution is an essential tool as it gives us the possibility to linearize Einstein Equations. In fact, they are highly non linear as they contain all the dynamics in the Universe, for instance the formation and evolution of large-scale structures. However, expanding the Einstein Equations order-by-order in perturbations to the metric and the stress tensor makes the complicated system of coupled PDEs manageable.

Of course, we start by fixing a spatially flat ($k = 0$) FRW background which is going to represent our $M_0$ and we perturb around it. In conformal time, then, we define the perturbations to the components of the metric $g_{\mu\nu}$ as

$$
\begin{aligned}
g_{00} &= -a^2(\eta)\left[1 + 2\sum_{r=1}^{\infty}\frac{1}{r!}\phi^{(r)}\right],\\
g_{0i} &= g_{i0} = a^2(\eta)\sum_{r=1}^{\infty}\frac{1}{r!}\omega_i^{(r)},\\
g_{ij} &= a^2(\eta)\left\{\left[1 - 2\sum_{r=1}^{\infty}\frac{1}{r!}\psi^{(r)}\right]\delta_{ij} + \sum_{r=1}^{\infty}\frac{1}{r!}\chi_{ij}^{(r)}\right\},
\end{aligned}
$$

where $\chi_{ij}^{(r)}$ is the traceless component of the spatial perturbation and index $r$ gives the order of the perturbation so that $r = 1$ correspond to the linear order, $r = 2$ is the second order and so on; $\psi^{(r)}$ and

$\varphi^{(r)}$ are respectively called *lapse* and *shift* functions. Notice that, in perturbation theory, Latin indexes are raised and lowered by $\delta^{ij}$ and $\delta_{ij}$.

It is convenient to separate the cosmological perturbations of the metric tensor in the scalar S, vectorial V and tensorial T component because it can be seen that at first order they evolve independently. So we can split

$$\omega_i^{(r)} = \delta_i \omega^S_{(r)} + \omega^V_{i(r)} \quad \text{with} \quad \partial^i \omega^V_{i(r)} = 0,$$

$$\chi_{ij}^{(r)} = D_{ij}\chi^S + \partial_i \chi^V_j + \partial_j \chi^V_i + \chi^T_{ij} \quad \text{with} \quad \begin{cases} \partial^i \chi^V_i = 0 \\ \partial^i \chi^T_{ij} = 0 \\ \chi^{i,T}_i = 0 \end{cases},$$

and we defined $D_{ij} \equiv \partial_i \partial_j - (1/3)\delta_{ij}\nabla^2$.

Subsequently, we have to perturb the source in the Einstein Equations, that is to say the energy-momentum tensor. Perturbations are evaluated around the $T^{\mu\nu}$ for a perfect fluid, admitting also off-diagonal components for anisotropic stress:

$$T_{\mu\nu} = (\rho + p)u_\mu u_\nu + p g_{\mu\nu} + \Pi_{\mu\nu},$$

where $\Pi_{\mu\nu}$ is the tensor taking into account anisotropic stresses and perturbed energy density, pressure and 4-velocity are given by

$$\rho = \rho_0 + \sum_{r=1}^{\infty} \frac{1}{r!}\delta^{(r)}\rho \qquad \text{with} \qquad \rho_0 \equiv \rho_0(t),$$

$$p = p_0 + \delta p = p_0 + \left.\frac{\partial p}{\partial \rho}\right|_{S=\text{const}} \delta\rho + \delta S \qquad \text{with generally} \quad p = p(\rho, S),$$

$$u^\mu = \frac{1}{a(\eta)}\left(\delta^\mu_0 + \sum_{r=1}^{\infty}\frac{1}{r!}v^\mu_{(r)}\right).$$

$\delta S$ is the entropic perturbation, $\left.\frac{\partial p}{\partial \rho}\right|_{S=\text{const}} = c_s^2$ is the squared adiabatic speed of sound, which comes from the equation of state between $p$ and $\rho$, and, again, $v^i_{(r)}$ can be split into

$$v^i_{(r)} = \partial^i v^S_{(r)} + v^{i,V}_{(r)} \quad \text{with} \quad \partial_i v^{i,V}_{(r)} = 0.$$

An interesting remark is that, thanks to the normalization $u^\mu u_\mu = g_{\mu\nu}u^\nu u^\mu = -1$ which holds at every perturbative order, we can determine $v^\mu_{(r)}$ as a function of the metric perturbations. For instance, at linear order we have $v^0_{(1)} = -\psi^{(1)}$; notice then that, for a comoving observer, $u^\mu = (1/a, 0)$.

Let us now go back to the gauge problem for a moment.

Consider again the diffeomorphism $x^\mu \longmapsto x'^\mu = x^\mu - \xi^\mu(x)$; without losing any generality, we can write

$$\xi^\mu = \left(\xi^0, \xi^i\right) = (a, \partial^i \beta + d^i) \qquad \text{with} \quad \partial_i d^i = 0.$$

We have 4 degrees of freedom: 2 coming from the scalars $a$ and $\beta$, and 2 from the vector $d^i$ (3-1 as we imposed the divergence free condition). Thus, choosing (or fixing) a gauge means to impose 2 conditions on the scalar perturbations and a condition on the vector perturbations.

In order to give an example, we can apply rule (2.1) on the cosmological perturbation of the energy density $\rho(\mathbf{x}, t)$:

$$\rho \quad \longrightarrow \quad \widetilde{\delta\rho} = \delta\rho + \mathcal{L}_\xi[\rho_0].$$

The Lie-derivative of a scalar quantity is simply

$$\mathcal{L}_\xi[\rho_0] = D_\mu \rho_0 \xi^\mu = \partial_\mu \rho_0 \xi^\mu = \rho_0' a,$$

where we used the fact that the background energy density $\rho_0$ depends only on (conformal) time and the notation $' \equiv \partial/\partial\eta$. So we have

$$\widetilde{\delta\rho} = \delta\rho + \rho_0' a.$$

It may be educational to show a couple of particular gauge choices:

- *Poisson gauge*

$$\text{scalars} \begin{cases} \omega^S = 0 \\ \chi^S = 0 \end{cases} \quad ; \quad \text{vector} \left\{ \chi_i^V = 0 \right. \quad .$$

  This is one of the most used gauge and it is also known as (conformal) Newtonian gauge, longitudinal gauge, or orthogonal zero shear gauge. The last name descends from the fact that, in this gauge, the geometrical shear $\sigma$ defined by

$$\sigma \equiv -\omega^S + \frac{\chi^S}{2}$$

  is null;

- *uniform density gauge*

$$\delta\rho = 0 \quad \text{in general} \quad \Longrightarrow \quad \widetilde{\delta\rho} = 0 = \delta\rho + \rho_0' a,$$

  which consequently fixes

$$\alpha = -\frac{\delta\rho}{\rho_0'}.$$

Notice that this condition is general in the sense that it is imposed on the Lie-dragged perturbation and not on the starting perturbation.

Let us now get to the point of this whole argument. We have said that in general the value of a cosmological perturbation can change according to a chosen gauge, and this is essentially what the gauge problem is. However, a physical observable cannot depend on a gauge choice, therefore there must exist some quantities which are *gauge-invariant*. By a quick study on the degrees of freedom, it is easy to see that one should seek 2 gauge-invariant combinations for scalars and 1 for vectors.

We will focus on a particular scalar gauge-invariant quantity which will represent an extremely interesting subject of study in the next Chapters as it possesses a very useful property. We are talking about the *curvature perturbation* on uniform density hyper-surfaces, indicated by $\zeta$ and defined by [20]

$$\zeta^{(1)} \equiv -\widehat{\psi}^{(1)} - \frac{a'}{a}\frac{\delta^{(1)}\rho}{\rho_0'},$$

where $\widehat{\psi}^{(1)} \equiv \psi^{(1)} + (1/6)\nabla^2\chi^S$ is another curvature perturbation of the metric.

We are interested in finding an evolution equation at linear order for the curvature perturbation $\zeta$. In order to ease the calculation we can take advantage of its gauge-invariance property and write it in the uniform density gauge:

$$\delta\rho = 0 \quad \Longrightarrow \quad \zeta = -\widehat{\psi},$$

where we omitted the superscript $(1)$ everywhere. From the temporal component of the continuity equation $D_\mu T^\mu_0$ at linear order then one gets [20]

$$\zeta' = -\frac{a'}{a}\frac{\delta p_{\text{non adiabatic}}}{\rho_0 + p_0} - \frac{1}{3}\nabla^2(V+\sigma) = 0,$$

where $V \equiv v^S + \omega^S$ and $\delta p_{\text{non adiabatic}}$ is the non-adiabatic perturbation to the pressure, which can be also seen as a perturbation to the entropy; notice that the adiabatic component $c_s^2\delta\rho = 0$ in the uniform density gauge.

Here comes the interesting part: trying to solve the evolution equation in Fourier space, $\nabla^2$ becomes $k^2$, which is negligible on super-horizon scales, since $k \ll aH$; then, if we have only adiabatic perturbations, we finally obtain:

$$\zeta' = 0 \qquad \Longrightarrow \qquad \zeta = \text{const.}$$

Therefore, after this curvature perturbation $\zeta$ is created in the inflatory epoch, it remains constant once it exits the horizon until it re-enters during radiation or, more likely, matter dominated epoch. This is indeed a remarkable result because it means that not only $\zeta$ is a gauge-invariant variable but it is

something that 'keeps memory' of physical processes acting in the very first moments of life of the Universe. Moreover, we will see that $\zeta$ characterizes the fluctuations amplitude during inflation and that's why our attention should now move from cosmological perturbations to perturbations of the scalar field $\varphi$ driving the inflationary process.

## 2.3 Quantum fluctuations of a scalar field

Perturbations to $\varphi$ appear in the form of quantum fluctuations $\delta\varphi$; first of all, we shall start by inserting the splitting of the scalar field (1.10) into the equation of motion (1.11) in order to obtain the equations for the fluctuations:

$$\begin{cases} \delta\ddot{\varphi} + 3H\delta\dot{\varphi} - \frac{1}{a^2}\nabla^2\delta\varphi = -V''\delta\varphi \\ \ddot{\varphi}_0 + 3H\dot{\varphi}_0 = -\frac{\partial V}{\partial\varphi_0}. \end{cases} \tag{2.2}$$

What we are interested in is find an expression for the modulus of the perturbation $|\delta\varphi|$ (which is precisely what will be converted in CMB anisotropies) but, of course, we must solve the first equation in (2.2) before. We use the very powerful tool represented by the Fourier expansion:

$$\delta\varphi(\mathbf{x}, t) = \int \frac{\mathrm{d}^3\mathbf{k}}{(2\pi)^3}\delta\varphi_{\mathbf{k}}(t)e^{i\mathbf{k}\cdot\mathbf{x}}.$$

Note that

- the Fourier integral is 3-dimensional and not 4-dimensional because symmetries in the RW metric are intended only on its spatial part;
- the plane wave expansion $e^{i\mathbf{k}\cdot\mathbf{x}}$ can be used because we consider a space-time with curvature $k = 0$.[1]

Thus, (2.2) becomes then

$$\delta\ddot{\varphi}_{\mathbf{k}} + 3H\delta\dot{\varphi}_{\mathbf{k}} + \frac{k^2}{a^2}\delta\varphi_{\mathbf{k}} = -V''\delta\varphi_{\mathbf{k}}. \tag{2.3}$$

Solutions to this equation can be sought in different simplified cases, to make some of the terms of the equation above negligible in respect with the others. However, we want to remain as general as possible so we are going to consider

- scalar field $\varphi$ with a mass $m_\varphi \neq 0$:

$$m_\varphi^2 = V'' \ll H^2 \quad \Longrightarrow \quad \eta = \frac{V''}{3H^2} = \frac{m_\varphi^2}{3H^2} \ll 1;$$

[1] Have we considered a curved space-time, we should have used solutions of the Hellmotz equations instead of plane waves:

$$\nabla^2 Q_{\mathbf{k}} + k^2 Q_{\mathbf{k}} = 0,$$

where $\nabla^2$ is the curved Laplacian.

- quasi De-Sitter expansion phase:

$$H \ncong \text{const.} \quad \Longrightarrow \quad \dot{H} = -\varepsilon H^2 \ll 1.$$

The solution to (2.3) will depend on a particular perturbation mode $\mathbf{k}$ to which we can associate a comoving wavelength $\lambda = 2\pi/k$. To make things simpler, recalling Fig. 1.4.3, we can imagine to set two borderline cases:

1) SUB-HORIZON REGIME
   For physical scales that are smaller than the Hubble radius: $\lambda_{\text{phys}} \ll H^{-1}$

$$\lambda_{\text{phys}} = a\lambda \sim \frac{a}{k} \quad \Longrightarrow \quad k \gg aH;$$

2) SUPER-HORIZON REGIME
   For physical scales that are greater than the Hubble radius: $\lambda_{\text{phys}} \gg H^{-1}$

$$\lambda_{\text{phys}} = a\lambda \sim \frac{a}{k} \quad \Longrightarrow \quad k \gg aH.$$

Now, note that $\delta\varphi$ is a comoving quantity, so if we want a physical quantity we must consider $\delta\widehat{\varphi} = a\delta\varphi$. Being a quantum fluctuation, we can write $\delta\widehat{\varphi}$ in terms of creation and annihilation operators $a_{\mathbf{k}}$ and $a_{\mathbf{k}}^\dagger$ and then Fourier expand it:

$$\delta\widehat{\varphi}(\eta, \mathbf{x}) = \int \frac{\mathrm{d}^3\mathbf{k}}{(2\pi)^3} \left[ u_{\mathbf{k}}(\eta) a_{\mathbf{k}} e^{i\mathbf{k}\cdot\mathbf{x}} + u_{\mathbf{k}}^*(\eta) a_{\mathbf{k}}^\dagger e^{-i\mathbf{k}\cdot\mathbf{x}} \right], \tag{2.4}$$

with

i) $u_{\mathbf{k}}(\eta)$ = classical functions of $\mathbf{k}$ and $\eta$ with the normalization,
   $u_{\mathbf{k}}(\eta)^* u_{\mathbf{k}}(\eta)' - u_{\mathbf{k}}(\eta) u_{\mathbf{k}}(\eta)^{*'} = -i$ (primes denotes derivatives w.r.t. $\eta$);

ii)
$$\begin{cases} a_{\mathbf{k}}|0\rangle = 0 & \forall \mathbf{k} \\ \langle 0|a_{\mathbf{k}}^\dagger = 0 & \forall \mathbf{k} \end{cases} \qquad \begin{cases} [a_{\mathbf{k}}, a_{\mathbf{k}'}] = [a_{\mathbf{k}}^\dagger, a_{\mathbf{k}'}^\dagger] = 0 \\ [a_{\mathbf{k}}, a_{\mathbf{k}'}^\dagger] = \hbar\delta^{(3)}(\mathbf{k} - \mathbf{k}') \end{cases};$$

iii) vacuum choice of Bunch-Davies: for a scalar field on a curved space-time we demand that the flat case is restored on very small scales, that is

$$u_{\mathbf{k}}(\eta) \xrightarrow[k \gg aH]{} \frac{e^{ik\eta}}{\sqrt{2k}}.$$

It is then customary to rewrite equation (2.3) in terms of the $u_{\mathbf{k}}(\eta)$ functions; with some easy algebra

one finds:

$$\begin{cases} u_{\mathbf{k}}(\eta_c)'' + \left(k^2 - \frac{\nu^2 - \frac{1}{4}}{\eta_c^2}\right) u_{\mathbf{k}}(\eta_c) = 0 \\ \nu^2 \simeq \frac{9}{4} + 3\varepsilon - 3\eta, \end{cases} \tag{2.5}$$

where conformal time is indicated with $\eta_c$ to distinguish it from the slow roll parameter $\eta$. Notice that $\nu$ is the parameter that takes into account the corrections terms coming from the little mass of $\varphi$ and the fact that the expansion phase is not De-Sitter, but quasi; in particular, in the simplest case where the field is massless and the expansion is perfect De-Sitter, $\varepsilon = 0 = \eta$ and $\nu^2 = 9/4$.

Solutions to (2.5) that one finds, without entering the technical details of the procedure, correspond to an oscillating $\delta\varphi$ at sub-horizon scales whereas $\delta\varphi \simeq$ const. at super-horizon scales [20]. After the horizon crossing the fluctuation no longer propagates and its amplitude remains constant; basically, it is a gravitational amplification mechanism and the modes once inside the horizon are then stretched outside of it, until they re-enter the horizon during radiation or matter dominated epoch.

Finally, recalling that $\delta\varphi = \delta\widehat{\varphi}/a \sim u_{\mathbf{k}}/a$ we can give the main result of this paragraph:

$$\left|\delta\varphi_{\mathbf{k}}\right| \simeq \frac{H}{\sqrt{2k^3}} \left(\frac{k}{aH}\right)^{\frac{3}{2}-\nu}. \tag{2.6}$$

Notice that in the simplified case when $\nu^2 = \frac{9}{4}$ the term in round brackets is just 1. The moment of horizon crossing of the fluctuations corresponds, in the momentum space, to the condition $k = aH$.

## 2.4 Power spectrum of cosmological perturbations

When we split the field in (1.10) we said that vacuum expectation value of its fluctuation is zero, i.e. $\langle\delta\varphi\rangle = 0$; this descends from the fact that the origin of the perturbation is of quantum nature. However, $\langle\delta\varphi^2\rangle \neq 0$ in general and we want to have a rough idea of what it is.

Since the creation of fluctuations is a statistic process, we will find extremely useful the *two points correlation function* for a scalar field:

$$\langle 0|\delta\varphi(\mathbf{x}, t)\delta\varphi(\mathbf{x} + \mathbf{r}, t)|0\rangle \equiv \xi(\mathbf{x}, \mathbf{x} + \mathbf{r}, t).$$

Actually, $\delta\varphi$ is an operator so the process of averaging over the vacuum state is necessary if we want a stochastic variable. Going more general, we can consider a perturbation $\delta(\mathbf{x}, t)$ which may be a perturbation in the scalar field $\varphi$ or a primordial energy density perturbation $\delta\rho/\rho(\mathbf{x}, t)$. As usual, it is very convenient to move into the Fourier space:

$$\delta(\mathbf{x}, t) = \int \frac{\mathrm{d}^3\mathbf{k}}{(2\pi)^3} \delta_{\mathbf{k}}(t) e^{i\mathbf{k}\cdot\mathbf{x}}.$$

Let us now assume that our system is isotropic so that the function $\xi$ depends only on the difference of the coordinates of the two chosen points $\mathbf{x} - (\mathbf{x} - \mathbf{r}) = \mathbf{r}$.Therefore, in the Fourier space, the two

points correlation function takes the form

$$\langle \delta_{\mathbf{k}_1} \delta_{\mathbf{k}_2} \rangle = (2\pi)^3 P(k_1) \delta^{(3)}(\mathbf{k}_1 + \mathbf{k}_2), \tag{2.7}$$

where $k_1$ is the modulus of the vector $\mathbf{k}_1$ and $P(k_1)$ is the *power spectrum*, a quantity that measures the amplitude of the fluctuations at a given scale $k$. The property of isotropy is reflected by the fact that the power spectrum depends on $k_1$ and not on $\mathbf{k}_1$, while the presence of the Dirac delta function $\delta^{(3)}(\mathbf{k}_1 + \mathbf{k}_2)$ introduces also a translation invariance, i.e. homogeneity. Notice that, according to our definition (2.7), we are implying that $P(k)$ is the Fourier transform of the correlation function $\xi$.

Another interesting statistic quantity is the variance

$$\langle \delta(x)^2 \rangle = \int_0^\infty \mathrm{d} \ln k \Delta^2(k) \qquad \text{with} \quad \Delta^2(k) \equiv \frac{k^3}{2\pi^2} P(k)$$

and $\Delta^2(k)$ is the *dimensionless power spectrum*; recalling that $k = 2\pi/\lambda$ is the wave number, we see that $P(k)$ has dimension of length cubed and then it gives the probe scale of the fluctuations.

We shall now enter a specific case for our discussion and consider the power spectrum for the inflaton fluctuations.

The object we are interested in is the correlation function $\langle 0 | \delta\varphi_{\mathbf{k}_1} \delta\varphi^*_{\mathbf{k}_2} | 0 \rangle$ where $\delta\varphi_{\mathbf{k}}$ is written in term of creation and annihilation operators $a_{\mathbf{k}}$ and $a^\dagger_{\mathbf{k}}$. Using the properties in ii) of the (2.4) we have

$$\langle 0 | \delta\varphi_{\mathbf{k}_1} \delta\varphi^*_{\mathbf{k}_2} | 0 \rangle = (2\pi)^3 |\delta\varphi_{\mathbf{k}_1}|^2 \delta^{(3)}(\mathbf{k}_1 - \mathbf{k}_2),$$

where we used that $\delta\varphi^*_{\mathbf{k}_2} = \delta\varphi_{-\mathbf{k}_2}$. The power spectrum $P(k)$ generated by the perturbations associated with the inflaton is precisely $|\delta\varphi_{\mathbf{k}_1}|^2$ and the dimensionless version of it can be obtained directly from the definition of $\Delta(k)$ and (2.6):

$$\Delta^2_{\delta\varphi}(k) \equiv \frac{k^3}{2\pi^2} P(k) = \frac{k^3}{2\pi^2} \frac{H^2}{2k^3} \left( \frac{k}{aH} \right)^{3-2\nu} = \left( \frac{H}{2\pi} \right)^2 \left( \frac{k}{aH} \right)^{3-2\nu}. \tag{2.8}$$

It is interesting to evaluate such quantity at the horizon crossing:

$$\Delta^2_{\delta\varphi}(k) \Big|_{k=aH} = \left( \frac{H}{2\pi} \right)^2 \Bigg|_{k=aH},$$

and the dependence on the mode $k$ is hidden in the time of horizon crossing $t_H(k)$ at which we calculate the Hubble constant $H$.

In order to better study the shape of the power spectrum $\Delta(k)$, it is customary to introduce the *spectral index n*

$$n - 1 \equiv \frac{\mathrm{d} \ln \Delta^2(k)}{\mathrm{d} \ln k};$$

- if $n$ =const., meaning that it does not depend on $k$, the spectrum is a power law:

$$\Delta^2(k) = \Delta^2(k_0) \left( \frac{k}{k_0} \right)^{n-1}, \tag{2.9}$$

where $k_0 = 0.002\ \mathrm{Mpc}^{-1}$ is a common pivot scale;

- if $n = 1$, $\Delta^2(k)$ is the Harrison-Z'eldovich spectrum:
  it is a scale invariant spectrum in the sense that there is no fluctuation dependence on the cosmological scale.

We can now benefit from one of the many great results of the inflation theory. In fact, the so-called *method of formalism* $\delta N$ [21] permits us to understand how quantum fluctuation in an expanding Universe $\delta\varphi$ gave birth to the primordial energy density perturbation $\delta\rho/\rho$.

Considering the number of e-folds and the fact that $H \simeq$const. during inflation we have

$$N = \int_{t_I}^{t_F} H(t)\mathrm{d}t \qquad \longrightarrow \qquad \delta N \simeq H\delta t.$$

It can be seen [20] that there is a temporal shift in the fluctuations $\delta t = -\delta\varphi/\dot{\varphi}_0$ in the sense that different points of the Universe experience the same history but at slightly different times, as the acceleration rate may vary from point to point. Then, since the inflaton dominates the energy density during the inflationary epoch, it is easy to see that

$$\delta N \simeq H\delta t = -H\frac{\delta\varphi}{\dot{\varphi}_0} \simeq -H\frac{\delta\rho}{\dot{\rho}}.$$

This is where the curvature perturbation quantity $\zeta$ comes into play. Thanks to its gauge-invariancy, we can write it in the spatially flat gauge where $\widehat{\psi}^{(1)} = 0$ so that:

$$\zeta = \delta N = -H\frac{\delta\varphi}{\dot{\varphi}_0} \simeq -H\frac{\delta\rho}{\dot{\rho}}. \tag{2.10}$$

Therefore, thanks to the fact that $\zeta \simeq$const. on super horizon scales, we can see that it is really tied to primordial inhomogeneities; for instance, if we assume that a particular comoving mode $\lambda$ re-enters the horizon during radiation dominated epoch, it can be easily proved that the inhomogeneities generated by quantum fluctuations $\delta\varphi$ are anisotropies $\delta T/T$ in the CMB. Fig. 2.4.1 can be helpful to visualize that.

Of course, from the dynamics equations we can see that the type of primordial perturbation generated is strictly related to the shape of the potential $V(\varphi)$, i.e. to the model of inflation considered.

With the relation (2.10) it is then possible to calculate the Power Spectrum for the curvature perturbation; some simple algebra leads us to

$$\Delta^2_\zeta(k) \simeq \frac{H^2}{\dot{\varphi}^2}\Delta^2_{\delta\varphi}(k)\bigg|_{t_H(k)} = \left(\frac{H^2}{2\pi\dot{\varphi}}\right)^2\bigg|_{t_H(k)},$$

with $t_H(k)$ the time at which the mode $k$ exits the horizon.

Interestingly, for the spectral index of $\Delta^2_\zeta(k)$, a straightforward calculation leads to the relation

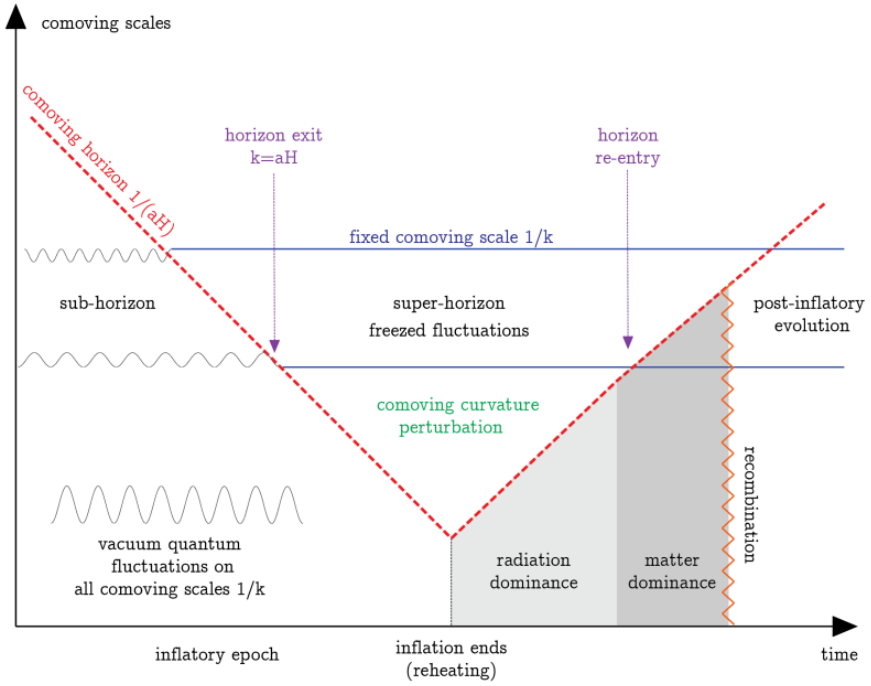


**Figure 2.4.1:** Evolution on super-horizon scales of a perturbation mode $\lambda$.

$$n_s - 1 = 2\eta - 6\varepsilon,$$

where we remind that $\eta$ and $\varepsilon$ are the two slow-roll parameters. If $n_s > 1$, the spectrum presents a 'blue-tilt' meaning that perturbations have more power on smaller scale, whereas if $n_s < 1$ the spectrum has a 'red-tilt' and the perturbations have less power on smaller scale. Notice that deviation from unity of $n_s$ is as tiny as important because it indicates an inflationary dynamics. We should also mention that more recent theories and experiments take into account the possibility that the spectral index is not scale invariant but presents a running, i.e. :

$$\frac{dn_s}{d\ln k} \neq 0.$$

However, we will not consider any running for $n_s$, also because otherwise we would have to change the shape of the power spectrum (2.9).

Since we are talking about power spectrum, before ending this section we should mention that also tensor perturbation produce their own spectrum $\Delta_T^2(k)$. These perturbation are an inevitable consequence of every inflationary models, they indeed would be created as vacuum fluctuation in the same way as the energy density perturbations. Tensor perturbations to the metric appear to us in the form of primordial gravitational waves, characterized by two degrees of freedom that propagate as two minimally coupled massless scalar fields. In fact, it can be proved that tensor perturbations and scalar quantum fluctuations behave similarly: they are both almost constant outside the horizon (see, e.g. [22]) and start to oscillate and decay once they enter it; this variation of amplitude generates anisotropies and polarization in the CMB. Gravitational waves were first guessed by Einstein himself as solutions to the

Einstein Equations in vacuum and their recent discovery made GR an even more robust theory.

We will not be interest in the metric tensor perturbations for more than concerns the fact that also their spectrum can be described by a spectral index $n_T$ which satisfies the relation

$$n_T = \frac{\mathrm{d}\ln \Delta_T^2}{\mathrm{d}\ln k} = -2\varepsilon.$$

Usually, from the comparison with observations in the CMB, it is convenient to introduce the ratio

$$r \equiv \frac{\Delta_T^2}{\Delta_\zeta^2}.$$

Single field slow roll inflationary models predict the consistency relation ('the holy grail of inflation')

$$r = 16\varepsilon = -8n_T,$$

which does not actually depend on the particular model considered. If experimentally verified, this relation would be an unequivocal prove for the inflationary theory since it does not exist another mechanism that can produce such relation. This is of course a very demanding task because one should measure $r$ and $n_T$ separately.

## 2.5 Current constraints on Cosmological Parameters

We have now all the ingredients to finally give the most recent constraints on the six parameters we mentioned at the very beginning of this work and that parameterize the ΛCDM fiducial model. We said that they are a total number of six but there is a high degree of arbitrariness on which six parameters are picked out. The ones we consider are:

- baryon density parameter $\Omega_b$;
- dark matter density parameter $\Omega_c$;
- scalar spectral index $n_s$;
- curvature fluctuation amplitude $\Delta_\zeta^2(k_\circ)$;
- reionization optical depth $\tau$;
- angular scale of the sound horizon at last-scattering $\theta_*$.

Without entering the details, we limit to say that the choice is based on what particular analysis techniques are enforced and this is also why they may be presented in more convenient expressions, for instance the angular scale of the sound horizon at last-scattering is listed as $\theta_{MC}$ that approximates $\theta_*$ in the CosmoMC code.

**Table 2.5.1:** Parameter 68% confidence limits for the base ΛCDM model from *Planck* CMB power spectra+lensing.

| Parameter | Value |
|---|---|
| $\Omega_b h^2$ | $0.02230 \pm 0.00014$ |
| $\Omega_c h^2$ | $0.1188 \pm 0.0010$ |
| $n_s$ | $0.9667 \pm 0.0040$ |
| $\ln\left(10^{10}\Delta^2_\zeta\left(k_0\right)\right)$ | $3.064 \pm 0.023$ |
| $\tau$ | $0.066 \pm 0.012$ |
| $100\theta_{MC}$ | $1.04093 \pm 0.00030$ |

Current constraints on the parameters can be found in one of the latest *Planck* collaboration releases [7] and are given in Table 2.5.1. Calculations have been made in combination with lensing reconstruction at 68% confidence limits.

Notice that not only the six parameters are arbitrary, but other parameters can be derived from them according to what is the topic studied and what quantities are kept fixed. For example, in [7] we can also find a constraint on the tensor-to-scalar ratio $r$:

$$r_{0.002} < 0.11 \qquad \text{at} \quad 95\% \quad \text{CL.}$$

The subscript on $r$ refers to the pivot scale $k_0$ in $\text{Mpc}^{-1}$. For *Planck*, $r_{0.002}$ is usually quoted, since a pivot scale of $0.002\ \text{Mpc}^{-1}$ is closer to the scale at which there is some sensitivity to tensor modes in the large-angle temperature power spectrum.

The list is quite long but we end it here as in the next chapters we are going to focus on different subjects which are of much more interest for us.

# 3

# Beyond the Standard Model

In this Chapter we are going to analyze two main features of the Cosmic Microwave Background Radiation that, in some ways, go beyond the Standard Model in Cosmology: *spectral distortions* and *primordial non-Gaussianity (NG)*.

The measurements of COBE/FIRAS have shown that the CMB spectrum is extremely close to a perfect black-body. There are, however, a number of processes in the early Universe that should create deviations from the black-body, i.e. spectral distortions, at a level which is within reach of present day/near future technology [23]. Accurate descriptions and understanding of the CMB spectral distortions can in fact lead us to a new world into the physics of inflation. We will firstly introduce the subject, describing what spectral distortions are and why they are important, and then we will focus on particular type: the so called $\mu$ (i.e. chemical potential)-type of distortions. They arise from dissipation (Silk damping) of acoustic waves on very small-scale range unexplored so far, namely $0.6\ \text{kpc} \lesssim \lambda \lesssim 1\ \text{Mpc}$ (or multipoles $10^5 \lesssim \ell \lesssim 10^8$) [24]. For our purposes, we will derive an analytic estimate for the $\mu$-distortion and the associated power spectrum.

In the second instance, we will take into consideration primordial non-Gaussianity in the CMB. There can be a wealth of information that is contained in deviations from a perfectly Gaussian distribution for the primordial perturbations - [3], [20], [25], [26] and [27] just to mention a few. In fact, cosmological measurements of primordial NG are a powerful way to bring us closer to the ultimate goal of particle physics, which is to determine the action (i.e. the fields, symmetries and couplings) as a function of energy scale. At low energies, $E < 1$ TeV, physics is completely described by the Standard Model of particle physics; whereas, to probe the physics at energy scales far exceeding the TeV scale, which will explain the inflationary era in the early Universe or be relevant for alternatives to inflation, we are likely

to require cosmological data.

Since the observed cosmological perturbations are of the order of $10^{-5}$, one might think that first-order perturbation theory will be adequate for all comparison with observations. Actually, things have changed as we have now reached a generation of satellite, starting from *Planck*, that are sensitive up to the second or higher order in the cosmological perturbations, hence to their level of non-Gaussianity [4]. Such level is tested on various cosmological scales through statistical properties like the *bispectrum* and the *trispectrum* of the CMB, which can also determine if the NG comes from secondary anisotropies or systematic effects [28], [29]. Accurate theoretical predictions for the statistics of CMB anisotropies can therefore convey fundamental information on primordial perturbations originated during or right after inflation.

We will end this Chapter by mentioning a few practical examples that will help us to better understand how primordial non-Gaussianity signals are generated in different inflationary models.

## 3.1 Spectral Distortions

The Cosmic Microwave Background temperature and polarization anisotropies provide the most stringent and robust constraints to theoretical models, allowing us to determine the key parameters of our Universe and address fundamental questions about inflation and early-Universe physics. But the CMB holds another, complementary and independent piece of invaluable information: its frequency spectrum. In particular, departures of the CMB frequency spectrum from a black-body are of paramount interest; they are commonly referred to as *spectral distortions* and encode information about the thermal history of the early Universe, from when it was a few month old until today [23]. As we have already anticipated, since the measurements with COBE/FIRAS, the average CMB spectrum is known to be extremely close to a perfect black-body, with possible distortions being limited to $\Delta I_\nu / I_\nu \lesssim 10^{-5} - 10^{-4}$. This impressive measurement, together with the discovery of anisotropy in the CMB, was awarded the Nobel prize in Physics 2006, and already rules out cosmologies with extended periods of significant energy release, disturbing the thermal equilibrium between matter and radiation in the early Universe.

No average CMB distortion was actually found, but it is still interesting to think about CMB spectral distortions since there is a long list of processes that could lead to them. These include both pre-and post-recombination epoch standard sources of distortions. The former, at high redshifts, are: cooling by adiabatically expanding ordinary matter, heating by decaying or annihilating relic particles, evaporation of primordial black holes and superconducting strings, dissipation of primordial acoustic modes and magnetic fields, cosmological recombination radiation; the latter, at low redshifts, are: signatures due to first supernovae and their remnants, shock waves arising due to large-scale structure formation, Sunyaev-Zel'dovich effect from clusters and effects of reionization and other exotic processes. Most importantly, many of these processes are part of our cosmological Standard Model and therefore should lead to guaranteed signals to search for.

Another reason for spectral distortion being interesting is due to technological advances. Proposed experimental concepts like PIXIE (Primordial Inflation Explorer) [2] and PRISM (Polarized Radiation

Imaging and Spectroscopy Mission) [1] may dramatically improve, in the future, our knowledge of the CMB spectrum, which is still in a similar state as more than 20 years ago. These types of experiments could possibly enhance the limits of COBE/FIRAS by more than three orders of magnitude, providing a unique way to learn about processes that are otherwise hidden from us. CMB spectral distortions posses indeed an immense potential which is becoming more and more recognized by the Cosmology community.

The energy spectrum of the CMB tells the tale about the thermal history of the Universe at very early times, well before any structures had formed and when the baryonic matter and radiation were tightly coupled via Compton scattering. It is well known that any perturbation of the full thermodynamic equilibrium between photons and baryons in the early Universe inevitably leads to spectral distortions in the CMB. However, the memory of any event which injects energy into the electromagnetic plasma is quickly erased in this thight coupling regime (apart from the change in the temperature of the plasma and the photons), through the process of thermalization.

At early times, i.e. for $z \gg 10^6$, the Universe is well described by a hot photon-baryon plasma. The number density of photons $n(\nu)$ per frequency interval is given to very high accuracy by the Planckian black-body spectrum

$$n_P(\nu) = \frac{1}{e^x - 1},$$

where $\nu$ is the photon frequency, $T$ is the temperature of the electromagnetic plasma and, in natural units, $x \equiv \nu/T$ is the dimensionless frequency. The equation that describes the subsequent evolution of the photon number density is the full Boltzmann equation, which, when restricted to Compton scattering, is known as the Kompaneet's equation. This equation has three interesting regimes:

- before $z \simeq z_{\mu,i} \equiv 2 \times 10^6$ any energy released into the photon-baryon plasma is quickly thermalized by elastic and double Compton scattering $e^- + \gamma \rightarrow e^- + 2\gamma$, which are still very efficient. The end result is again a black-body spectrum with now a higher $T$ and a larger total number of photons $N$. After $z_{\mu,i}$, double Compton scattering, as well as bremsstrahlung, becomes less efficient and the total number of photons is approximately frozen;

- for $z \gtrsim z_{\mu,f}$, with $z_{\mu,f} \equiv 5 \times 10^4$, equilibrium is still achieved after an energy injection due to elastic Compton scattering $e^- + \gamma \rightarrow e^- + \gamma$, but since this process does not change the number of photons the end result is a Bose-Einstein distribution, i.e.

  $$n_{BE}(\nu) = \frac{1}{e^{x+\mu(x)} - 1},$$

  where $\mu$ is a frequency dependent chemical potential, already rescaled by $T$ so that it is dimensionless. The Kompaneet's equation shows that $\mu(x)$ deviates from a constant only at very low frequencies, i.e. $\mu(x) = \mu_0 e^{-x_c/x}$, with $x_c \simeq 5 \times 10^{-3}$. Henceforth we can approximate $\mu$ as constant, which is valid everywhere except deep in the Rayleigh-Jeans tail ($\nu \rightarrow 0$). Distortions created in this period are called $\mu$-type;

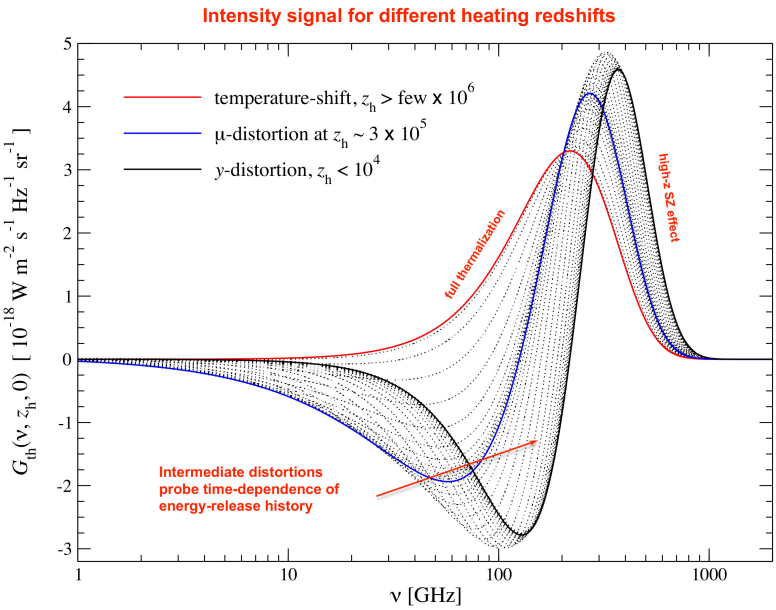


**Figure 3.1.1:** Energy releases at different heating redshifts $z_h$ alter the CMB spectrum. At $z \gtrsim$ few $\times\ 10^6$, there is a temperature shift. Pure $\mu$ and $y$ spectral distortions appear, respectively, around $z \simeq 3 \times 10^5$ and at at $z \lesssim 10^4$. Intermediate distortions, which are neither $\mu$ nor $y$ but a superposition of the two of them, contain information about the time dependency of the process that releases energy (Picture taken from [23]).

- finally for $z \lesssim z_{\mu,f}$ even Compton scattering is not efficient enough to establish kinetic equilibrium between matter and radiation. The distortion created after this moment is known as $y$-type and is relevant for example for the Sunyaev-Zel'dovich effect (a mechanism generating secondary anisotropies in the CMB via inverse Compton scattering when photons travel across a ionized gas, typically inside a cluster of galaxies).

Of course this is a simplified picture since there is no sharp transition between one regime and the next. It was shown that the distortion signature from different energy-release scenarios is generally not just given by a superposition of pure $\mu$- and $y$-distortion. From Fig. 3.1.1 we see that the small residual beyond $\mu$- and $y$-distortion contains information about the exact time-dependence of the energy-release history.

Using future CMB spectroscopy, some interesting scenarios from inflation can be constrained. For more in depth reading and overview we refer to [30], [31], [32], [33] and [34]; a few examples, just to illustrate the potential of CMB spectral distortions [23], are: reionization and structure formation, decay and annihilation of long-lived relic particles with lifetimes $t_X \simeq 10^9\text{sec} - 10^{10}\text{sec}$, shape of the small-scale power spectrum if the amplitude of primordial curvature perturbations exceeds $\Delta^2_\zeta(k) \simeq$ few $\times\ 10^{-8}$ at wavenumber $k \simeq 45\text{Mpc}^{-1}$ and cosmological recombination of hydrogen and helium[1]. More recently, it has been also demonstrated that measurements with a PIXIE-like experiment could

[1]Notice that without improvements accounting for several previously omitted atomic physics and radiative transfer effects in the recombination calculation, the value for $n_s$ would be biased by $\Delta n_s \simeq -0.01$ to $n_s \simeq 0.95$ instead of $n_s \simeq 0.96$. In other words, we would be discussing different inflation models without these corrections.

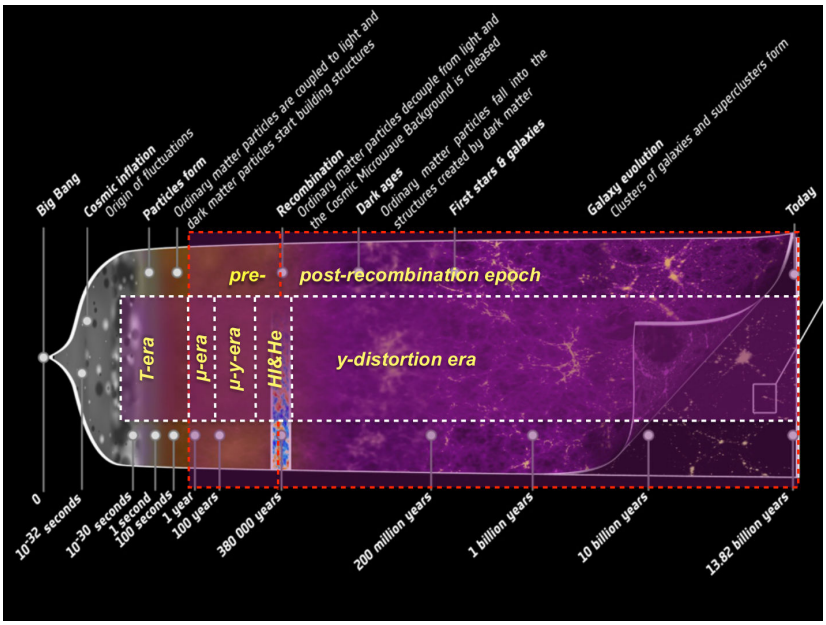


**Figure 3.1.2:** Thermal history of the Universe during pre- and post-recombination era is probed by CMB spectral distortions. Energy release at $z \gtrsim$ few $\times\, 10^6$ only causes a change of the CMB temperature. $\mu$-type and $y$-type distortions arises, respectively, from energy release at $3 \times 10^5 \lesssim z \lesssim$ few $\times\, 10^6$ and $z \lesssim 10^4$. A superposition of $\mu$- and $y$-distortion is created at $10^4 \lesssim z \lesssim 3 \times 10^5$). In the recombination era, $10^3 \lesssim z \lesssim 10^4$, atomic transitions of hydrogen and helium cause additional spectral features (Picture taken from [23]).

provide constraints on gravitino decay and the scale of inflation [35] as well as dark matter interactions with Standard Model particles [36].

CMB spectral distortions measurements thus provide a unique way for studying early-Universe models and particle physics at very different stages of the Universe, as indicated in Fig. 3.1.2.

Recent works (see, e.g. [37], [31] and [24]) developed efficient methods for computing the CMB spectral distortions and we are getting to a more and more precise understanding of the energy-release processes mentioned above. For instance, information from intermediate distortions, which are neither pure $\mu$ nor pure $y$ but a superposition of the two of them, can be used to study the time dependency of processes occurring at $10^4 \lesssim z \lesssim 3 \times 10^5$, allowing us to build an exact energy-release scenario. There are also effects from pre-recombination (i.e. at $z \gtrsim 10^3$) atomic transitions that can make the thermalization problem even richer; $\mu$- and $y$-eras can be in fact deeper investigated by studying the spectrum of the cosmological recombination radiation.

In this thesis, we will focus exclusively on the $\mu$-type distortions and how they can be used to probe primordial non-Gaussianity, as we are going to see in the next Chapter. Being interested in analytical estimates, we will take the period responsible for their creation to be $5 \times 10^4 \equiv z_{\mu,f} \lesssim z \lesssim z_{\mu,i} \equiv 2 \times 10^6$. We will see that the dependence on the size of this interval is logarithmic and so, even if we change the values for $z$ by factors of order unity, the main results will not be altered. Nevertheless, it should be clear that if one is looking for precise predictions, a numerical study of the system is needed.

We know very little about primordial curvature perturbations on scales smaller than about a Mpc and measurements of the $\mu$-type distortion of the CMB spectrum provide the unique opportunity to probe these scales over the unexplored range from 50 to $10^4$ Mpc$^{-1}$ [3]. It is very hard to find accurate probes of the initial conditions of our Universe since most of the scales specifying the probability distribution function of the adiabatic mode have evolved in a complicated and often non-linear way until today. However, CMB radiation together with large scale structures today, which still have not entered a fully non-linear regime, represent two notable exceptions. Because Silk damping on the one side and complicated non-linear dynamics on the other, both probes are useful only at scales of order a Mpc or larger.

We have seen that the physics of the processes that inject energy into the electromagnetic plasma is very rich. For our purposes, we will be interested in the energy injection coming from the dissipation of acoustic waves of the adiabatic mode, basically a Silk damping, as these re-enter the horizon and start oscillating. For the moment, our working assumption here is that either all other sources lead to a smaller and therefore negligible distortion, as it is the case if the primordial power spectrum is not too red tilted, or that all other relevant effects are understood with a high enough precision to be subtracted off leaving the $\mu$-distortion caused by Silk damping as the only signal.

The primordial perturbations excite standing sound waves in the tightly coupled baryon-photon fluid as they enter the horizon. The mean free path of the photons for Thomson scattering on free electrons is very small during this time, they can however still diffuse to scales larger than the ones given by this mean free path by doing a random walk in the sea of electrons. The diffusion damping scale $k_D(z)$ is given during the radiation dominated era by (including both thermal conductivity and radiative viscosity) [6]:

$$\begin{aligned} k_D(z) &= \left[\int_0^\eta \mathrm{d}\eta' \frac{1+z}{6(1+R)n_e\sigma_T}\left(\frac{R^2}{1+R}+\frac{16}{15}\right)\right]^{-1/2} \\ &\simeq (1+z)^{3/2} 4.1\times 10^{-6}\mathrm{Mpc}^{-1}, \end{aligned}$$

where $R \equiv 3\rho_b/4\rho_\gamma$, $\rho_b$ is the baryon energy density, $\rho_\gamma$ is the photon energy density, $\sigma_T$ is the Thomson cross section, $n_e(\eta)$ is the electron number density and, of course, $\eta$ in conformal time. Notice that the diffusion (or dissipation) scale depends on the gravitational redshift $z$ and we have

$$\begin{aligned} k_D(z_{\mu,i}) &\simeq 1.1\times 10^4 \mathrm{Mpc}^{-1}, \\ k_D(z_{\mu,f}) &\simeq 46 \mathrm{Mpc}^{-1}. \end{aligned}$$

The photon diffusion erases the perturbations on the diffusion scales, moving the energy in the perturbations or sound waves into the local CMB monopole spectrum, giving a chemical potential to the spectrum.

Now, following [38], [39] and [37], we derive a formula which relates the late time $\mu$-distortion to the

primordial curvature perturbations $\zeta$; in order to do that, let us start by defining a deformation parameter $\mu(\mathbf{x})$ which depends on the position in space $\mathbf{x}$.

From the Bose-Einstein distribution properties together with the fact that the total number of photons is constant it can be shown that an amount of energy (density) $\delta E$ released into the photon-baryon plasma gives

$$\mu \simeq 1.4 \frac{\delta E}{E}.$$

In order to consider the energy injection due to damping of acoustic waves, let us recall that the energy density in acoustic waves in the photon-baryon plasma (neglecting the baryon energy density) is

$$Q = \frac{\rho_\gamma \langle \delta_\gamma(\mathbf{x})^2 \rangle_p c_s^2}{1 + c_s^2},$$

where $c_s^2 \sim 1/3$ is sound speed squared and $\delta_\gamma \equiv \delta\rho_\gamma/\overline{\rho_\gamma}$ is the dimensionless perturbation in the photon density at position $\mathbf{x}$ averaged over a period (indicated by $\langle\rangle_p$ to differentiate it from the quantum/ensemble average $\langle\rangle$).

Then one has

$$\frac{\delta E}{E} \simeq -\int_{z_{\mu,i}}^{z_{\mu,f}} \frac{\mathrm{d}}{\mathrm{d}z}\frac{Q}{\rho_\gamma} \simeq \frac{1}{4}\langle \delta_\gamma(\mathbf{x})^2 \rangle_p \Big|_{z_{\mu,f}}^{z_{\mu,i}}. \tag{3.1}$$

One can perform the following Fourier space expansion

$$\delta_\gamma(\mathbf{x}) = \frac{1}{(2\pi)^3}\int \mathrm{d}^3\mathbf{k} e^{i\mathbf{k}\cdot\mathbf{x}} \widetilde{\delta_\gamma}(\mathbf{k}) = \frac{1}{(2\pi)^3}\int \mathrm{d}^3\mathbf{k} e^{i\mathbf{k}\cdot\mathbf{x}} \zeta_\mathbf{k} \Delta_\gamma(k).$$

Notice that the fundamental relation between $\mu$-distortion and the primordial curvature perturbation $\zeta_\mathbf{k}$ lies in the quantity $\widetilde{\delta_\gamma}(\mathbf{k})$, as it can be directly connected to the primordial quantity $\zeta_\mathbf{k}$ via the transfer function $\Delta_\gamma(k)$. Intuitively, a good approximation is to write it as an oscillating term times a decreasing exponential term which mimics a process of Silk damping [40]:

$$\Delta_\gamma(k) \simeq 3\cos(kr) e^{-k^2/k_D^2},$$

where, using that the baryon-to-photon ratio $R \ll 1$, [3]

$$kr = \int_0^t \frac{k\mathrm{d}t'}{a\sqrt{3(1+R)}} \simeq \frac{kt}{a\sqrt{3}},$$

with $r$ a physical distance so that the combination inside the cosine $kr$ is dimensionless.

We are now ready to evaluate (3.1):

$$\begin{aligned}\langle\delta_\gamma(\mathbf{x})^2\rangle_p &= 1.45\left\langle\frac{1}{(2\pi)^3}\int \mathrm{d}^3\mathbf{k}_1 e^{i\mathbf{k}_1\cdot\mathbf{x}}\zeta_{\mathbf{k}_1}\Delta_\gamma(k_1)\frac{1}{(2\pi)^3}\int \mathrm{d}^3\mathbf{k}_2 e^{i\mathbf{k}_2\cdot\mathbf{x}}\zeta_{\mathbf{k}_2}\Delta_\gamma(k_2)\right\rangle_p \\ &= 1.45\int\frac{\mathrm{d}^3\mathbf{k}_1\mathrm{d}^3\mathbf{k}_2}{(2\pi)^6}\zeta_{\mathbf{k}_1}\zeta_{\mathbf{k}_2}\langle\Delta_\gamma(k_1)\Delta_\gamma(k_2)\rangle_p e^{i(\mathbf{k}_1+\mathbf{k}_2)\cdot\mathbf{x}}.\end{aligned}$$

The numerical coefficient 1.45 has been added a posteriori as a term that adds the contribution of neutrinos [39]. An important remark is due here: we can see that $\mu \sim \langle\delta_\gamma^2\rangle_p$ is not linear but it is intrinsically of second order in the primordial curvature perturbation $\zeta$; we shall bear this fact in mind for what we are about to see in the next Chapter.

Therefore, the deformation parameter $\mu(\mathbf{x})$ is related to $\zeta$ by

$$\begin{aligned}\mu(\mathbf{x}) &\simeq 1.4\frac{\delta E}{E} \simeq \frac{1.4}{4}\langle\delta_\gamma(\mathbf{x})^2\rangle_p\Big|_{z_{\mu,f}}^{z_{\mu,i}} \\ &= \frac{1.4}{4}1.45\int\frac{\mathrm{d}^3\mathbf{k}_1\mathrm{d}^3\mathbf{k}_2}{(2\pi)^6}\zeta_{\mathbf{k}_1}\zeta_{\mathbf{k}_2}\int\mathrm{d}^3\mathbf{k}_3\delta^{(3)}\left(\sum_{n=1}^3\mathbf{k}_n\right)\langle\Delta_\gamma(k_1)\Delta_\gamma(k_2)\rangle_p\Big|_{z_{\mu,f}}^{z_{\mu,i}} \\ &\qquad e^{-i\mathbf{k}_3\cdot\mathbf{x}}W\left(\frac{k_3}{k_s}\right) \\ &= 4.6\int\frac{\mathrm{d}^3\mathbf{k}_1\mathrm{d}^3\mathbf{k}_2}{(2\pi)^6}\zeta_{\mathbf{k}_1}\zeta_{\mathbf{k}_2}\int\mathrm{d}^3\mathbf{k}_3\delta^{(3)}\left(\sum_{n=1}^3\mathbf{k}_n\right)\langle\cos(k_1 r)\cos(k_2 r)\rangle_p \\ &\qquad \left[e^{-(k_1^2+k_2^2)/k_D^2(z)}\right]_{z_{\mu,f}}^{z_{\mu,i}} e^{-i\mathbf{k}_3\cdot\mathbf{x}}W\left(\frac{k_3}{k_s}\right). \qquad (3.2)\end{aligned}$$

$W(k_3/k_s)$ is the Fourier transform of the top-hat filter

$$W(x) \equiv 3\frac{j_1(x)}{x},$$

which accounts for the fact that $\mu$ arises from a thermalization process and smears the dissipated energy over a volume of radius $k_s^{-1} \gtrsim k_{D,f}^{-1}$.

Having the CMB revealed itself compatible with a black-body so far, the bound on $\mu$-distortion put by COBE/FIRAS is $|\mu| < 9\times10^{-5}$, whereas a PIXIE-like experiment could achieve $\Delta_\mu \simeq 10^{-8}$ at 1-$\sigma$ [2].

It is interesting to estimate the vacuum expectation value, that is the quantum/ensemble average, of $\mu(\mathbf{x})$:

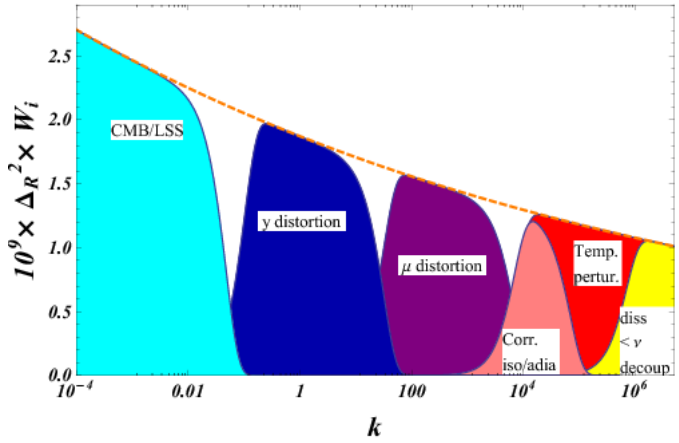


**Figure 3.1.3:** The different k-space windows responsible for different observables. The CMB anisotropies are visible at $k \lesssim 0.1\ \mathrm{Mpc}^{-1}$, where the smale-scale cut-off is introduced by Silk damping. The purple area indicated by $\mu$ is the difference of the power spectrum (including the window function $W_\mu$) between $z_{\mu,i}$ and $z_{\mu,f}$. Once integrated over $\log k$ this gives the $\mu$-distortion. $R = -\zeta$ is an alternative variable to indicate the primordial curvature perturbation (Picture taken from [27]).

$$\langle \mu(\mathbf{x}) \rangle \simeq 4.6 \int \frac{\mathrm{d}^3\mathbf{k}_1 \mathrm{d}^3\mathbf{k}_2}{(2\pi)^6} \langle \zeta_{\mathbf{k}_1} \zeta_{\mathbf{k}_2} \rangle \int \mathrm{d}^3\mathbf{k}_3 \delta^{(3)} \left( \sum_{n=1}^{3} \mathbf{k}_n \right) e^{-i\mathbf{k}_3 \cdot \mathbf{x}} W\left(\frac{k_3}{k_s}\right) \langle \cos(k_1 r) \cos(k_2 r) \rangle_p \left[ e^{-(k_1^2+k_2^2)/k_D^2(z)} \right]_{z_{\mu,f}}^{z_{\mu,i}}.$$

We can take $k_s$ to be $k_D(z_f)$ as we are interested in a lower bound on the $\mu$ distortion, then the function $W(k_3/k_s)\left[e^{-(k_1^2+k_2^2)/k_D^2(z)}\right]_{z_{\mu,f}}^{z_{\mu,i}}$ filters the squeezed limit $k_1, k_2 > k_D(z_f) > k_3$, i.e. $W(k_3/k_s) \simeq 1$ and $e^{-i\mathbf{k}_3 \cdot \mathbf{x}} \simeq 1$:

$$\langle \mu(\mathbf{x}) \rangle \simeq 2.3 \int \frac{\mathrm{d}^3\mathbf{k}_1 \mathrm{d}^3\mathbf{k}_2}{(2\pi)^6} (2\pi)^3 \delta^{(3)}(\mathbf{k}_1 + \mathbf{k}_2) \frac{2\pi^2 \Delta_\zeta^2(k_1)}{k_1^3} \left[ e^{-(k_1^2+k_2^2)/k_D^2(z)} \right]_{z_{\mu,f}}^{z_{\mu,i}},$$

where, as customary, we used the estimate $\langle \cos(k_1 r) \cos(k_2 r) \rangle_p \simeq 1/2$. We also employed the definitions

$$\langle \zeta_{\mathbf{k}_1} \zeta_{\mathbf{k}_2} \rangle \equiv (2\pi)^3 \delta^{(3)}(\mathbf{k}_1 + \mathbf{k}_2) P_\zeta(k),$$
$$P_\zeta(k) \equiv \frac{2\pi^2 \Delta_\zeta^2(k)}{k^3},$$

which descend directly from (2.7) when the perturbation considered is the primordial curvature $\zeta$ that generates the power spectrum $P_\zeta(k)$. The dimensionless power spectrum $\Delta_\zeta^2(k)$ is a power law exactly like the one in (2.9):

$$\Delta^2_\zeta(k) = \Delta^2_\zeta(k_\circ)\left(\frac{k}{k_\circ}\right)^{n_s-1},$$

with $\Delta^2_\zeta(k_\circ) \simeq 2.142 \times 10^{-9}$, taken directly from Table 2.5.1. We remind that we are not considering any running for $n_s$.

Thus, we finally obtain:

$$\begin{aligned}\langle\mu(\mathbf{x})\rangle &\simeq 2.3\int \frac{\mathrm{d}^3\mathbf{k}}{4\pi}\frac{\Delta^2_\zeta(k)}{k^3}\left[e^{-2k^2/k_D^2(z)}\right]^{z_{\mu,i}}_{z_{\mu,f}}\\ &= 2.3\int \mathrm{d}\log k\Delta^2_\zeta(k)\left[e^{-2k^2/k_D^2(z)}\right]^{z_{\mu,i}}_{z_{\mu,f}}.\end{aligned} \tag{3.3}$$

To visualize this, in Fig. 3.1.3 we plot the power spectrum with Silk damping probed at different scales by different observables. The purple-filled region quantifies the amount of dissipated energy and hence $\mu$-distortion. Interestingly, it is the usual log$k$-integration of a power spectrum coming from a cosmological perturbation and appearing in the variance of the cosmological perturbation, now with an extra window term, which reminds us that $\mu$-distortions occur only at small scales. Evaluating the expression (3.3) using a scale invariant spectrum, i.e. $n_s = 1$ and $\Delta^2_\zeta(k) = \Delta^2_\zeta(k_\circ) = 2.142 \times 10^{-9}$, yields to $\langle\mu\rangle \simeq 2.7 \times 10^{-8}$.

## 3.2 Primordial non-Gaussianity in the CMB

Simple inflationary models predict that the CMB anisotropy field is nearly Gaussian with random phases, and that two-point statistics completely specify statistical properties of CMB. However, our Universe may not be so simple and there may be deviations from a pure Gaussian statistics in the mechanism chosen by Nature to produce the structures we see today. Said deviations could give rise to non vanishing higher-order connected correlation functions of CMB anisotropies, i.e., using the curvature perturbation $\zeta$ as a parameter:

$$\langle\zeta_{\mathbf{k}_1}\zeta_{\mathbf{k}_2}\cdots\zeta_{\mathbf{k}_n}\rangle = (2\pi)^3\delta^{(3)}(\mathbf{k}_1+\mathbf{k}_2+\cdots+\mathbf{k}_n)S(\mathbf{k}_2,\cdots,\mathbf{k}_n),$$

where $S(\mathbf{k}_2,\cdots,\mathbf{k}_n)$ is the *polyspectrum* and is defined as the Fourier transform of the $n$-point correlation function $\xi$:

$$S(\mathbf{k}_2,\cdots,\mathbf{k}_n) \equiv \int \mathrm{d}^3\mathbf{x}_2\cdots\mathrm{d}^3\mathbf{x}_n e^{-i(\mathbf{k}_2\cdot\mathbf{x}_2+\cdots+\mathbf{k}_n\cdot\mathbf{x}_n)}\xi(\mathbf{x}_2,\cdots,\mathbf{x}_n).$$

Notice that, because of homogeneity, the polyspectrum only depends on $n$-1 out of the $n$ wavevectors in the $n$-point function. Remind that if the fluctuation is Gaussian, then the two–point correlation function specifies all the statistical properties of $\zeta_{\mathbf{k}}$, for all odd-$n$ polyspectra vanish and the two–point correlation function is the only parameter left.

Potential probes of the physics of generating the primordial fluctuations are represented by the first

two higher order statistics: the three-point correlation function in Fourier space, called *bispectrum*, and the four-point correlation function in Fourier space, the *trispectrum*. Since gravitationally induced non-linearities are small at $z_* \sim 1300$, CMB is expected to be the best probe of the *primordial non-Gaussianity* [41]. The adjective 'primordial' descends from the fact that we are considering non-Gaussianity (NG), i.e. non-linearity, in the primordial curvature perturbation $\zeta$ produced in the very early Universe by inflation (or an alternative). Both the functional form, i.e. the *shape*, and strength of the bispectrum and the trispectrum are model dependent, therefore constraints on different inflationary scenarios can be obtained by fitting their predicted bispectrum and trispectrum shapes to the data, and extracting the corresponding amplitude parameters $f_{NL}$ (for the bispectrum), $g_{NL}$ and $\tau_{NL}$ (for the trispectrum).

The first inflation-motivated primordial NG model to be considered in the literature was the so called *local model*, which is characterized by the following ansatz in real space [28]

$$\zeta(\mathbf{x}) = \zeta_g(\mathbf{x}) - \frac{3}{5} f_{NL}^{loc} \left( \zeta_g(\mathbf{x})^2 - \langle \zeta_g^2 \rangle \right) + \frac{9}{25} g_{NL}^{loc} \left( \zeta_g(\mathbf{x}) \right)^3 ,$$

where $\zeta_g$ is the Gaussian part of the curvature perturbation field and the NG components are local functionals of the Gaussian part. At linear order during the matter-dominated epoch and on large scales $\zeta = -5/3\phi$ and this fixes the coefficient $3/5$ in front of the $f_{NL}^{loc}$ parameter. One can also consider models in which $\zeta_g$ is modulated by a second, uncorrelated, Gaussian field $\sigma$, giving rise to a $\tau_{NL}^{loc}$ trispectrum:

$$\zeta(\mathbf{x}) = \zeta_g(\mathbf{x}) + \sqrt{\tau_{NL}^{loc}} \sigma(\mathbf{x}) \zeta_g(\mathbf{x}).$$

As we just mentioned, different primordial models can generate a large variety of different bispectrum and trispectrum shapes, and to each of them correspond different NG amplitudes.

The focus of our work will however be specifically on local-type bispectra, i.e. we will consider the case when $g_{NL}^{loc} = 0 = \tau_{NL}^{loc}$.

A crucial aspect when considering NG of the primordial type is that it suffers from contamination by other non-linear effects which mimic a three-point correlation function similar in shape to the primordial one. Namely, different sources for a non-Gaussian CMB [42] are:

1) second-order non-Gaussianity: arising from non-linearities in the transfer function relating $\zeta$ to the CMB temperature anisotropy $\Delta T/T$ at recombination;

2) secondary non-Gaussianity: generated by 'late' time effect after recombination (e.g. lensing);

3) foreground non-Gaussianity: created by galactic and extra-galactic sources.

which are generated during inflation by substantially two classes of mechanisms:

i) quantum-mechanical effects at or before horizon exit;

ii) classical non-linear evolution after horizon exit.

All of these sources contribute to the observed signal and it is important to understand them both theoretically and empirically. Only if we understand the secondary non-Gaussianity well enough can we hope to extract the primordial signal reliably. Having said that, for the remainder of this work we will focus entirely on the microphysical origin of primordial non-Gaussianity and a contamination like the one in point 2) given by a particular term in the temperature anisotropy at second order (Sachs-Wolfe effect).

Let us now examine a bit more the primordial bispectrum, which is important since it represents the lowest order statistics able to distinguish non–Gaussian from Gaussian perturbations. We start from the definition

$$\langle \zeta_{\mathbf{k}_1} \zeta_{\mathbf{k}_2} \zeta_{\mathbf{k}_3} \rangle \equiv B(\mathbf{k}_1, \mathbf{k}_2, \mathbf{k}_3).$$

For perturbations around an FRW background, the momentum dependence of the bispectrum simplifies considerably: because of homogeneity, or translation invariance, the bispectrum is proportional to a delta function of the sum of the momenta, $B(\mathbf{k}_1, \mathbf{k}_2, \mathbf{k}_3) \propto \delta^{(3)}(\mathbf{k}_1 + \mathbf{k}_2 + \mathbf{k}_3)$, i.e. the sum of the momentum 3-vectors must form a closed triangle. Because of isotropy, or rotational invariance, the bispectrum only dependence on the magnitudes of the momentum vectors, but not on their orientations, so we obtain:

$$B(\mathbf{k}_1, \mathbf{k}_2, \mathbf{k}_3) = (2\pi)^3 \delta^{(3)}(\mathbf{k}_1 + \mathbf{k}_2 + \mathbf{k}_3) B(k_1, k_2, k_3).$$

If the bispectrum is scale-invariant, its shape only depends on two ratios of $k_i$'s, say $x_2 \equiv k_2/k_1$ and $x_3 \equiv k_3/k_1$:

$$B(k_1, k_2, k_3) = k_1^{-6} B(1, x_2, x_3).$$

These two variables $x_2$ and $x_3$ define a plane with all possible configurations for the modulus of $\mathbf{k}_1$, $\mathbf{k}_2$ and $\mathbf{k}_3$; we can see from Fig. 3.2.1 that there are three particular configurations to which we usually refer to:

- *squeezed*: $k_2 \sim k_3 \gg k_1$;
- *equilateral*: $k_1 = k_2 = k_3$;
- *folded*: $k_1 = k_2 + k_3$ (and cyclic).

Going into details, the bispectrum of local non-Gaussianity (see, e.g., [44]) is found to be:

$$\begin{aligned} B_{loc}(k_1, k_2, k_3) &= \left( -\frac{6}{5} f_{NL}^{loc} \right) \times [P_\zeta(k_1) P_\zeta(k_2) + 2 \text{ perm's}] \\ &= \left( -\frac{6}{5} f_{NL}^{loc} \right) A^2 \left( \frac{1}{k_1^{4-n_s} k_2^{4-n_s}} + 2 \text{ perm's} \right), \end{aligned}$$

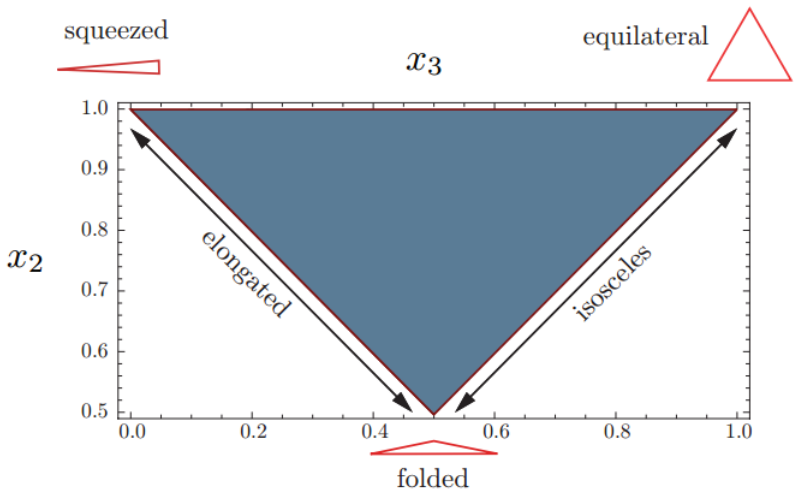


**Figure 3.2.1:** Momentum configurations of the bispectrum in terms of the two ratios $x_2 \equiv k_2/k_1$ and $x_3 \equiv k_3/k_1$. The fact that the sum of the momentum 3-vectors must form a closed triangle comes from the presence of the Dirac delta $\delta^{(3)}(\mathbf{k}_1+\mathbf{k}_2+\mathbf{k}_3)$ in the definition of $B(\mathbf{k}_1, \mathbf{k}_2, \mathbf{k}_3)$ (Picture taken from [43]).

where in the second line we assumed a weak scale dependent spectrum like the one in (2.9), $P_\zeta(k) = A/k^{4-n_s}$ with $A$ the normalization and $n_s$ the scalar spectral index.

Notice the presence of two permutations: they come from the fact that in the three-point correlation function $\langle \zeta_{\mathbf{k}_1} \zeta_{\mathbf{k}_2} \zeta_{\mathbf{k}_3} \rangle$, the second order correction in the $\zeta(\mathbf{k})$ is taken into account, by turns, in the first, in the second and in the third place. Moreover, the bispectrum is proportional to the magnitude of the parameter $f_{NL}^{loc}$ and, similarly, if we had considered a first order, Gaussian, correlation we would have obtained $\langle \zeta_g(\mathbf{k}_1)\zeta_g(\mathbf{k}_2)\zeta_g(\mathbf{k}_3)\rangle = 0$.

Without loss of generality, let us order the momenta such that $k_1 \leq k_2 \leq k_3$. The bispectrum for local non-Gaussianity is then largest in the squeezed limit, i.e. when $k_1 \ll k_2 \sim k_3$; by momentum conservation, the other two momenta are then nearly equal and the bispectrum takes the form:

$$\lim_{k_1 \ll k_2 \sim k_3} B_{loc}(k_1, k_2, k_3) = \left(-\frac{6}{5} f_{NL}^{loc}\right) \cdot 2 \cdot P_\zeta(k_1) P_\zeta(k_2). \tag{3.4}$$

There is an important statement on how the local non-Gaussianity can be used to distinguish inflation models [45]:

> *a detection of a large local non-Gaussian component in the bispectrum can rule out all single field inflation models.*

The size of local non-Gaussianity which can be detected with high confidence level in the near future is $f_{NL}^{loc} \gg 1$. By single field inflation models, we include not only the slow-roll single field models with Bunch-Davies vacuum, but also all other inflation models that have one field responsible for both the inflation and creation of curvature perturbation. The statement is based on Maldacena's consistency condition for the single field models ([46], [45]), that relates a particular geometrical limit of the 3-point function of density perturbations to the spectrum and tilt of the 2-point function:

$$\lim_{k_1\to 0}\langle\zeta_{\mathbf{k}_1}\zeta_{\mathbf{k}_2}\zeta_{\mathbf{k}_3}\rangle = -(2\pi)^3\delta^{(3)}\left(\sum_{i=1}^{3}\mathbf{k}_i\right)(n_s-1)P_\zeta(k_1)P_\zeta(k_2).$$

By a comparison with (3.4) we can immediately see that $f_{NL}^{loc} \sim n_s - 1$, which is of order the slow-variation parameter $\mathcal{O}(\varepsilon) \sim \mathcal{O}(0.01)$ at the leading and non-oscillatory order. Therefore these models predict very small local non-Gaussianity.

Notice that the derivation of this condition relies on a very general assumption: for single field, the only effect of a long wavelength mode on short wavelength modes is to provide a constant rescaling of the background scale factor. In fact, it is easy to see [47] that the effect of a background wave is exactly balanced by a coordinate transformation.

It can be proved that also higher-derivative corrections during inflation can lead to large non-Gaussianities [4]. A key characteristic of derivative interactions is that they are suppressed when any individual mode is far outside the horizon. This suggests that the bispectrum is maximal when all three moves have wavelengths equal to the horizon size. The bispectrum therefore has a shape that peaks in the equilateral configuration, $k_1 = k_2 = k_3$. The CMB analysis that searches for these signals uses the following template for the bispectrum formula [48]:

$$B_{equil}(k_1,k_2,k_3) = -\frac{18}{5}A^2 f_{NL}^{equil}\left[-\frac{1}{k_1^{4-n_s}k_2^{4-n_s}} - \frac{1}{k_2^{4-n_s}k_3^{4-n_s}} - \frac{1}{k_3^{4-n_s}k_1^{4-n_s}} - \frac{2}{(k_1k_2k_3)^{2(4-n_s)/3}} + \left(\frac{1}{k_1^{(4-n_s)/3}k_2^{2(4-n_s)/3}k_3^{4-n_s}} + 5\text{ perm's}\right)\right],$$

which is also obtained starting from a weak scale dependent power spectrum $P_\zeta(k) = A/k^{4-n_s}$.

Finally, a third shape can be introduced by considering that the CMB may be truly non-Gaussian but was searched with the wrong bispectra templates. As we explained above, assuming isotropy, the shape function depends only on two momentum ratios $x_2 \equiv k_2/k_1$ and $x_3 \equiv k_3/k_1$ and we can define the scalar product of two different shapes $B_1$ and $B_2$ as

$$B_1 \cdot B_2 \equiv \int_{\mathcal{V}} B_1(x_2,x_3)B_2(x_2,x_3)\mathrm{d}x_2\mathrm{d}x_3,$$

where the integrals are only over physical momenta satisfying the triangle inequality: $0 \leq x_2 \leq 1$ and $1 - x_2 \leq x_3 \leq 1$. Thus, there exist a phenomenological shape that is orthogonal to both the local and equilateral templates [49], i.e. $B_{ortho} \cdot B_{loc} = B_{ortho} \cdot B_{equil} \equiv 0$:

$$B_{ortho}(k_1,k_2,k_3) = -\frac{18}{5}A^2 f_{NL}^{ortho}\left[-\frac{3}{k_1^{4-n_s}k_2^{4-n_s}} - \frac{3}{k_2^{4-n_s}k_3^{4-n_s}} - \frac{3}{k_3^{4-n_s}k_1^{4-n_s}} - \frac{8}{(k_1k_2k_3)^{2(4-n_s)/3}} + \left(\frac{3}{k_1^{(4-n_s)/3}k_2^{2(4-n_s)/3}k_3^{4-n_s}} + 5\text{ perm's}\right)\right],$$

**Table 3.2.1:** Latest constraints obtained by *Planck* measurements of CMB temperature (T) and temperature+polarization (T+E) data. Results are at 68% CL.

| | T | T+E |
|---|---|---|
| $f_{NL}^{loc}$ | $2.5 \pm 5.7$ | $0.8 \pm 5.0$ |
| $f_{NL}^{equil}$ | $-16 \pm 70$ | $-4 \pm 43$ |
| $f_{NL}^{ortho}$ | $-34 \pm 33$ | $-26 \pm 21$ |

which peaks in the folded limit $k_1 = k_2 + k_3$ (and cyclic) and, just like the equilateral shape, emerges in models characterized by more general higher-derivative interactions.

Currently, the most stringent constraint on the primordial non-Gaussianity parameters comes from *Planck* measurements of the CMB temperature and polarization bispectra [4]; results are given at 68% CL and are summarized in Table 3.2.1. We separately show the constraints obtained first from the temperature data alone (T) and then combining temperature and polarization data (T+E). Notice that, unfortunately, $f_{NL}^{loc}$ and $f_{NL}^{equil}$ are still compatible with 0 in both measurements.

### Non-Gaussianity from inflation

As we said, different classes of inflationary models generate a distinctive NG signal. Within each class a common underlying physical process gives rise to the corresponding NG shape, illustrated by concrete realizations of inflationary models. Following primarly [4] and [20], we are now going to illustrate some of the most pedagogic and common examples, but, of course, the list is much more longer.

#### 1.General single-field models of inflation

This class of models includes inflationary models with a non-standard kinetic term (or more general higher-derivative interactions), in which the inflaton fluctuations propagate with an effective sound speed $c_s$ which can be smaller than the speed of light. For example, models with a non-standard kinetic term are described by an inflaton Lagrangian $\mathcal{L} = P(X, \phi)$, where $X = g^{\mu\nu}\partial_\mu\phi\partial_\nu\phi$, with at most one derivative on $\phi$, and the sound speed is given by

$c_s^2 = (\partial P/\partial X)/(\partial P/\partial X + 2X(\partial^2 P/\partial X^2))$.

Since usually there are two dominant interaction terms of the inflaton field giving rise to the overall NG signal, there are two characteristic NG shapes in this class of models: the *equilateral* and the *orthogonal*, which we already saw.

The higher-derivative operators considered are of the form $X^n/\Lambda^{4n-4}$ and, in principle, they could lead to strong interactions. In fact, non derivative operators such as $\phi^n/\Lambda^{n-4}$ form part of the inflaton potential and are therefore strongly constrained by the background. In other words, the existence of a slow-roll phase requires the non-Gaussianity associated with these operators to be small.

For instance, the leading correction to the slow-roll Lagrangian $P_{s.r.}((\partial\phi)^2, \phi)$ is

$$P(X,\phi) = P_{\rm s.r.}((\partial\phi)^2,\phi) + \frac{X^2}{8\Lambda^4}.$$

Physically well-motivated examples of the $P(X,\phi)$-model are provided by Dirac-Born-Infeld (DBI)inflationary models based on string theory. They are characterized by an almost equilateral NG with $f_{NL}^{equil} = -(35/108)c_s^{-1}$ for $c_s \ll 1$, which typically is $f_{NL}^{equil} < -5$.

Furthermore, equilateral and orthogonal shapes emerge also in models characterized by more general higher-derivative interactions, such as ghost inflation, effective field theories of inflation, or the so 'Galileon-like' models of inflation. The latter model is constructed starting from some specific underlying symmetry for the inflaton field, and is characterized by strongly constrained derivative interactions.

### 2.The curvaton scenario

In order to generates initially adiabatic perturbation deep in the radiation era, the curvaton mechanism represents an alternative to the standard scenario described in the previous sections. In fact, in the curvaton scenario the cosmological perturbations are produced from quantum fluctuations of a light scalar field $\sigma$ (different from the inflaton) during a period of inflation, in the case where the perturbations from the inflaton field $\phi$ are considered to be negligible. The scalar field is sub-dominant during inflation and thus its fluctuations are initially of isocurvature type, i.e. a curvature perturbation is sourced on large scales. The curvature perturbation will become relevant when the energy density of the curvaton field is a significant fraction of the total energy. This happens after the end of inflation when the curvaton field begins to oscillate around the minimum of its potential once its mass has dropped below the Hubble rate, behaving like non-relativistic matter. Finally, well before primordial nucleosynthesis, the curvaton field is supposed to completely decay into thermalized radiation thus generating a final adiabatic perturbation. From this epoch onwards the 'standard' radiation dominated phase takes place.

The curvaton mechanism produces a bispectrum that peaks in the squeezed limit; in the (simplest) adiabatic models, when the curvaton field has a quadratic potential, the local $f_{NL}$ parameter was found to be

$$f_{NL}^{loc} = \frac{5}{4r_D} - \frac{5}{6}r_D - \frac{5}{3},$$

where $r_D = 3\rho_{\rm curvaton}/(3\rho_{\rm curvaton} + 4\rho_{\rm radiation})$ is the 'curvaton decay fraction' evaluated at the epoch of the curvaton decay in the sudden decay approximation. It is then easy to see that, for low values of $r_D$, a high level of NG can be generated.

Notice that, in order to achieve an $f_{NL}^{loc} = 2.5 \pm 5.7$ (68% CL), one would need $r_D \gtrsim 0.15$ at 95% CL.

### 3. The inhomogeneous reheating scenario

This mechanism acts during the reheating stage after inflation and can be also found with the name 'modulated reheating'. As in the curvaton scenario, it is supposed that the perturbations coming from the inflaton fluctuations are negligible. To reheat the Universe the inflaton has to couple to ordinary

particles and has to decay into radiation with a decay rate $\Gamma$ which depends on the couplings of the inflaton field. In the standard scenario of inflation such a coupling is constant, i.e. $\delta\Gamma = 0$. In fact it may be determined by the vacuum expectation value of fields $\chi$'s of the underlying theory. It could be the case of supersymmetric theories or theories inspired by superstrings, with the scalar fields $\chi$'s being some scalar super-partner or the so-called moduli fields. If those fields are light during inflation fluctuations $\delta\chi \sim H/2\pi$, where $H$ is the Hubble rate during inflation, are left imprinted on super-horizon scales. These perturbations lead to spatial fluctuations in the decay rate $\Gamma$ of the inflaton field to ordinary matter

$$\frac{\delta\Gamma}{\Gamma} \sim \frac{\delta\chi}{\chi} \neq 0,$$

thus producing fluctuations in the radiation and in the reheating temperature in different regions of the Universe. These fluctuations are of isocurvature type and will be converted into curvature fluctuations after reheating, once the thermalized radiation starts do dominate the energy density.

Unsurprisingly, also in this case we find a bispectrum of the local shape, as the non-Gaussianity is coming from local non-linearities in real space. Using the $\delta N$ formalism and expanding $\delta\Gamma = \Gamma'\delta\chi + \frac{1}{2}\Gamma''(\delta\chi)^2$ we find

$$f_{NL}^{loc} = 5\left[\frac{\Gamma''\Gamma}{(\Gamma')^2} - 1\right].$$

This can lead to large non-Gaussianity if the dependence of the decay rate on the modulus $\chi$ is non-linear, $\Gamma''\Gamma \gg (\Gamma')^2$.

## 4. Multi-field models

This class of models can be seen as a generalization of the curvaton scenario as it is characterized by the presence of additional light scalar degrees of freedom besides the inflaton. Fluctuations of these fields give rise, or contribute, to the final primordial curvature perturbation at the end of inflation. This includes the case of 'multiple-field inflation', where inflation is driven by more than one scalar field, as well as scenarios in which additional scalar fields remain subdominant during the inflationary expansion.

From the point of view of primordial NG, the element in common to all these models is that a potentially detectable level of NG in the curvature perturbation is generated via a transfer of super-horizon non-Gaussian isocurvature perturbations in the second field (not necessarily the inflaton) to the adiabatic (curvature) density perturbations, accompanied by non-linearities in the transfer mechanism.

In fact, as we may have already pointed out, in the single field models perturbations along inflationary trajectory are 'born' adiabatic and so they are Gaussian because of slow-roll. But when other fields come into play, new isocurvature directions are available and thanks to their arbitrariness they produce non-Gaussian perturbations. The conversion from isocurvature to adiabatic perturbations is provided by the turning of these trajectories, the modulated reheating and the curvaton mechanism.

This process typically takes place on super-horizon scales, thus implying a local form of NG in real space. When going to Fourier space, this leads to a correlation between large and small scale modes.

The bispectrum for this class of models is indeed largest on squeezed triangles, generating a local shape with generally $f_{NL}^{loc} \sim \mathcal{O}(1)$.

Just to have an idea of how this model works, consider inflation with many (scalar) fields; assuming gradient flow, at any point in field space we can compute the number of e-folds $N(\varphi)$ until the adiabatic attractor is reached. On super-Hubble scales, the $\delta N$ formalism gives

$$\zeta = \delta N = \frac{\partial N}{\partial \varphi^I} \delta\varphi^I + \cdots ,$$

so that the observed perturbations come from the gradient of $N(\varphi)$ (Fig. 3.2.2 (a)). Consider then constant $V$ surfaces normal to the gradient $\partial V/\partial\varphi^I \equiv V_{,I}$; in effective single field, the gradients of $V$ and $N$ are parallel, but in multifield models we can define (Fig. 3.2.2 (b))

$$\cos\theta \equiv \frac{\dot{\varphi}^I N_{,I}}{|\dot{\varphi}^I||N_{,I}|}.$$

Notice that, in fact, $\cos\theta \neq 1$ is exactly the definition of multifield.

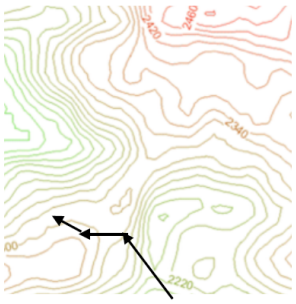

(a) Gradient flow of $N(\varphi)$ in constant N lines

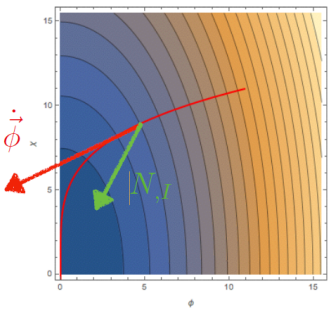


(b) Gradients of constant $N$ (green) and constant $V$ (red) surfaces

**Figure 3.2.2:** Definition of multifield model of inflation.

Before ending, we should report a final remark. We have already seen that a few observables such as isocurvature perturbations and local NG can rule out single fields models, but ruling out the multifield paradigm is more of a demanding task as computing multi-field predictions requires understanding of inflation, reheating, coupling to Standard Model physics and thermalization. Anyway, be aware that one should investigate quite complicated models since there are simple multifield models that produce no local primordial NG, e.g.

$$V(\varphi_1, \varphi_2) = \frac{1}{2} m_1^2 \varphi_1^2 + \frac{1}{2} m_2^2 \varphi_2^2.$$

Thus, in the pessimistic view where $f_{NL}^{loc} < \mathcal{O}(1)$, new single field consistency relations should be tested both for tensors and, more recently, scalars:

$$r = 8 n_T \cos\theta^2,$$
$$f_{NL}^{equil} = \frac{\mathrm{d}n_s}{\mathrm{d}\ln k}.$$

As might be expected, these two relations are extremely challenging to test observationally.

# 4

# Probing primordial non-Gaussianity via CMB spectral distortions

It has finally come the time to get to the heart of the matter. In the previous Chapter we introduce two peculiar features of the CMB, namely spectral distortions and non-Gaussianity, and we are now ready to see how they mix together to convey precious information about the primordial Universe.

In particular, in the context of more futuristic scenarios, the enhancement sensitivity on NG parameters has recently been one of the goals in modern Cosmology. In order to achieve it, three main approaches have been proposed. One is to look at the higher-order correlation functions of full-sky 21-cm radiation surveys, in the redshift range $30 < z < 100$ (e.g., [50]). Another possibility is to study scale-dependent bias in future radio surveys probing high redshifts (e.g., [51]). The third approach, which is the focus of this work, was recently introduced in [3]. It consists in measuring cross-correlations between CMB chemical potential ($\mu$) spectral distortions, arising from dissipation of acoustic waves in the primordial photon-baryon plasma, and temperature anisotropies $\Delta T/T$. As already anticipated and originally pointed out by the authors of [3], the $\mu$T correlation probes the local bispectrum at wavenumbers $50\ \mathrm{Mpc}^{-1} \lesssim k \lesssim 10^4\ \mathrm{Mpc}^{-1}$, i.e. on scales which are unaccessible by CMB temperature or polarization anisotropies, or by any other cosmological probe, including future galaxy and 21-cm surveys.

An ideal, cosmic-variance dominated experiment could extract a very large number of modes in this range of scales, allowing in principle constraints on $f_{NL}^{loc} \lesssim 10^{-3}$ [3] . Moreover, by the same reasoning, cosmic variance dominated $\mu\mu$ measurements could constrain $\tau_{NL}^{loc}$ with an significant level of precision as well. These original findings have been followed by further studies from several groups, showing that $\mu$T correlations could be used to study several other NG signatures besides standard local-type NG.

Recent $f_{NL}^{loc}$ constraints with this technique were obtained in [52] using *Planck* data.

However, notice that there is one interesting primordial NG parameter that $\mu$T and $\mu\mu$ correlations are unable to determine, and it is the $g_{NL}^{loc}$ trispectrum amplitude. It was in fact shown in [28] that $\mu\mu$ correlations are not sensitive to $g_{NL}^{loc}$-type local NG, but it can still be measured by going beyond two-point correlations and using the $TT\mu$ bispectrum. Authors of [28] showed that $TT\mu$ allows to measure not only $g_{NL}^{loc}$, but also to extract additional information on $\tau_{NL}^{loc}$. By a simple Fisher matrix forecast, they concluded that $TT\mu$ bispectrum estimates could in principle allow a sensitivity $\Delta g_{NL}^{loc} = \mathcal{O}(1)$ in the ideal, cosmic variance dominated case. This high level of precision is made possible thanks to the very large number of primordial bispectrum modes that are contained in the $TT\mu$ three-point function.

It is then clear that from $\mu$T cross correlation we can extract plenty of information about primordial NG; but, for the remainder of our work, we will focus only on the $\mu$T local bispectrum shape and one of its possible contamination, which we will see in the next Chapter. In order to ease the notation, we are going to drop the label *loc* of $f_{NL}^{loc}$ as we are not going to consider any other NG shape and so no ambiguity will be present.

## 4.1 $\mu$T CROSS CORRELATION AND PRIMORDIAL NG

In this section we take advantage of the fact that the $\mu$T two-point correlation is proportional to the very squeezed limit of the primordial bispectrum and hence measures $f_{NL}$.

Our first aim is to reproduce formula (16) of [3] in order to give a rigorous derivation and understand every underlying approximation. To gently enter the subject, we start from the case of a scale invariant power spectrum and later on we will introduce a weak scale dependence.

The first result we consider is then the correlation

$$C_\ell^{\mu T} \simeq \frac{2.2 \times 10^{-16}}{\ell(\ell+1)}, \tag{4.1}$$

which directly descends from the general definition

$$\langle a^{\mu}_{\ell_1 m_1} a^{T}_{\ell_2 m_2} \rangle \equiv (-1)^{m_1} \delta^{\ell_2}_{\ell_1} \delta^{-m_2}_{m_1} C^{\mu T}_{\ell_1}. \tag{4.2}$$

In order to relate with the observations, both the direction dependent $\mu$-distortion $\mu(\hat{\mathbf{n}})$ and temperature anisotropy $\Delta T(\hat{\mathbf{n}})$ signals are decomposed in spherical harmonics, an orthonormal basis more appropriate for a 2D field on the surface of a sphere, i. e. the Last Scattering Surface.

The coefficient for the temperature multipoles expansion reads

$$\begin{aligned} a^T_{\ell m} &\equiv \int \mathrm{d}\hat{\mathbf{n}} \Theta(\hat{\mathbf{n}}) Y^*_{\ell m}(\hat{\mathbf{n}}) \\ &= \int \mathrm{d}\hat{\mathbf{n}} \underbrace{\int \frac{\mathrm{d}^3\mathbf{k}}{(2\pi)^3} e^{i\mathbf{k}\cdot r_L \hat{\mathbf{n}}} \Theta(\mathbf{k})}_{\Theta(\hat{\mathbf{n}})} Y^*_{\ell m}(\hat{\mathbf{n}}), \end{aligned} \tag{4.3}$$

where $\Theta(\widehat{\mathbf{n}}) \equiv \Delta T/T(\widehat{\mathbf{n}})$ is the observed temperature anisotropy for a specific direction $\widehat{\mathbf{n}}$ in the sky and $\Theta(\mathbf{k})$ is its Fourier transform.

At first order, the Sachs-Wolfe (SW) limit [53] in Fourier space becomes:

$$\Theta(\mathbf{k}) = \frac{1}{3}\phi_{\mathbf{k}} = \frac{1}{3}\left(-\frac{3}{5}\zeta_{\mathbf{k}}\right) = -\frac{1}{5}\zeta_{\mathbf{k}},$$

$\phi_{\mathbf{k}}$ and $\zeta_{\mathbf{k}}$ being respectively the primordial Newtonian gravitational potential (at first order) and curvature perturbation in Fourier space. We dropped the superscript $(1)$ everywhere to lighten the notation.

We can then expand the exponential term in plane waves using the following identities

$$e^{i\mathbf{k}\cdot r_L\widehat{\mathbf{n}}} = \sum_{\ell'}(2\ell'+1)i^{\ell'}P_{\ell'}(\widehat{\mathbf{k}}\cdot\widehat{\mathbf{n}})j_{\ell'}(kr_L),$$

$$P_{\ell'}(\widehat{\mathbf{k}}\cdot\widehat{\mathbf{n}}) = \frac{4\pi}{2\ell'+1}\sum_{m'=-\ell'}^{\ell'} Y_{\ell'm'}(\widehat{\mathbf{n}})Y^*_{\ell'm'}(\widehat{\mathbf{k}}),$$

which are also known as the Rayleigh equation when mixed together; so we get

$$a^T_{\ell m} = \int \frac{\mathrm{d}^3\mathbf{k}}{(2\pi)^3}\underbrace{\int \mathrm{d}\widehat{\mathbf{n}}}\sum_{\ell'}(2\ell'+1)i^{\ell'}\frac{4\pi}{2\ell'+1}\sum_{m'=-\ell'}^{\ell'}\underbrace{Y_{\ell'm'}(\widehat{\mathbf{n}})}$$
$$Y^*_{\ell'm'}(\widehat{\mathbf{k}})j_{\ell'}(kr_L)\left(-\frac{1}{5}\zeta_{\mathbf{k}}\right)\underbrace{Y^*_{\ell m}(\widehat{\mathbf{n}})}.$$

The terms grouped by the curly brackets can be reduce thanks to the spherical harmonics normalization

$$\int \mathrm{d}\widehat{\mathbf{n}}Y_{\ell'm'}(\widehat{\mathbf{n}})Y^*_{\ell m}(\widehat{\mathbf{n}}) = \delta^{\ell'}_{\ell}\delta^{m'}_{m}.$$

Thus, we obtain

$$a^T_{\ell m} = 4\pi i^{\ell}\int\frac{\mathrm{d}^3\mathbf{k}}{(2\pi)^3}\zeta_{\mathbf{k}}\left(-\frac{j_\ell(kr_L)}{5}\right)Y^*_{\ell m}(\widehat{\mathbf{k}}) \underset{SW}{\simeq} 4\pi i^{\ell}\int\frac{\mathrm{d}^3\mathbf{k}}{(2\pi)^3}\zeta_{\mathbf{k}}\mathcal{T}_\ell(k)Y^*_{\ell m}(\widehat{\mathbf{k}}), \tag{4.4}$$

where $\mathcal{T}_\ell(k)$ is the *radiation transfer function* and the last equivalence holds in the Sachs - Wolfe limit, for which $\mathcal{T}_\ell(k) \longrightarrow -(1/5)j_\ell(kr_L)$. This transfer function encapsulates all the effects that CMB photons suffered in their journey from the decoupling to us and by taking the SW limit we are reducing it to just a geometrical projection on the Last Scattering Surface. Nevertheless, in most cases this is a good approximation and for a more detailed version one should take into account several effects and rely on numerical codes.

As regard the $\mu$-distortion instead, we can perform a multipoles expansion on a spherical harmonics

basis in perfect analogy with the case of the temperature anisotropy just by plugging (3.2) in (4.3):

$$
\begin{aligned}
a^{\mu}_{\ell m} &= \int \mathrm{d}\widehat{\mathbf{n}}\mu(\mathbf{x})Y^{*}_{\ell m}(\widehat{\mathbf{n}}) \\
&= \int \mathrm{d}\widehat{\mathbf{n}} 4.6 \int \frac{\mathrm{d}^3\mathbf{k}_1\mathrm{d}^3\mathbf{k}_2}{(2\pi)^6}\zeta_{\mathbf{k}_1}\zeta_{\mathbf{k}_2}\int \mathrm{d}^3\mathbf{k}_3\delta^{(3)}\left(\sum_{n=1}^{3}\mathbf{k}_n\right)\left\langle\cos(k_1 r)\cos(k_2 r)\right\rangle_p \\
&\qquad \left[e^{-(k_1^2+k_2^2)/k_D^2(z)}\right]_{z_{\mu,f}}^{z_{\mu,i}} e^{-i\mathbf{k}_3\cdot\mathbf{x}}W\left(\frac{k_3}{k_s}\right)Y^{*}_{\ell m}(\widehat{\mathbf{n}}) \\
&= \underbrace{\int \mathrm{d}\widehat{\mathbf{n}}}\, 4.6 \int \frac{\mathrm{d}^3\mathbf{k}_1\mathrm{d}^3\mathbf{k}_2}{(2\pi)^6}\zeta_{\mathbf{k}_1}\zeta_{\mathbf{k}_2}\int \mathrm{d}^3\mathbf{k}_3\delta^{(3)}\left(\sum_{n=1}^{3}\mathbf{k}_n\right)\left\langle\cos(k_1 r)\cos(k_2 r)\right\rangle_p \\
&\qquad \left[e^{-(k_1^2+k_2^2)/k_D^2(z)}\right]_{z_{\mu,f}}^{z_{\mu,i}}\sum_{\ell'}(2\ell'+1)(-i)^{\ell'}\frac{4\pi}{2\ell'+1}\sum_{m'=-\ell'}^{\ell'}\underbrace{Y_{\ell' m'}(\widehat{\mathbf{n}})}\,Y^{*}_{\ell' m'}(\widehat{\mathbf{k}}_3) \\
&\qquad j_{\ell'}(k_3 r_L)W\left(\frac{k_3}{k_s}\right)\underbrace{Y^{*}_{\ell m}(\widehat{\mathbf{n}})} \\
&= 18.4\pi(-i)^{\ell}\int \frac{\mathrm{d}^3\mathbf{k}_1\mathrm{d}^3\mathbf{k}_2}{(2\pi)^6}\zeta_{\mathbf{k}_1}\zeta_{\mathbf{k}_2}\int \mathrm{d}^3\mathbf{k}_3\delta^{(3)}\left(\sum_{n=1}^{3}\mathbf{k}_n\right)\left\langle\cos(k_1 r)\cos(k_2 r)\right\rangle_p \\
&\qquad \left[e^{-(k_1^2+k_2^2)/k_D^2(z)}\right]_{z_{\mu,f}}^{z_{\mu,i}} j_{\ell}(k_3 r_L)W\left(\frac{k_3}{k_s}\right)Y^{*}_{\ell m}(\widehat{\mathbf{k}}_3). \qquad (4.5)
\end{aligned}
$$

We are then finally ready to cross correlate (4.5) with (4.4):

$$
\begin{aligned}
\left\langle a^{\mu}_{\ell_1 m_1} a^{T}_{\ell_2 m_2}\right\rangle &= 18.4\pi(-i)^{\ell_1}4\pi i^{\ell_2}\int \frac{\mathrm{d}^3\mathbf{k}_1\mathrm{d}^3\mathbf{k}_2}{(2\pi)^6}\int \mathrm{d}^3\mathbf{k}_3\delta^{(3)}\left(\sum_{n=1}^{3}\mathbf{k}_n\right)\int\frac{\mathrm{d}^3\mathbf{k}}{(2\pi)^3} \\
&\qquad \left\langle\cos(k_1 r)\cos(k_2 r)\right\rangle_p\left[e^{-(k_1^2+k_2^2)/k_D^2(z)}\right]_{z_{\mu,f}}^{z_{\mu,i}} j_{\ell_1}(k_3 r_L)W\left(\frac{k_3}{k_s}\right) \\
&\qquad Y^{*}_{\ell_1 m_1}(\widehat{\mathbf{k}}_3)\mathcal{T}_{\ell_2}(k)Y^{*}_{\ell_2 m_2}(\widehat{\mathbf{k}})\langle\zeta_{\mathbf{k}_1}\zeta_{\mathbf{k}_2}\zeta_{\mathbf{k}}\rangle. \qquad (4.6)
\end{aligned}
$$

An interesting thing has just happened here. We started with a two-point correlation function but we actually ended up with a three-point correlation $\langle\zeta_{\mathbf{k}_1}\zeta_{\mathbf{k}_2}\zeta_{\mathbf{k}}\rangle$. As anticipated when we first introduced the $\mu$ distortions and wrote (3.2), this is because $\mu(x)\propto\zeta^2$ so that $\langle\mu\Delta T/T\rangle\propto\langle\zeta^2\zeta\rangle\propto\langle\zeta^3\rangle$, at lowest order.

Therefore, constraints on the primordial NG parameter $f_{NL}$ are obtained just by plugging the local bispectrum formula

$$
\langle\zeta_{\mathbf{k}_1}\zeta_{\mathbf{k}_2}\zeta_{\mathbf{k}}\rangle = (2\pi)^3\delta^{(3)}(\mathbf{k}_1+\mathbf{k}_2+\mathbf{k})\left(-\frac{6}{5}f_{NL}\right)[P_\zeta(k_1)P_\zeta(k_2)+2\text{ perm's}], \qquad (4.7)
$$

into (4.6):

$$\langle a^{\mu}_{\ell_1 m_1} a^{T}_{\ell_2 m_2}\rangle = -73.6\pi^2 i^{\ell_2-\ell_1}\cdot\frac{6}{5}\int\frac{d^3\mathbf{k}_1 d^3\mathbf{k}_2}{(2\pi)^6}\int d^3\mathbf{k}_3\delta^{(3)}(\mathbf{k}_1+\mathbf{k}_2+\mathbf{k}_3)$$
$$\langle\cos(k_1 r)\cos(k_2 r)\rangle_p\left[e^{-(k_1^2+k_2^2)/k_D^2(z)}\right]^{z_{\mu,i}}_{z_{\mu,f}} j_{\ell_1}(k_3 r_L) W\left(\frac{k_3}{k_s}\right)$$
$$Y^*_{\ell_1 m_1}(\widehat{\mathbf{k}}_3) Y^*_{\ell_2 m_2}(\widehat{\mathbf{k}}_3)\mathcal{T}_{\ell_2}(k_3) f_{NL}[P_\zeta(k_1)P_\zeta(k_2) + 2\text{ perm's}].$$

Now, let us first consider the scale invariant power spectrum

$$P_\zeta(k) = \frac{2\pi^2\Delta^2_\zeta(k)}{k^3} = \frac{2\pi^2\Delta^2_\zeta(k_o)}{k^3},$$

with $k_o \equiv 0.002\text{Mpc}^{-1}$ the common pivot scale we already saw at which $\Delta^2_\zeta(k_o) = 2.142\cdot 10^{-9}$. The transfer function $W(k_3/k_s)\left[e^{-(k_1^2+k_2^2)/k_D^2(z)}\right]^{z_{\mu,i}}_{z_{\mu,f}}$ filters the squeezed limit $k_1 \sim k_2 \gg k_3$, that is

- $\delta^{(3)}(\mathbf{k}_1+\mathbf{k}_2+\mathbf{k}_3) \longrightarrow \delta^{(3)}(\mathbf{k}_1+\mathbf{k}_2)$;
- $W\left(\frac{k_3}{k_s}\right) \overset{k_3\to o}{\longrightarrow} 1$;
- $\langle\cos(k_1 r)\cos(k_2 r)\rangle_p \simeq \frac{1}{2}$;
- $\left[e^{-(k_1^2+k_2^2)/k_D^2(z)}\right]^{z_{\mu,i}}_{z_{\mu,f}} \longrightarrow \left[e^{-2k_1^2/k_D^2(z)}\right]^{z_{\mu,i}}_{z_{\mu,f}}$;
- and we can neglect the first of the three terms coming from the permutations in the primordial bispectrum

$$[P_\zeta(k_1)P_\zeta(k_2) + P_\zeta(k_1)P_\zeta(k_3) + P_\zeta(k_2)P_\zeta(k_3)] =$$
$$= 4\pi^4\Delta^4_\zeta(k_o)\left(\frac{1}{k_1^3}\frac{1}{k_2^3} + \frac{1}{k_1^3}\frac{1}{k_3^3} + \frac{1}{k_2^3}\frac{1}{k_3^3}\right)$$
$$\simeq 8\pi^4\Delta^4_\zeta(k_o)\left(\frac{1}{k_1^3}\frac{1}{k_3^3}\right).$$

Taking also the SW approximation where $\mathcal{T}_{\ell_2}(k_3) \longrightarrow -(1/5)j_{\ell_2}(k_3 r_L)$, we obtain:

$$\langle a^{\mu}_{\ell_1 m_1} a^{T}_{\ell_2 m_2}\rangle = 73.6 i^{\ell_2-\ell_1}\pi^2\cdot\frac{6}{5}\cdot\frac{1}{2}\cdot\frac{8}{5}\pi^4 f_{NL}\Delta^4_\zeta(k_o)\int\frac{d^3\mathbf{k}_1 d^3\mathbf{k}_3}{(2\pi)^6} j_{\ell_1}(k_3 r_L)$$
$$j_{\ell_2}(k_3 r_L) Y^*_{\ell_1 m_1}(\widehat{\mathbf{k}}_3) Y^*_{\ell_2 m_2}(\widehat{\mathbf{k}}_3)\frac{1}{k_1^3}\frac{1}{k_3^3}\left[e^{-2k_1^2/k_D^2(z)}\right]^{z_{\mu,i}}_{z_{\mu,f}}$$
$$= 9.2\cdot\frac{3}{25} i^{\ell_2-\ell_1} f_{NL}\Delta^4_\zeta(k_o)\int 4\pi k_1^2 dk_1\int dk_3\,\underbrace{d\widehat{\mathbf{k}}_3}\, k_3^2 j_{\ell_1}(k_3 r_L)$$
$$j_{\ell_2}(k_3 r_L)\,\underbrace{Y^*_{\ell_1 m_1}(\widehat{\mathbf{k}}_3) Y^*_{\ell_2 m_2}(\widehat{\mathbf{k}}_3)}\,\frac{1}{k_1^3}\frac{1}{k_3^3}\left[e^{-2k_1^2/k_D^2(z)}\right]^{z_{\mu,i}}_{z_{\mu,f}},$$

and, thanks to the spherical harmonics normalization

$$\int \mathrm{d}\widehat{\mathbf{k}}_3 Y^*_{\ell_1 m_1}(\widehat{\mathbf{k}}_3) Y^*_{\ell_2 m_2}(\widehat{\mathbf{k}}_3) = (-1)^{m_1} \delta^{\ell_2}_{\ell_1} \delta^{-m_2}_{m_1}, \tag{4.8}$$

it all reduces to (recall definition (4.2))

$$C^{\mu T}_\ell = 9.2 \cdot \frac{12}{25} \pi f_{NL} \Delta^4_\zeta(k_0) \underbrace{\int \mathrm{d}k_3 \frac{j^2_\ell(k_3 r_L)}{k_3}}_{(A)} \underbrace{\int \mathrm{d}k_1 \frac{\left[e^{-2k_1^2/k_D^2(z)}\right]^{z_{\mu,i}}_{z_{\mu,f}}}{k_1}}_{(B)},$$

where $\ell = \ell_1 = \ell_2$. In order to ease the reading of the calculation, we separately evaluate integrals $(A)$ and $(B)$. In $(A)$, by performing a variable change $k_3 r_L \overset{s}{=} x$ we get

$$(A) = \int \mathrm{d}(k_3 r_L) \frac{j^2_\ell(k_3 r_L)}{k_3 r_L} = \int \mathrm{d}x \frac{j^2_\ell(x)}{x},$$

and this can be simplified using the general formula (see, for instance, [6])

$$\int \mathrm{d}x x^{n-2} j^2_\ell(x) = 2^{n-4} \pi \frac{\Gamma\left(\ell + \frac{n}{2} - \frac{1}{2}\right) \Gamma(3-n)}{\Gamma\left(\ell + \frac{5}{2} - \frac{n}{2}\right) \Gamma^2\left(2 - \frac{n}{2}\right)}, \tag{4.9}$$

with $\Gamma$ being the Euler Gamma Function. In our case $n = 1$, so

$$(A) = \frac{\pi}{8} \frac{\Gamma(\ell)\Gamma(2)}{\Gamma(\ell+2)\Gamma^2\left(\frac{3}{2}\right)} = \frac{\pi}{8} \frac{(\ell-1)!}{(\ell+1)\ell(\ell-1)!} \frac{4}{\pi} = \frac{1}{2\ell(\ell+1)}.$$

Integral $(B)$ gives instead

$$\begin{aligned}
(B) &= \int_0^\infty \mathrm{d}k_1 \frac{\left[e^{-(\sqrt{2}k_1)^2/k^2_{D,i}} - e^{-(\sqrt{2}k_1)^2/k_{D,f}}\right]}{k_1} = \int_0^\infty \mathrm{d}\frac{x}{\sqrt{2}} \frac{\sqrt{2}}{x} \left[e^{-x^2/k^2_{D,i}} - e^{-x^2/k^2_{D,f}}\right] \\
&= \int_{\tilde{x}}^{k_{D,i}} \mathrm{d}x \frac{1}{x} - \int_{\tilde{x}}^{k_{D,f}} \mathrm{d}x \frac{1}{x} = \ln(x)\Big|_{\tilde{x}}^{k_{D,i}} - \ln(x)\Big|_{\tilde{x}}^{k_{D,f}} = \ln\left(\frac{k_{D,i}}{\tilde{x}}\right) - \ln\left(\frac{k_{D,f}}{\tilde{x}}\right) \\
&= \ln\left(\frac{k_{D,i}}{\tilde{x}} \cdot \frac{\tilde{x}}{k_{D,f}}\right) = \ln\left(\frac{k_{D,i}}{k_{D,f}}\right),
\end{aligned}$$

where we approximated the decreasing exponential term from the Silk damping as a cut-off on the integration. Also, we used as lower bound $\tilde{x}$ primarily because $x \propto k$ and it would not have any physical meaning consider $k = 0$ in the integral, as it would correspond to an infinite wavelength mode contributing only to the monopole and impossible to be observed; secondly, it can be seen from the calculation that the integral lower bound, whatever it is, cancels off.

Finally, we come to the result

$$C_\ell^{\mu T} = 9.2 \cdot \frac{12}{25}\pi f_{NL}\Delta_\zeta^4(k_*)\frac{1}{2\ell(\ell+1)}\ln\left(\frac{k_{D,i}}{k_{D,f}}\right)$$
$$\simeq \frac{1.8\cdot 10^{-16}}{\ell(\ell+1)}f_{NL}, \tag{4.10}$$

where we used $k_{D,i} \simeq 1.1\cdot 10^4 \mathrm{Mpc}^{-1}$ and $k_{D,f} \simeq 46\mathrm{Mpc}^{-1}$; notice that the numerical coefficient is slightly different from the one in (4.1), but this is simply because we used a more up-to-date value for $\Delta_\zeta^2(k_*)$.

We managed to reproduce the first result we were interested in, highlighting every approximation and assumption taken, but we can take a step further and consider, more realistically, a power spectrum with a weak scale dependence and no running ($\mathrm{d}n_s/\mathrm{d}\ln k = 0$), i.e

$$P_\zeta(k) = \frac{2\pi^2\Delta_\zeta^2(k)}{k^3} = \frac{2\pi^2\Delta_\zeta^2(k_*)}{k^3}\left(\frac{k}{k_*}\right)^{(n_s-1)} = \frac{2\pi^2\Delta_\zeta^2(k_*)}{k_*^{(n_s-1)}}k^{(n_s-4)}.$$

Then, in the squeezed limit $k_1 \sim k_2 \gg k_3$:

$$\left[P_\zeta(k_1)P_\zeta(k_2) + P_\zeta(k_1)P_\zeta(k_3) + P_\zeta(k_2)P_\zeta(k_3)\right] =$$
$$\frac{4\pi^4\Delta_\zeta^4(k_*)}{k_*^{2(n_s-1)}}\left[k_1^{(n_s-4)}k_2^{(n_s-4)} + k_1^{(n_s-4)}k_3^{(n_s-4)} + k_2^{(n_s-4)}k_3^{(n_s-4)}\right]$$
$$\simeq \frac{8\pi^4\Delta_\zeta^4(k_*)}{k_*^{2(n_s-1)}}\left[k_1^{(n_s-4)}k_3^{(n_s-4)}\right]$$

and the $\mu$T cross-correlation is found to be

$$C_\ell^{\mu T} = 9.2\cdot\frac{12}{25}\pi f_{NL}\frac{\Delta_\zeta^4(k_*)}{k_*^{2(n_s-1)}}\underbrace{\int \mathrm{d}k_1 k_1^{(n_s-2)}\left[e^{-2k_1^2/k_D^2(z)}\right]_{z_{\mu,i}}^{z_{\mu,f}}}_{(A)}\underbrace{\int \mathrm{d}k_3 k_3^{(n_s-2)}j_\ell^2(k_3 r_L)}_{(B)}.$$

Again, we evaluate separately integrals $(A)$ and $(B)$. For $(A)$, by following the same reasoning adopted in the previous case, we find an analogous result:

$$
\begin{aligned}
(A) &= \int_0^\infty \mathrm{d}k_1 k_1^{(n_s-2)} \left[e^{-(\sqrt{2}k_1)^2/k_D^2(z)}\right]_{z_{\mu,f}}^{z_{\mu,i}} = \int_0^\infty \mathrm{d}\frac{x}{\sqrt{2}} \frac{x^{(n_s-2)}}{\sqrt{2}^{(n_s-2)}} \left[e^{-x^2/k_D^2(z)}\right]_{z_{\mu,f}}^{z_{\mu,i}} \\
&= \frac{1}{\sqrt{2}^{(n_s-1)}} \int_0^\infty \mathrm{d}x x^{(n_s-2)} \left[e^{-x^2/k_{D,i}^2} - e^{-x^2/k_{D,f}^2}\right] \\
&= \frac{1}{\sqrt{2}^{(n_s-1)}} \left[\int_{\tilde{x}}^{k_{D,i}} \mathrm{d}x x^{(n_s-2)} - \int_{\tilde{x}}^{k_{D,f}} \mathrm{d}x x^{(n_s-2)}\right] \\
&= \frac{1}{\sqrt{2}^{(n_s-1)}} \left[\frac{1}{n_s-1} x^{(n_s-1)}\Big|_{\tilde{x}}^{k_{D,i}} - \frac{1}{n_s-1} x^{(n_s-1)}\Big|_{\tilde{x}}^{k_{D,f}}\right] \\
&= \frac{1}{(n_s-1)\sqrt{2}^{(n_s-1)}} \left[k_{D,i}^{(n_s-1)} - \tilde{x}^{(n_s-1)} - k_{D,f}^{(n_s-1)} + \tilde{x}^{(n_s-1)}\right] \\
&= \frac{1}{n_s-1} \left[\left(\frac{k_D}{\sqrt{2}}\right)^{(n_s-1)}\right]_{z_{\mu,f}}^{z_{\mu,i}}.
\end{aligned}
$$

Whereas, for the $(B)$ term, the general formula (4.9) still holds and so we have

$$
\begin{aligned}
(B) &= \frac{1}{r_L^{(n_s-1)}} \int \mathrm{d}(k_3 r_L)(k_3 r_L)^{(n_s-2)} j_\ell^2(k_3 r_L) = \frac{1}{r_L^{(n_s-1)}} \int \mathrm{d}x x^{(n_s-2)} j_\ell^2(x) \\
&= \frac{1}{r_L^{(n_s-1)}} 2^{(n_s-4)} \pi \frac{\Gamma\left(\ell + \frac{n_s}{2} - \frac{1}{2}\right)\Gamma(3-n_s)}{\Gamma\left(\ell + \frac{5}{2} - \frac{n_s}{2}\right)\Gamma^2\left(2 - \frac{n_s}{2}\right)} \\
&= \frac{1}{r_L^{(n_s-1)}} \frac{\sqrt{\pi}}{4} \frac{\Gamma\left(\ell + \frac{n_s}{2} - \frac{1}{2}\right)\Gamma\left(\frac{3-n_s}{2}\right)}{\Gamma\left(\ell + \frac{5}{2} - \frac{n_s}{2}\right)\Gamma\left(2 - \frac{n_s}{2}\right)},
\end{aligned}
$$

where for the last equality we used the known Gamma function property: $\Gamma(2z) = (2\pi)^{-1/2} 2^{2z-1/2} \Gamma(z)\Gamma(z+1/2)$.

Putting it all together we eventually come to:

$$
C_\ell^{\mu T} \simeq \frac{4.42\pi f_{NL} \Delta_\zeta^4(k_0) r_L^{1-n_s}}{k_0^{2(n_s-1)}} \frac{\sqrt{\pi}}{4} \frac{\Gamma\left(\ell + \frac{n_s}{2} - \frac{1}{2}\right)\Gamma\left(\frac{3-n_s}{2}\right)}{\Gamma\left(\ell + \frac{5}{2} - \frac{n_s}{2}\right)\Gamma\left(2 - \frac{n_s}{2}\right)} \left[\frac{2}{n_s-1} 2^{-(n_s+1)/2} k_D(z)^{n_s-1}\Big|_{z_{\mu,f}}^{z_{\mu,i}}\right]. \quad (4.11)
$$

We can easily see that our result is compatible with (5.24) of [52]. In particular, our term $2/(n_s-1)$ is actually the leading term in the expansion of $\Gamma\left((n_s-1)/2\right)$ for $n_s - 1 \to 0$[1]; the difference in the numerical coefficient, i.e. 4.42 vs 4.86, is probably just a matter of approximation throughout the

[1] In fact, it is well known that a Laurent series expansion at $z = 0$ for $\Gamma(z)$ gives

$$
\Gamma(z) \overset{0}{\sim} \frac{1}{z} - \gamma + \frac{1}{12}(6\gamma^2 + \pi^2) + \mathcal{O}(z^2)
$$

where $\gamma = 0.5772\ldots$ is the Euler-Mascheroni constant. In our case, $z = (n_s-1)/2$ and the expansion at $z = 0$ is justified by the fact that, as we saw in Table 2.5.1, $n_s$ is very close to 1.

calculation and we do not think it deserves an investigation more accurate than this. Moreover, notice that we prefer to relate to the result (5.24) given by authors of [52] instead of (18) in [3] as it has a much clearer derivation, as we have just proved.

It may be interesting to note, lastly, that primordial non-Gaussianity acts as a spatial modulation of the small-scale power spectrum $\Delta^2_\zeta(k)$ by long-wavelength mode $k_D(z)$ [27]: the change in time of the damping scale $k_D(z)$ correlates different patches of the Universe where, on small scales, spectral distortions of the $\mu$-tyre are being created.

## 4.2 Future expected constraints on local NG

The entire issue of constraining the primordial NG by simply evaluating the two-point correlation function between CMB $\mu$-type spectral distortion and temperature anisotropy $\Delta T/T$ is encapsulated in the fact that both (4.10) and (4.11) give

$$C_\ell^{\mu T} \propto f_{NL},$$

in the very squeezed limit of the primordial bispectrum. This is a result that has been pointed out quite recently in several papers (such as [3], [52], [29], [26] and of course [4]) and it is now well established.

However, there is a claim that we reported at the beginning of this Chapter and that must be inspected more; in particular, authors of [3] stated that, in principle, a cosmic variance limited experiment could reach $\Delta f_{NL} \sim \mathcal{O}(10^{-3})$. By performing a Fisher forecast, they used results for $C_\ell^{\mu T}$ and $C_\ell^{\mu\mu}$ to put bounds on the local $f_{NL}$ parameter from $\mu$ distortions. The figure of merit (PIXIE) for the signal-to-noise ratio they found is

$$\frac{S}{N} \simeq 0.7 \times 10^{-3} b f_{NL} \left( \frac{\sqrt{4\pi} \times 10^{-8}}{w_\mu^{-1/2}} \right),$$

i.e. $\Delta f_{NL} \lesssim 10^3$ with current technology. A few caveats are due here:

- $\Delta\mu = 10^{-8}$ is the estimated 1-$\sigma$ error on the $\mu$-distortion monopole of an experiment like PIXIE;
- $b$ is a parameter that takes into account the $k$-dependence of the power spectrum:

  $$b \simeq 1 + \frac{n_s - 1}{2} \ln \left( \frac{k_{D,i} k_{D,f}}{4 k_\star^2} \right) \simeq 1 + 12(n_s - 1),$$

  for a weak scale dependence spectrum so that $b \simeq 1$ in the case of scale invariance;
- $w_\mu$ is the sensitivity to $\mu$ defined in the noise model for $\mu$, which is a Gaussian beam:

  $$C_\ell^{\mu\mu,N} \simeq w_\mu^{-1} e^{\ell^2/\ell^2_{\max}}.$$

  For example, for PIXIE the beam size is $\theta_{\rm FWHM} = 1^\circ.6$, i.e $\ell_{\max} \simeq 84$, and $w_\mu^{-1/2} \simeq \sqrt{4\pi} \times 10^{-8}$.

As indicated in [3], there are at least two classes of models in which the $\mu$T correlation could provide the strongest constraints on non-Gaussianity already with PIXIE's sensitivity. First, models in which the power spectrum grows at small scales, since then $b \gg 1$. In most of these models $b$ can be as large as $\mathcal{O}(10^2)$ leading to $\Delta f_{NL} \sim \mathcal{O}(10)$ for PIXIE. Second, models in which the bispectrum diverges faster than the local template in the squeezed limit, i.e. $\langle \zeta^3 \rangle \propto k_3^{-a}$ for $k_3 \to 0$ with $a > 3$.

Notice that, even though instrumental noise can be improved, there is still a lower bound imposed by nature and known as cosmic variance. One of its most important property is that it scales with the number of $k$-mode $N_k$ as $N_k^{-1/2}$. For instance, for the $TTT$ bispectrum (the three-point correlation in temperature anisotropy) it is useful to consider only short modes and it can be seen that

$$\left(\frac{S}{N}\right)_{TTT} \propto N_k^{1/2} \sim \ell_{\max} \ln^{1/2} \ell_{\max}.$$

But, unfortunately, because of Silk damping, we are limited to $\ell_{\max} \sim 2000$. In this respect, the important advantage offered by the $\mu$T cross correlation is that it possesses a much larger number of short modes and so one can find

$$\left(\frac{S}{N}\right)_{\mu T} \propto N_k^{1/2} \sim \sqrt{\frac{k_{D,f}^3}{k_s r_L^{-2}}} \sim 10^6,$$

where we remind that $k_s^{-1}$ is the radius that defines the spherical volume within which $\mu$ distortions are dissipated.

Therefore, for comic variance limited experiments, the bispectrum's sensitivity is $\Delta f_{NL} \sim \mathcal{O}(5)$, while using $\mu$T correlation one can in principle reach $\Delta f_{NL} \sim \mathcal{O}(10^{-3})$.

This is indeed all true, but we think it may be a too optimistic prediction. In §[3.2] we saw that, being a second order effect, the primordial non-Gaussianity signal suffers from many contamination and we now want to try to quantitatively evaluate a particular large-scale source of non-primordial NG which mimic an $f_{NL} \neq 0$: the Sachs-Wolfe effect at second order.

# 5

# Second order contamination

Every gravitational process enters, sooner or later, a non-linear regime. At the mildly non-linear level, to mention a few examples related to the physics of CMB anisotropies, on large angular scales Sachs-Wolfe (SW) effect at second-order in the cosmological perturbations arises, together with both second-order early and late Integrated Sachs-Wolfe (ISW) effects as well as second order metric tensor perturbations [54]. On small scales, several non-linear effects, such as gravitational lensing, Shapiro time-delay, Rees-Sciama effects and, of course, non-linear Boltzmann equation for the photon-matter fluid are involved (see, e.g., [38]).

All these effect should be necessarily taken into consideration as they too carry important information; for instance, Einstein equivalence principle can be tested with CMB spectral distortions [55]. Said effects are likely to cause a contamination to primordial non-Gaussianity in the CMB three-point correlation function and several efforts have been made in the literature of the past years toward this direction. For instance, it has been shown that second-order CMB effects yield negligible contamination to primordial NG; just to mention a few examples, see [47], [56], [57], [58], [59], [60], [61], [62], [63], [64] and [65]. The contamination was found to be of $\sim \mathcal{O}(1)$ in the $f_{NL}$ parameter and precise numerical values calculated depend on the specific shape of the three-point function: local, equilateral, orthogonal or in between.

We have seen that, more recently, primordial NG has been tested through the $\mu$T cross-correlation and it is legitimate to ask ourselves if the non-linear evolution (mild, second- or higher- order) can contaminate the primordial signal. As a matter of fact, given the increasing sensitivity of the measurements of the primordial $f_{NL}$ parameter, such question is particularly important. Easier said than done, in fact in order to find an answer one would have to employ numerical codes like CAMB and solve Boltzmann

equations at second order. However, since this represents an extremely new subject, we think it may be instructive to start from an analytic estimate, perhaps a bit naive.

In a general and schematic way, we can look at the process of mimicking a local bispectrum and consequently affecting measurements of the true primordial $f_{NL}$ parameter as follows: the bispectrum arising from an $f_{NL} \neq 0$ refers to a primordial non-Gaussian contribution that is transferred (e.g. to the CMB anisotopies linearly), but, in general, in terms of the primordial gravitational potential $\phi$, we have

$$\langle \phi^3 \rangle \sim f_{NL} \langle \phi^2 \rangle^2 + f_{NL}^{cont} \langle \phi^2 \rangle^2. \tag{5.1}$$

The second term is the one giving the contamination and contains all that contributions that are not primordial. In the explicit computations, to arrive at a structure like the one of (5.1), we will see that we will use the Wick Theorem to expand the four-point function of the contamination as a sum of terms given by multiplied two-point correlation functions.

From the study of CMB temperature anisotropies we know that $\phi \sim 10^{-5}$ ([9], [6], [12]), i.e.

$$\langle \phi^3 \rangle \sim f_{NL} \langle 10^{-10} \rangle^2 + f_{NL}^{cont} \langle 10^{-10} \rangle^2.$$

Thus, the claim of a sensitivity to $f_{NL} \sim 10^{-3}$ via the CMB temperature-$\mu$ cross-correla tion must be reviewed, because it all depends on the magnitude of the contamination coefficient $f_{NL}^{cont}$ (and the shape of the contamination) since the second contribution could dominate on the first one corresponding to the primordial bispectrum.

Let us now enter into some details of the issue. We can retrieve the general expression for large-scale CMB anisotropies up to second order from gravitational perturbations from [54]; the extension up to second order of the Sachs-Wolfe effect at large angular scales has been derived in the Poisson gauge (for adiabatic perturbations). Considering non-linearities arising from inflation and from post-inflationary epoch, we have

$$\frac{\Delta T}{T} = \frac{1}{3}\phi_*^{(1)} + \frac{1}{18}\left(\phi_*^{(1)}\right)^2 - \frac{\mathcal{K}}{10} - \frac{1}{3} f_{NL}\left(\phi_*^{(1)}\right)^2, \tag{5.2}$$

where $\phi_*^{(1)}$ indicates that the gravitational potential (at first order) at emission on the last scattering surface and

$$\mathcal{K} \equiv 10\nabla^{-4}\partial_i\partial^j(\partial^i\phi_*^{(1)}\partial_j\phi_*^{(1)}) - \nabla^{-2}\left(\frac{10}{3}\partial^i\phi_*^{(1)}\partial_i\phi_*^{(1)}\right).$$

Notice that expression (5.2) resembles the one for the local non-Gaussianity with $1/18$ in the place of $-3/5 f_{NL}$.

As already anticipated in §4.2, as a first computation we choose to focus on the second order SW effect, i.e. the second term in (5.2), inspired by the idea that the calculation for the $\mu$T correlation from this term, in principle, should be analogous to the one in the bispectrum formula derivation, with the exception that the coefficient $f_{NL}$ is substituted by $1/18$; see §III. A. in [44] as a reference. For the remainder of this Chapter, it may be then useful to keep in mind the definition

$$\frac{\Delta T^{(2)}}{T} \equiv \Theta^{(2)} = \frac{1}{18}\left(\phi_*^{(1)}\right)^2,$$

and we will be interested in the correlation

$$C_\ell^{\mu T,(2)} \sim \left\langle \mu \frac{\Delta T^{(2)}}{T} \right\rangle \sim \langle \zeta^2 \zeta^2 \rangle .$$

## 5.1 $\mu$T cross correlation from Sachs-Wolfe effect at second order

In practical terms, we want now to cross correlate (4.5) with the temperature anisotropy coefficient

$$a_{\ell m}^{T,(2)} = \int d\hat{\mathbf{n}} \Theta^{(2)}(\hat{\mathbf{n}}) Y_{\ell m}^*(\hat{\mathbf{n}}) = \int d\hat{\mathbf{n}} \int \frac{d^3\mathbf{k}_3}{(2\pi)^3} e^{i\mathbf{k}_3 \cdot r_L \hat{\mathbf{n}}} \Theta^{(2)}(\mathbf{k}_3) Y_{\ell m}^*(\hat{\mathbf{n}}). \tag{5.3}$$

Unlike the case of the first order SW effect, the CMB temperature anisotropy is proportional to the square of the gravitational potential $\phi$, and therefore its Fourier transform gives a convolution in the Fourier space, resulting in an additional integration:

$$\begin{aligned}\Theta^{(2)}(\mathbf{k}_3) &= \frac{1}{18}\mathcal{F}[\phi^2] = \frac{1}{18}\mathcal{F}[\phi] * \mathcal{F}[\phi] = \frac{1}{18}\int d^3\mathbf{k}_4 \phi_{\mathbf{k}_3-\mathbf{k}_4}\phi_{\mathbf{k}_4} \\ &= \frac{1}{18}\left(-\frac{3}{5}\right)\left(-\frac{3}{5}\right)\int d^3\mathbf{k}_4 \zeta_{\mathbf{k}_3-\mathbf{k}_4}\zeta_{\mathbf{k}_4} = \frac{9}{450}\int d^3\mathbf{k}_4 \zeta_{\mathbf{k}_3-\mathbf{k}_4}\zeta_{\mathbf{k}_4},\end{aligned} \tag{5.4}$$

where we dropped labels (1) and $*$ in $\phi_*^{(1)}$. Again, using the Rayleigh identity to expand the exponential $e^{i\mathbf{k}_3\cdot r_L\hat{\mathbf{n}}}$ and the normalization of spherical harmonics we get

$$\begin{aligned}a_{\ell m}^{T,(2)} &= \frac{9}{450}\int d\hat{\mathbf{n}} \int \frac{d^3\mathbf{k}_3}{(2\pi)^3}\sum_{\ell'}(2\ell'+1) i^{\ell'} j_{\ell'}(k_3 r_L)\frac{4\pi}{2\ell'+1}\sum_{m'=-\ell'}^{\ell'} Y_{\ell' m'}(\hat{\mathbf{n}}) Y_{\ell' m'}^*(\hat{\mathbf{k}_3}) \\ &\qquad \int d^3\mathbf{k}_4 \zeta_{\mathbf{k}_3-\mathbf{k}_4}\zeta_{\mathbf{k}_4} Y_{\ell m}^*(\hat{\mathbf{n}}) \\ &= \frac{36\pi i^\ell}{450}\int \frac{d^3\mathbf{k}_3}{(2\pi)^3}\int d^3\mathbf{k}_4 j_\ell(k_3 r_L)\zeta_{\mathbf{k}_3-\mathbf{k}_4}\zeta_{\mathbf{k}_4} Y_{\ell m}^*(\hat{\mathbf{k}_3}).\end{aligned}$$

Having an explicit expression for $a_{\ell m}^{T,(2)}$, we can then try to analytically evaluate the cross correlation, i.e. the two-point correlation function, between $\mu$ distortions and temperature anisotropy from the second order SW effect:

$$\langle a^{\mu}_{\ell_1 m_1} a^{T,(2)}_{\ell_2 m_2}\rangle = 1.47\pi^2 i^{\ell_2-\ell_1}\int\frac{d^3\mathbf{k}_1 d^3\mathbf{k}_2}{(2\pi)^6}\int\frac{d^3\mathbf{k}_3 d^3\mathbf{k}_4}{(2\pi)^3}\int d^3\mathbf{k}\,\delta^{(3)}(\mathbf{k}_1+\mathbf{k}_2+\mathbf{k})$$
$$\langle\cos(k_1 r)\cos(k_2 r)\rangle_p\left[e^{-(k_1^2+k_2^2)/k_D^2(z)}\right]_{z_{\mu,f}}^{z_{\mu,i}} j_{\ell_1}(kr_L)W\left(\frac{k}{k_s}\right)$$
$$Y^*_{\ell_1 m_1}(\widehat{\mathbf{k}})j_{\ell_2}(k_3 r_L)Y^*_{\ell_2 m_2}(\widehat{\mathbf{k}}_3)\langle\zeta_{\mathbf{k}_1}\zeta_{\mathbf{k}_2}\zeta_{\mathbf{k}_3-\mathbf{k}_4}\zeta_{\mathbf{k}_4}\rangle. \tag{5.5}$$

As already anticipated, we have now a four-point correlation function in the curvature perturbation $\zeta$ and we can avail ourselves of the Wick Theorem. Thus, we actually have a sum of paired two-point functions, each one of them giving a power spectrum $P_\zeta(k)$:

$$\begin{aligned}\langle\zeta_{\mathbf{k}_1}\zeta_{\mathbf{k}_2}\zeta_{\mathbf{k}_3-\mathbf{k}_4}\zeta_{\mathbf{k}_4}\rangle &= \langle\zeta_{\mathbf{k}_1}\zeta_{\mathbf{k}_2}\rangle\langle\zeta_{\mathbf{k}_3-\mathbf{k}_4}\zeta_{\mathbf{k}_4}\rangle + \langle\zeta_{\mathbf{k}_1}\zeta_{\mathbf{k}_3-\mathbf{k}_4}\rangle\langle\zeta_{\mathbf{k}_2}\zeta_{\mathbf{k}_4}\rangle + \langle\zeta_{\mathbf{k}_1}\zeta_{\mathbf{k}_4}\rangle\langle\zeta_{\mathbf{k}_2}\zeta_{\mathbf{k}_3-\mathbf{k}_4}\rangle\\ &= \underbrace{(2\pi)^6\delta^{(3)}(\mathbf{k}_1+\mathbf{k}_2)\delta^{(3)}(\mathbf{k}_3)P_\zeta(k_1)P_\zeta(k_4)}_{(A)}\\ &\quad+\underbrace{(2\pi)^6\delta^{(3)}(\mathbf{k}_1+\mathbf{k}_3-\mathbf{k}_4)\delta^{(3)}(\mathbf{k}_2+\mathbf{k}_4)P_\zeta(k_1)P_\zeta(k_2)}_{(B)}\\ &\quad+\underbrace{(2\pi)^6\delta^{(3)}(\mathbf{k}_1+\mathbf{k}_4)\delta^{(3)}(\mathbf{k}_2+\mathbf{k}_3-\mathbf{k}_4)P_\zeta(k_1)P_\zeta(k_2)}_{(C)}.\end{aligned} \tag{5.6}$$

The first term, (A), is proportional to $\delta^{(3)}(\mathbf{k}_3)$ so it corresponds to a perturbation mode acting on an infinite wavelength scale which contributes only to the monopole. As a matter of fact, this is a disconnected term that vanishes with a little precaution we did not take. To see this, notice that when we took the expression for the temperature anisotropy up to the second order in the SW effect, we did not consider that the observed $\Delta T/T$ must have a zero mean value:

$$\frac{\Delta T}{T} = \frac{1}{3}\phi + \frac{1}{18}\phi^2 \quad\Longrightarrow\quad \left\langle\frac{\Delta T}{T}\right\rangle = \frac{1}{18}\langle\phi^2\rangle \neq 0,$$

where the gravitational potential $\phi$ is taken at linear order so that $\langle\phi\rangle = 0$. In order to adjust for this shift, we shall redefine the temperature anisotropy as

$$\frac{\Delta T}{T} = \frac{1}{3}\phi + \frac{1}{18}\left(\phi^2 - \langle\phi^2\rangle\right).$$

In fact, by following again §III. A. in [44], we can define

$$\Theta^{(2)}(\mathbf{k}_3) \equiv \frac{1}{18}\left(\mathcal{F}[\phi]*\mathcal{F}[\phi] - (2\pi)^6\delta^{(3)}(\mathbf{k}_3)\langle\phi^2(\mathbf{x})\rangle\right).$$

Redoing the calculation and using the fact that $\langle\phi^2(\mathbf{x})\rangle = (2\pi)^{-3}\int d^3\mathbf{k}P_\zeta(k)$, it can be easily seen that the additional term proportional to $-1/18\langle\phi^2\rangle$ exactly cancels off the term (A) in (5.6).

Let us then go back to (5.6) and consider the other two terms, (B) and (C); we can see that they are

symmetric in the switching $\mathbf{k}_1 \leftrightarrow \mathbf{k}_2$ and since also the integrals in (5.5) have the same symmetry, we can substitute the four-point correlation function with just 2(B). So we have

$$\begin{aligned}\langle a^{\mu}_{\ell_1 m_1} a^{T,(2)}_{\ell_2 m_2}\rangle = 1.47\pi^2 i^{\ell_2-\ell_1}\int\frac{\mathrm{d}^3\mathbf{k}_1\mathrm{d}^3\mathbf{k}_2}{(2\pi)^6}\int\frac{\mathrm{d}^3\mathbf{k}_3\mathrm{d}^3\mathbf{k}_4}{(2\pi)^3}\int\mathrm{d}^3\mathbf{k}\delta^{(3)}(\mathbf{k}_1+\mathbf{k}_2+\mathbf{k})\\ \left[e^{-(k_1^2+k_2^2)/k_D^2(z)}\right]^{z_{\mu,i}}_{z_{\mu,f}} j_{\ell_1}(kr_L)W\left(\frac{k}{k_s}\right)Y^*_{\ell_1 m_1}(\widehat{\mathbf{k}})j_{\ell_2}(k_3 r_L)\\ Y^*_{\ell_2 m_2}(\widehat{\mathbf{k}_3})(2\pi)^6\delta^{(3)}(\mathbf{k}_1+\mathbf{k}_3-\mathbf{k}_4)\delta^{(3)}(\mathbf{k}_2+\mathbf{k}_4)P_\zeta(k_1)P_\zeta(k_2),\end{aligned} \tag{5.7}$$

where, again, we used the customary approximation $\langle\cos(k_1 r)\cos(k_2 r)\rangle_p \simeq 1/2$. Integrating in $\mathrm{d}^3\mathbf{k}_4$ and $\mathrm{d}^3\mathbf{k}$ we find the constraints $\mathbf{k}_4 = -\mathbf{k}_2$ and $\mathbf{k} = -\mathbf{k}_1 - \mathbf{k}_2 = \mathbf{k}_3$ and therefore the three Dirac deltas are reduced to just one, i.e.:

$$\begin{aligned}\langle a^{\mu}_{\ell_1 m_1} a^{T,(2)}_{\ell_2 m_2}\rangle = 1.47\pi^2 i^{\ell_2-\ell_1}\int\frac{\mathrm{d}^3\mathbf{k}_1\mathrm{d}^3\mathbf{k}_2}{(2\pi)^3}\int\mathrm{d}^3\mathbf{k}_3\delta^{(3)}(\mathbf{k}_1+\mathbf{k}_2+\mathbf{k}_3)W\left(\frac{k_3}{k_s}\right)\\ \left[e^{-(k_1^2+k_2^2)/k_D^2(z)}\right]^{z_{\mu,i}}_{z_{\mu,f}} j_{\ell_1}(k_3 r_L)Y^*_{\ell_1 m_1}(\widehat{\mathbf{k}_3})j_{\ell_2}(k_3 r_L)\\ Y^*_{\ell_2 m_2}(\widehat{\mathbf{k}_3})P_\zeta(k_1)P_\zeta(k_2).\end{aligned} \tag{5.8}$$

Now, we could take the squeezed limit $k_1 \sim k_2 \gg k_3$ as we did in the previous Chapter and write $\delta^{(3)}(\mathbf{k}_1+\mathbf{k}_2+\mathbf{k}_3) \to \delta^{(3)}(\mathbf{k}_1+\mathbf{k}_2)$, $W(k_3/k_s)\to 1$ and $\left[e^{-(k_1^2+k_2^2)/k_D^2(z)}\right]^{z_{\mu,i}}_{z_{\mu,f}} \to \left[e^{-2k_1^2/k_D^2(z)}\right]^{z_{\mu,i}}_{z_{\mu,f}}$; but since we are moving the first steps in a so far unexplored territory, we prefer to follow a more formal, and a rigorous (and probably safer) approach. We start by using the Rayleigh identity to expand the Dirac delta as

$$\delta^{(3)}(\mathbf{k}_1+\mathbf{k}_2+\mathbf{k}_3) = 8\int_0^\infty r^2\mathrm{d}r\left[\prod_{n=1}^{3}\sum_{L_n M_n} j_{L_n}(k_n r)Y^*_{L_n M_n}(\widehat{\mathbf{k}_n})\right](-1)^{\frac{L_1+L_2+L_3}{2}}\mathcal{G}^{L_1L_2L_3}_{M_1M_2M_3},$$

where $\mathcal{G}^{L_1L_2L_3}_{M_1M_2M_3}$ is the so-called *Gaunt factor* defined by

$$\mathcal{G}^{L_1L_2L_3}_{M_1M_2M_3} \equiv \sqrt{\frac{(2L_1+1)(2L_2+1)(2L_3+1)}{4\pi}}\begin{pmatrix} L_1 & L_2 & L_3\\ 0 & 0 & 0\end{pmatrix}\begin{pmatrix} L_1 & L_2 & L_3\\ M_1 & M_2 & M_3\end{pmatrix}.$$

The two matrices, known as Wigner 3j-Symbol, are quantities that arise in considering coupled angular momenta in two quantum systems as they are the result of an integration of three spherical harmonics. An important property of this coefficient is that they are not null if and only if the following selection rules are satisfied:

i) $M_i \in \{-|L_i|, \ldots, |L_i|\} \quad \forall i = 1, 2, 3;$

ii) $M_1 + M_2 + M_3 = 0;$

iii) $|L_1 - L_2| \leq L_3 \leq L_1 + L_2$ (triangular inequality).

Moreover, notice that $i) + ii) + iii) \implies L_1 + L_2 + L_3$ is an integer.

In (5.8), we can then take advantage of the fact that the angular dependence of $\mathbf{k}_1$ and $\mathbf{k}_2$ is all contained in $Y^*_{L_1M_1}(\widehat{\mathbf{k}_1})$ and $Y^*_{L_2M_2}(\widehat{\mathbf{k}_2})$; so, writing explicitly $\int \mathrm{d}^3\mathbf{k}_{1,2} = \int k^2_{1,2}\mathrm{d}k_{1,2} \int \mathrm{d}\widehat{\mathbf{k}_{1,2}}$ we find

$$\int \mathrm{d}\widehat{\mathbf{k}_1} Y^*_{L_1M_1}(\widehat{\mathbf{k}_1}) = \sqrt{4\pi}\delta^{\circ}_{L_1}\delta^{\circ}_{M_1},$$
$$\int \mathrm{d}\widehat{\mathbf{k}_2} Y^*_{L_2M_2}(\widehat{\mathbf{k}_2}) = \sqrt{4\pi}\delta^{\circ}_{L_2}\delta^{\circ}_{M_2}.$$

The Gaunt factor becomes $\mathcal{G}^{\circ\circ L_3}_{\circ\circ M_3}$ and, at this point, selection rules $ii)$ and $iii)$ imposes also $L_3 = 0 = M_3$. Therefore, for (5.8) we obtain

$$\begin{aligned}\left\langle a^{\mu}_{\ell_1 m_1} a^{T,(2)}_{\ell_2 m_2}\right\rangle = 11.76\pi^2 i^{\ell_2-\ell_1} \int \mathrm{d}\widehat{\mathbf{k}_3} Y^*_{\ell_1 m_1}(\widehat{\mathbf{k}_3}) Y^*_{\ell_2 m_2}(\widehat{\mathbf{k}_3}) \int \frac{k_1^2\mathrm{d}k_1 k_2^2 \mathrm{d}k_2 k_3^2 \mathrm{d}k_3}{(2\pi)^3} \\ \int_0^{\infty} r^2 \mathrm{d}r j_0(k_1 r) j_0(k_2 r) j_0(k_3 r) W\left(\frac{k_3}{k_s}\right) \left[e^{-(k_1^2+k_2^2)/k_D^2(z)}\right]^{z_{\mu,i}}_{z_{\mu,f}} \\ j_{\ell_1}(k_3 r_L) j_{\ell_2}(k_3 r_L) P_\zeta(k_1) P_\zeta(k_2),\end{aligned}$$

where we used that $\mathcal{G}^{000}_{000} = 1/\sqrt{4\pi}$ and $Y^*_{00}(\widehat{\mathbf{k}_3}) = 1/\sqrt{4\pi}$. If we aim for proceeding further with our analytic estimation for the $\mu$T cross correlation at second order, it has come the time to go in the squeezed limit and see what happens. In fact, assuming $k_1 \sim k_2 \gg k_3$, then $j_0(k_3 r) \longrightarrow 1$ and we can approximate

$$\int_0^{\infty} r^2 \mathrm{d}r j_0(k_1 r) j_0(k_2 r) j_0(k_3 r) \simeq \frac{\pi\delta(k_1 - k_2)}{2k_2^2}.$$

Finally, from the spherical harmonics normalization (4.8), the correlation amplitude reads:

$$C_\ell^{\mu T,(2)} \simeq 0.74 \int k_1^2 \mathrm{d}k_1 \left[e^{-2k_1^2/k_D^2(z)}\right]^{z_{\mu,i}}_{z_{\mu,f}} P_\zeta(k_1)^2 \int k_3^2 \mathrm{d}k_3 j_\ell^2(k_3 r_L) W\left(\frac{k_3}{k_s}\right),$$

with $\ell = \ell_1 = \ell_2$.

If we now plug the usual power spectrum formula with a weak scale dependence

$$P_\zeta(k) = \frac{2\pi^2 \Delta^2_\zeta(k_0)}{k_0^{(n_s-1)}} k^{(n_s-4)},$$

we are left with

$$C_\ell^{\mu T,(2)} \simeq 2.96 \frac{\pi^4 \Delta^4_\zeta(k_0)}{k_0^{2(n_s-1)}} \underbrace{\int \mathrm{d}k_1 k_1^{2(n_s-3)} \left[e^{-2k_1^2/k_D^2(z)}\right]^{z_{\mu,i}}_{z_{\mu,f}}}_{(A)} \underbrace{\int \mathrm{d}k_3 k_3^2 j_\ell^2(k_3 r_L) W\left(\frac{k_3}{k_s}\right)}_{(B)}. \tag{5.9}$$

Contribution $(A)$ can be integrated out just like we did before and gives the numerical factor

$$(A) = \frac{2^{\frac{5}{2}-n_s}}{2n_s - 5} \left[k_D(z)^{2n_s-5}\right]_{z_{\mu,f}}^{z_{\mu,i}}.$$

On the other hand, contribution $(B)$ is indeed quite problematic. First of all, even if we took $W(k_3/k_s) \to 1$ in the squeezed limit we would not be able to use the general formula $(4.9)$ as it holds only if the real part of $n$, $Re[n]$, satisfies $1 < Re[n] < 3$, wheres unfortunately in our case $n = 4$. We shall then look for other ways to solve it, but we can immediately realize that $(B)$ is actually a formally divergent integral: being proportional to the squared of a spherical Bessel function, the integrand behaves like a function that keeps oscillating and never decades. We will come back on this issue with a deeper insight in a few moment, in §5.2.

Inspecting more carefully the derivation of $(5.9)$, we can see that something odd has happened: when we calculated the $\mu$T cross correlation at first order in the SW effect plugging the primordial bispectrum formula $(4.7)$, we discarded the first of the three terms, i.e. $P_\zeta(k_1)P_\zeta(k_2)$, since in the squeezed limit it was negligible compared with the other two. Curiously, when we calculate the $\mu$T cross correlation at second order in the SW effect we get a four-point correlation which, applying the Wick Theorem $(5.6)$, gives only contributions proportional to $P_\zeta(k_1)P_\zeta(k_2)$.

This behavior has actually a very accurate explanation: the bispectrum formula descends from the $TTT$ correlation where a non-linear (second-order) term in the gravitational potential $\phi$ is taken primarily in the first place, then in the second one and finally in the third one, hence the permutations $P_\zeta(k_1)P_\zeta(k_2) + P_\zeta(k_1)P_\zeta(k_3) + P_\zeta(k_2)P_\zeta(k_3)$. On the contrary, if the non linearity comes from the second order SW effect in the correlation $\mu$T, then the non linear $\phi$ term is fixed at the second place, therefore no permutation arise and we only find terms proportional to $P_\zeta(k_1)P_\zeta(k_2)$ (remember that (A) in $(5.6)$ is a non physical term).

Before attempting to find other methods to solve this awkward apparent divergence, it may be educative to take advantage of the so-called *flat-sky approximation* and have the chance to look at this divergence from another point of view.

### Flat-sky approximation

This approximation is widely used in Cosmology and has its basis in the observation that cosmological surveys in general and CMB in particular are naturally constructed on our celestial sphere. Because of the statistical isotropy, cosmological statistical properties, such as the angular power spectra or the bispectra, find a natural definition in the harmonic space. However, in general, since most of the physical mechanisms at play arise at small scales, they should not affect the whole sky properties. For instance, at scales corresponding to less than a degree on our observed sky, CMB spectral distortions themselves are determined by small-scale interactions. Moreover, decomposition in spherical harmonics introduces a lot of geometrical complication in the calculations, but on the other hand does not carry much physical insight into these mechanisms and, ironically, almost smudges the physics at play.

In this respect, a flat-sky approximation [66] allow us to use simple Fourier transforms that drastically

simplify CMB computations and it is intuitively expected to be accurate at small scales. It consists in considering directions very close to some fiducial direction, and ignoring the curvature of the sky taking $\widehat{\mathbf{n}}$ to lie in the plane perpendicular to the fiducial direction. This is equivalent to approximating the sphere in a neighborhood of a point by the tangent plane at that point. In this limit the equivalent of spherical harmonic transformation becomes simply a Fourier transform, i.e.

$$\Theta(\widehat{\mathbf{n}}) = \sum_{\ell=0}^{\infty} \sum_{m=-\ell}^{\ell} a^T_{\ell m} Y_{\ell m}(\widehat{\mathbf{n}}) \longrightarrow \int \frac{\mathrm{d}^2\vec{\ell}}{(2\pi)^2} a^T(\vec{\ell}) e^{i\vec{\ell}\cdot\,\widehat{\mathbf{n}}}.$$

As a result, the multipoles coefficients expansion become, under this approximation, the Fourier anti-transform of the temperature anisotropy. In our case, where we consider the second order Sachs-Wolfe effect, we then have

$$a^{T,(2)}(\vec{\ell}) = \int \mathrm{d}^2\widehat{\mathbf{n}} e^{-i\vec{\ell}\cdot\,\widehat{\mathbf{n}}} \Theta^{(2)}(\widehat{\mathbf{n}}) = \int \frac{\mathrm{d}^3\mathbf{k}_3}{(2\pi)^3} \Theta^{(2)}(\mathbf{k}_3) \int \mathrm{d}^2\widehat{\mathbf{n}} e^{-i\vec{\ell}\cdot\,\widehat{\mathbf{n}}} e^{i\mathbf{k}_3\cdot r_L\widehat{\mathbf{n}}}, \tag{5.10}$$

where $\Theta^{(2)}(\mathbf{k}_3)$ defined as in (5.4).

Analogously, taking the $\mu$-distortion parameter $\mu(\mathbf{x})$ from (3.2) and performing a Fourier anti-transform as in (5.10) we find

$$\begin{aligned} a^{\mu}(\vec{\ell}) &= \int \mathrm{d}^2\widehat{\mathbf{n}'} \mu(\mathbf{x}) e^{-i\vec{\ell}\cdot\,\widehat{\mathbf{n}}'} \\ &\simeq 2.3 \int \mathrm{d}^2\widehat{\mathbf{n}'} e^{-i\vec{\ell}\cdot\,\widehat{\mathbf{n}}'} \int \frac{\mathrm{d}^3\mathbf{k}_1 \mathrm{d}^3\mathbf{k}_2}{(2\pi)^6} \zeta_{\mathbf{k}_1} \zeta_{\mathbf{k}_2} \int \mathrm{d}^3\mathbf{k} \delta^{(3)}(\mathbf{k}_1 + \mathbf{k}_2 + \mathbf{k}) \\ &\quad \left[e^{-(k_1^2+k_2^2)/k_D^2(z)}\right]_{z_{\mu,f}}^{z_{\mu,i}} W\left(\frac{k}{k_s}\right) e^{-i\mathbf{k}\cdot r_L\widehat{\mathbf{n}}'}, \end{aligned}$$

where we took $\mathbf{x} = r_L\widehat{\mathbf{n}'}$ and the standard approximation $\langle \cos(k_1 r)\cos(k_2 r)\rangle_p \simeq 1/2$.

Now, in order to obtain the the correct estimation for the cross correlation, we must substitute the definition (4.2) with

$$\langle (a^{\mu}(\vec{\ell}_1))^* a^T(\vec{\ell}_2)\rangle = (2\pi)^2 \delta^{(2)}(\vec{\ell}_1 + \vec{\ell}_2) C_\ell^{\mu T},$$

with $\ell = \ell_1 = \ell_2$. So, we can start by calculating the LHS of the equation above. Again, we can use the Wick Theorem to simplify the four-point correlation function of primordial curvature perturbation $\zeta$ and write, under the sign of integral, that

$$\int \langle \zeta_{\mathbf{k}_1}\zeta_{\mathbf{k}_2}\zeta_{\mathbf{k}_3-\mathbf{k}_4}\zeta_{\mathbf{k}_4}\rangle \longrightarrow \int 2(2\pi)^6 \delta^{(3)}(\mathbf{k}_1 + \mathbf{k}_3 - \mathbf{k}_4)\delta^{(3)}(\mathbf{k}_2 + \mathbf{k}_4) P_\zeta(k_1) P_\zeta(k_2).$$

After some easy algebra with the Dirac delta functions, just like in the case of no flat-sky approximation, we find that $\mathbf{k} = \mathbf{k}_3$. Then, the crucial step here is to decompose vector $\mathbf{k}_3$ into two pieces that depend on the wavevectors parallel and perpendicular to the tangent plane:

$$\mathbf{k}_3 = k_3^z \widehat{\mathbf{n}} + \vec{k}_3^{\,\parallel}.$$

Evaluating the integrals over $\widehat{\mathbf{n}}$ and $\widehat{\mathbf{n}}'$ we recover two 2D $\delta$ functions that require $\vec{\ell}_1$ and $\vec{\ell}_2$ to be equal to, respectively, minus and plus the projected wavevector $\vec{k}_3^{\,\parallel}$ times the distance to the last scattering of the observed photon $r_L$. In formulas

$$\int \mathrm{d}^2\widehat{\mathbf{n}}' e^{i\vec{\ell}_1\cdot\,\widehat{\mathbf{n}}'} e^{i\vec{k}_3^{\,\parallel}\cdot r_L\widehat{\mathbf{n}}'} = \int \mathrm{d}^2\widehat{\mathbf{n}}' e^{i(\vec{\ell}_1+\vec{k}_3^{\,\parallel} r_L)\cdot\widehat{\mathbf{n}}'} = (2\pi)^2\delta^{(2)}(\vec{\ell}_1 + \vec{k}_3^{\,\parallel} r_L)$$
$$\int \mathrm{d}^2\widehat{\mathbf{n}} e^{-i\vec{\ell}_2\cdot\,\widehat{\mathbf{n}}} e^{i\vec{k}_3^{\,\parallel}\cdot r_L\widehat{\mathbf{n}}} = \int \mathrm{d}^2\widehat{\mathbf{n}} e^{-i(\vec{\ell}_2-\vec{k}_3^{\,\parallel} r_L)\cdot\widehat{\mathbf{n}}} = (2\pi)^2\delta^{(2)}(\vec{\ell}_2 - \vec{k}_3^{\,\parallel} r_L).$$

Notice that, as slightly anticipated, this approximation will break down when the tangent plane needed to define a mode with wavenumber $\ell$ has large deviations from the surface of the sphere that defines the Last Scattering Surface (LSS), that is to say when considering large angular scales.

For the second order $\mu$T cross correlation we then find

$$\langle (a^\mu(\vec{\ell}_1))^* a^T(\vec{\ell}_2)\rangle = 0.18\pi \int \mathrm{d}^3\mathbf{k}_1\mathrm{d}^3\mathbf{k}_2\mathrm{d}^3\mathbf{k}_3 \left[e^{-(k_1^2+k_2^2)/k_D^2(z)}\right]_{z_{\mu,f}}^{z_{\mu,i}} W\left(\frac{k_3}{k_s}\right) e^{i2k_3^z r_L}$$
$$\delta^{(3)}(\mathbf{k}_1+\mathbf{k}_2+\mathbf{k}_3) P_\zeta(k_1) P_\zeta(k_2) \delta^{(2)}(\vec{\ell}_1 + \vec{k}_3^{\,\parallel} r_L)\delta^{(2)}(\vec{\ell}_2 - \vec{k}_3^{\,\parallel} r_L),$$

and, considering that $\delta^{(2)}(\vec{\ell}_1 + \vec{k}_3^{\,\parallel} r_L)\delta^{(2)}(\vec{\ell}_2 - \vec{k}_3^{\,\parallel} r_L) = \delta^{(2)}(\vec{\ell}_1 + \vec{\ell}_2)\delta^{(2)}(\vec{\ell}_1 + \vec{k}_3^{\,\parallel} r_L)$, we recover

$$C_\ell^{\mu T,(2)} = \frac{0.18\pi}{(2\pi)^2} \int \mathrm{d}^3\mathbf{k}_1\mathrm{d}^3\mathbf{k}_2\mathrm{d}^3\mathbf{k}_3 \left[e^{-(k_1^2+k_2^2)/k_D^2(z)}\right]_{z_{\mu,f}}^{z_{\mu,i}} W\left(\frac{k_3}{k_s}\right) e^{i2k_3^z r_L}$$
$$\delta^{(3)}(\mathbf{k}_1+\mathbf{k}_2+\mathbf{k}_3) P_\zeta(k_1) P_\zeta(k_2) \delta^{(2)}(\vec{\ell} + \vec{k}_3^{\,\parallel} r_L).$$

In order to proceed with an analytic estimation, we should factorize the integrals as it can be seen in [67]. However, in our case the inner nature of the calculation is different and the quickest analytic way to deal with this fact is probably to take the squeezed limit, i.e. $\delta^{(3)}(\mathbf{k}_1+\mathbf{k}_2+\mathbf{k}_3) \xrightarrow{k_3\to 0} \delta^{(3)}(\mathbf{k}_1+\mathbf{k}_2)$. Moreover, we are interested only in the divergent integral in (5.9) and the limit in which $k_1 \sim k_2 \gg k_3$ is not going to affect the level of divergence.

Finally, we come to

$$C_\ell^{\mu T,(2)} \simeq 1.4\times 10^{-2} \int \mathrm{d}k k^2 \left[e^{-2k^2/k_D^2(z)}\right]_{z_{\mu,f}}^{z_{\mu,i}} P_\zeta(k)^2 \int \mathrm{d}k_3^z e^{2ik_3^z r_L} W\left(\frac{\sqrt{(k_3^z)^2 + (\ell/r_L)^2}}{k_s}\right),$$

where the divergent integral is, of course, the one in the second line. We left the filter function $W$ in its place just to show explicitly that the effect of the $\delta^{(2)}$ is to force the component $\vec{k}_3^{\,\parallel}$ to be equal to $-\vec{\ell}/r_L$

in the modulus of $\mathbf{k}_3$. We already saw that in the squeezed limit the $W$ function can be substituted with 1 and so the divergence becomes evident: it is a plane wave integrated on the entire domain of $k_3^z$.

It feels like such divergence is actually a pure formality and the only possible conclusion is that we are missing something here. In particular, the physics behind the contamination on the $\mu$T cross correlation is extremely complicated since it includes, for instance, intrinsic second order effects in the temperature anisotropy (just like the one we are studying) and non-linear evolution of the gravitational potentials which CMB photons interact with. Therefore, our next step aimed at finding a better understanding of this entire matter is to focus a bit more on the radiation transfer function that we disregarded so far.

## 5.2 Second-order radiation transfer function on large-scales

The term that is now giving us a divergent integral is the very same that in the bispectrum formula can be neglected in the squeezed limit (see also the discussion about this specific point in [52]). This is precisely what prompt us to think that this is a mere formal divergence and should be independent of the physics and of CMB anisotropies. This is to say that, perhaps, if we want to consider the CMB temperature anisotropy given by the large-scale Sachs-Wolfe effect at second order, we shall use a more accurate radiation transfer function than $\mathcal{T}_\ell(k) \longrightarrow -(1/5)j_\ell(kr_L)$. Such transfer function is indeed derived in the SW approximation and it just represents a geometrical projection of the anisotropies on the Last Scattering Surface, but it is clear that being large-scale anisotropies they will get damped at some cut-off scale $k_c$. In other words, the spherical Bessel function $j_\ell(kr_L)$ should be multiplied, in a first very rough estimate, by a Theta function which is 1 up to some $k_c$ and 0 for $k > k_c$ (remind that large $k$'s mean small scales).

However, before investigating toward such direction, it may be instructive to check that our second order temperature multipoles $a_{\ell m}^{T,(2)}$ are compatible with the more general expression found by authors of [54] in (5.1). First of all, let us rewrite the anisotropy Fourier transformation as

$$\Theta^{(2)}(\mathbf{k}_3) = \frac{9}{450}\int \mathrm{d}^3\mathbf{k}_4 \zeta_{\mathbf{k}_3-\mathbf{k}_4}\zeta_{\mathbf{k}_4} = \frac{1}{18}\int \mathrm{d}^3\mathbf{k}_4\mathrm{d}^3\mathbf{k}_5\delta^{(3)}(\mathbf{k}_4+\mathbf{k}_5-\mathbf{k}_3)\phi_{\mathbf{k}_4}\phi_{\mathbf{k}_5},$$

where we used $\zeta_{\mathbf{k}} = -5/3\phi_{\mathbf{k}}$. Remind that $\phi_{\mathbf{k}}$ is the gravitational potential at linear order at the epoch of matter dominance, thus it is the very same quantity that authors of [54] call $\phi_m(\mathbf{k})$.

Therefore, we have

$$a_{\ell m}^{T,(2)} = 4\pi i^\ell \int \frac{\mathrm{d}^3\mathbf{k}}{(2\pi)^3}\int \mathrm{d}^3\mathbf{k}_1\mathrm{d}^3\mathbf{k}_2\delta^{(3)}(\mathbf{k}_1+\mathbf{k}_2-\mathbf{k})\left[\frac{1}{18}j_\ell(k_3r_L)\right]\phi_{\mathbf{k}_1}\phi_{\mathbf{k}_2}Y^*_{\ell m}(\widehat{\mathbf{k}}), \tag{5.11}$$

where we renamed modes $\mathbf{k}_3$, $\mathbf{k}_4$ and $\mathbf{k}_5$ respectively as $\mathbf{k}$, $\mathbf{k}_1$ and $\mathbf{k}_2$ since they are dummy variables once integrated out. Now, it easy to see that the quantity $a_{NL}$ introduced in [54] is $a_{NL} = 3/5f_{NL} + 1$, so

(3.24) and (3.25) of [54] becomes

$$f_0(\mathbf{k}_1, \mathbf{k}_2, \mathbf{k}) = -f_{NL} - 1 = -1,$$
$$f_1(\mathbf{k}_1, \mathbf{k}_2, \mathbf{k}) = 1,$$
$$f_2(\mathbf{k}_1, \mathbf{k}_2, \mathbf{k}) = 0.$$

Notice that the kernel $f_2$ is null as it comes from the Fourier transform of the term proportional to $\mathcal{K}$ in (5.2), but we are not considering it in our case; moreover, we took $f_{NL} = 0$ because the second order contamination is obviously calculated excluding the contribution from primordial NG. The kernels $f_n(\mathbf{k}_1, \mathbf{k}_2, \mathbf{k})$ define just as many convolutions in Fourier space $K_n(\mathbf{k})$, given by

$$K_n(\mathbf{k}) = \frac{1}{(2\pi)^3} \int d^3\mathbf{k}_1 d^3\mathbf{k}_2 \delta^{(3)}(\mathbf{k}_1 + \mathbf{k}_2 - \mathbf{k}) f_n(\mathbf{k}_1, \mathbf{k}_2, \mathbf{k}) \phi_m(\mathbf{k}_1) \phi_m(\mathbf{k}_2).$$

Having these identifications and using also (5.6) and (5.7) in [54] we immediately see that

$$\begin{aligned} &K_0(\mathbf{k})\Delta_\ell^{0(2)}(k) + K_1(\mathbf{k})\Delta_\ell^{1(2)}(k) + K_2(\mathbf{k})\Delta_\ell^{2(2)}(k) = \\ &= \frac{1}{(2\pi)^3} \int d^3\mathbf{k}_1 d^3\mathbf{k}_2 \delta^{(3)}(\mathbf{k}_1 + \mathbf{k}_2 - \mathbf{k}) \left[ -\frac{1}{3} j_\ell(k(\eta_0 - \eta_*)) + \frac{7}{18} j_\ell(k(\eta_0 - \eta_*)) \right] \phi_m(\mathbf{k}_1) \phi_m(\mathbf{k}_2) \\ &= \frac{1}{(2\pi)^3} \int d^3\mathbf{k}_1 d^3\mathbf{k}_2 \delta^{(3)}(\mathbf{k}_1 + \mathbf{k}_2 - \mathbf{k}) \left[ \frac{1}{18} j_\ell(k(\eta_0 - \eta_*)) \right] \phi_m(\mathbf{k}_1) \phi_m(\mathbf{k}_2), \end{aligned} \tag{5.12}$$

with $\eta_0 - \eta_* \equiv r_L$ the comoving distance between the Last Scattering Surface and us.

Finally, invoking also (5.9) of [54] it is evident that the results for the non-linear part of multipoles $a_{\ell m}$ are compatible; compare (5.12) with (5.11). The slight differences due to the sign in front of the imaginary unity and the extra factor $1/(2\pi)^3$ depend on the definition of Fourier transform (in particular we are referring to the sign in the exponential term) and of the convolution between modes $\mathbf{k}_1$ and $\mathbf{k}_2$.

Reinforced by the confirmation of the goodness of our result for the coefficient $a_{\ell m}^{T,(2)}$, let us then go back to the assumption that there should be some sort of damping in the transfer function filtering temperature anisotropies according to a cut-off scale $k_c$ and write

$$a_{\ell m}^{T,(2)} = 4\pi i^\ell \int \frac{d^3\mathbf{k}_3}{(2\pi)^3} \int d^3\mathbf{k}_4 d^3\mathbf{k}_5 \delta^{(3)}(\mathbf{k}_4 + \mathbf{k}_5 - \mathbf{k}_3) \zeta_{\mathbf{k}_4} \zeta_{\mathbf{k}_5} \left[ \frac{9}{450} j_\ell(k_3 r_L) \Theta(k_c - k_3) \right] Y_{\ell m}^*(\widehat{\mathbf{k}_3}). \tag{5.13}$$

Thus, the $\mu$T cross correlation between (4.5) and (5.13) follow the same steps illustrated in §5.1 with the only caveat

$$\int d^3\mathbf{k}_3 = \int d^2\widehat{\mathbf{k}_3} \int_0^{k_c} dk_3$$

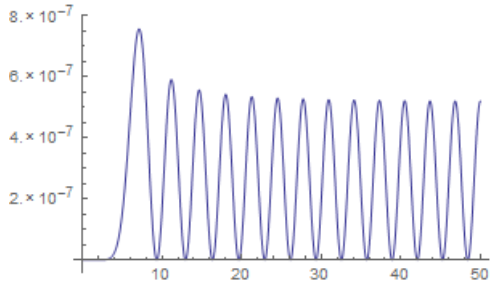


**Figure 5.2.1:** Evolution of the integrand in $(B)$, $I_\ell(x) = x j_\ell^2(x) j_1(x/(644 \cdot 10^3))$, on varying of $x$ for $\ell = 5$.

and, in the case of a weak scale dependence of the power spectrum $P_\zeta(k)$, we come to the correlation amplitude

$$C_\ell^{\mu T,(2)} \simeq 2.96 \frac{\pi^4 \Delta_\zeta^4(k_0)}{k_0^{2(n_s-1)}} \frac{2^{\frac{5}{2}-n_s}}{2n_s-5} \left[k_D(z)^{2n_s-5}\right]_{z_{\mu,f}}^{z_{\mu,i}} \underbrace{\int_0^{k_c} dk_3 k_3^2 j_\ell^2(k_3 r_L) W\left(\frac{k_3}{k_s}\right)}_{(B)}. \tag{5.14}$$

Contribution $(B)$ appears now with an upper bound in the integration interval and this treats the formal divergence that would arise if we integrated up to infinite. Of course, given the nature of the integrand, the outcome of the evaluation of $(B)$ will turn out to be extremely cut-off dependent and one should choose the scale $k_c$ very carefully. To better visualize this, let us perform the variable change $k_3 r_L \doteq x$ and set, as smearing scale for the $\mu$-distortion, $k_s \simeq k_D(z_{\mu,f}) \simeq 46 \text{Mpc}^{-1}$ in $(B)$, obtaining

$$(B) = 3 \frac{k_D(z_{\mu,f})}{r_L^2} \int_0^{x_c} dx x j_\ell^2(x) j_1\left(\frac{x}{644 \cdot 10^3}\right) = 3 \frac{k_D(z_{\mu,f})}{r_L^2} \int_0^{x_c} dx I_\ell(x), \tag{5.15}$$

where we defined $I_\ell(x) \equiv x j_\ell^2(x) j_1\left(\frac{x}{644 \cdot 10^3}\right)$ and used $W(k) \equiv 3 j_1(k)/k$ and $x_c = k_c r_L$. It is then straightforward to see why $(B)$ is so sensitive to the value we choose for the cut-off: if we try to plot $I_\ell(x)$ for, let's say, $\ell = 5$ we can see in Fig. 5.2.1 that it is an oscillating function which never decades, i.e. the bigger the cut-off $x_c$, the bigger the final result of integral $(B)$.

Now, recalling that CMB temperature anisotropies from second order Sachs-Wolfe effect arise, by definition, only on very large scale, it may be an appropriate choice to consider a cut-off $k_c$ on scales corresponding also to the ISW effect, pretty much at the order of the cosmological horizon today. Therefore, taking advantage of the relation connecting the Fourier $k$-space with the angular momentum $\ell$-space $\ell \sim k\eta_0$, if we set, for instance, $\ell = \ell_c = 10$ we have

$$\ell_c \sim k_c \eta_0 \quad \Longrightarrow \quad k_c \simeq 1.13 \times 10^{-3} \text{Mpc}^{-1},$$

where for the conformal time today we used the approximated value valid for a matter dominated Universe $\eta_0 = 2c/H_0$, with $c \simeq 3 \times 10^8$ ms$^{-1}$ the speed of light and $H_0 \simeq 67.74$ km s$^{-1}$ Mpc$^{-1}$ the Hubble constant today. We can see that $k_c$ is indeed very low, meaning that we are filtering the

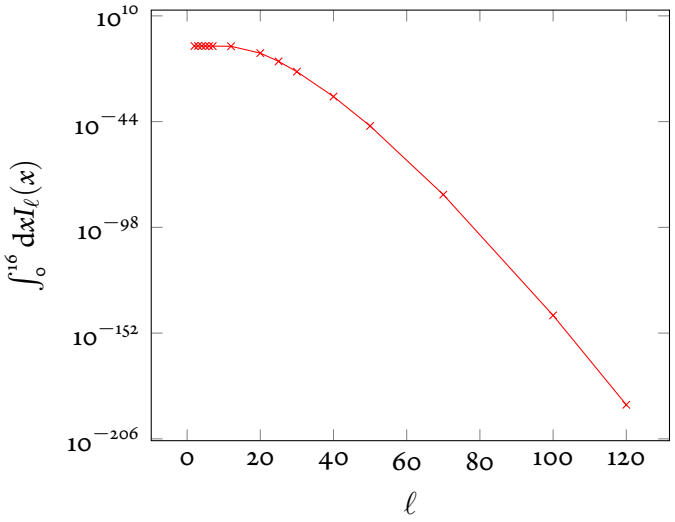


**Figure 5.2.2:** Different results at different values of $\ell$ for the formerly divergent integral arising in the $\mu$T cross correlation when temperature anisotropy is taken up to the second order in the Sachs-Wolfe effect. Lowest $\ell$'s correspond to values of order $10^{-6}$ and the trend is decreasing.

anisotropies to select only perturbation modes with very large wavelength $\lambda = 2\pi/k$.

After the variable change, the cut-off becomes $x_c = k_c r_L \simeq 16$ and we are finally able to evaluate it. Unfortunately, we can not proceed with an analytic approach further than this and we must rely on numerical methods; we employed the software *Mathematica* to find the outcomes of the formerly divergent integral appearing in $(B)$ for different values of $\ell$ and we summarized this procedure in the plot of Fig. 5.2.

We can see that, luckily, the integral has more or less the trend we were hoping for, i.e. it decreases when $\ell$ increases with lowest values of $\ell$'s, namely $\ell \lesssim 12$, corresponding to integral values of order $\sim 10^{-6}$.

Let us now be more quantitative and try to estimate the second order contamination. First of all, notice that using $(5.15)$ for $(B)$ in $(5.14)$, we correctly obtain a dimensionless value for $C_\ell^{\mu T,(2)}$; in fact the three terms carrying dimension combine themselves to give

$$\begin{aligned} [k_0^{2(n_s-1)}] &= \mathrm{Mpc}^{-2n_s+2} \\ [k_D(z)^{2n_s-5}] &= \mathrm{Mpc}^{-2n_s+5} \\ [(B)] &= \mathrm{Mpc}^{-3} \end{aligned} \qquad \Longrightarrow \left[\frac{k_D(z)^{2n_s-5}(B)}{k_0^{2(n_s-1)}}\right] = \mathrm{Mpc}^0 = 1.$$

Thus, assuming the most contaminated case, i.e. when $\ell \lesssim 12$, if we plug the numbers we find

$$(B) = 3\frac{k_D(z_{\mu,f})}{r_L^2} \times 10^{-6}\mathrm{Mpc}^{-3} \simeq 7 \times 10^{-13}\mathrm{Mpc}^{-3},$$

which implies, for a scale invariant $n_s = 1$ power spectrum, that

$$C^{\mu T,(2)}_{\ell=12} \simeq 8.9 \times 10^{-33}.$$

Recovering our expression for the $\mu$T cross-correlation induced by primordial non-Gaussianity when $n_s = 1$ (4.10), at $\ell = 12$ we have

$$C^{\mu T}_{\ell=12} \simeq 1.2 f_{NL} \times 10^{-18}.$$

It is then evident that, since currently $f_{NL} \sim \mathcal{O}(1)$, even in the case when integral $(B)$ gives its maximum value, the contamination from the second order SW effect to the primordial NG signal is indeed negligible, with a ratio

$$\frac{C^{\mu T,(2)}_{\ell=12}}{C^{\mu T}_{\ell=12}} \simeq 7.4 f^{-1}_{NL} \times 10^{-15}.$$

Therefore, if we believe in our choice for a cut-off at a scale corresponding to $k_c \simeq 1.13 \times 10^{-3}\mathrm{Mpc}^{-1}$, we are legitimated to think that the temperature anisotropies coming from the second order Sachs-Wolfe effect do not contaminate the primordial non-Gaussianity signal probed by the cross correlation between $\mu$-distortion and first order SW effect in temperature.

We shall stress that this conclusion is valid only on the very large angular scales the second-order Sachs-Wolfe effect refers to.

In order to refine the use of the second-order radiation transfer function we did not stop here but we looked for other different approaches. For instance, a natural extension of our supposition on the damping of the radiation transfer function is to imagine that every curvature perturbation $\zeta_{\mathbf{k}}$ coming from large-scale temperature anisotropies should be equipped with a window step function, i.e.

$$\zeta_{\mathbf{k}} \longrightarrow \zeta_{\mathbf{k}} \Theta(k_c - k) \tag{5.16}$$

This would ensure that no perturbation $\zeta_{\mathbf{k}}$ contributes to physical processes taking place on scale smaller than the ones at which the perturbation is generated. Notice in fact that, in order to obtain (5.2), all the wavenumbers in both the corresponding Fourier series and convolutions have been considered as large scales.

In this case, for the temperature anisotropy we would then find

$$a^{T,(2)}_{\ell m} = 4\pi i^{\ell} \int \frac{\mathrm{d}^3\mathbf{k}}{(2\pi)^3} \int \mathrm{d}^3\mathbf{k}_4 \mathrm{d}^3\mathbf{k}_5 \delta^{(3)}(\mathbf{k}_4 + \mathbf{k}_5 - \mathbf{k}) \zeta_{\mathbf{k}_4} \zeta_{\mathbf{k}_5} Y^*_{\ell m}(\widehat{\mathbf{k}}) \times \\ \times \left[ \frac{9}{450} j_{\ell}(k r_L) \Theta(k_c - k_4) \Theta(k_c - k_5) \right], \tag{5.17}$$

and recalling the equivalent multipoles expansion for the $\mu$-type spectral distortions (4.5)

$$a^{\mu}_{\ell m} = 18.4\pi(-i)^{\ell}\int \frac{\mathrm{d}^3\mathbf{k}_1\mathrm{d}^3\mathbf{k}_2}{(2\pi)^6}\zeta_{\mathbf{k}_1}\zeta_{\mathbf{k}_2}\int \mathrm{d}^3\mathbf{k}_3\delta^{(3)}\left(\sum_{n=1}^{3}\mathbf{k}_n\right)\langle\cos(k_1 r)\cos(k_2 r)\rangle_p\times$$
$$\times\left[e^{-(k_1^2+k_2^2)/k_D^2(z)}\right]_{z_{\mu,f}}^{z_{\mu,i}} j_\ell(k_3 r_L)W\left(\frac{k_3}{k_s}\right)Y^*_{\ell m}(\widehat{\mathbf{k}}_3).$$

the two point cross correlation obtained is

$$\langle a^{\mu}_{\ell_1 m_1} a^{T,(2)}_{\ell_2 m_2}\rangle \simeq \frac{0.37}{\pi} i^{\ell_2-\ell_1}\int \mathrm{d}^3\mathbf{k}_1\mathrm{d}^3\mathbf{k}_2\mathrm{d}^3\mathbf{k}_3\delta^{(3)}\left(\sum_{n=1}^{3}\mathbf{k}_n\right)j_{\ell_1}(k_3 r_L)W\left(\frac{k_3}{k_s}\right)Y^*_{\ell_1 m_1}(\widehat{\mathbf{k}}_3)\times$$
$$\times\left[e^{-(k_1^2+k_2^2)/k_D^2(z)}\right]_{z_{\mu,f}}^{z_{\mu,i}}\langle\cos(k_1 r)\cos(k_2 r)\rangle_p\int \mathrm{d}^3\mathbf{k}\mathrm{d}^3\mathbf{k}_4\mathrm{d}^3\mathbf{k}_5\delta^{(3)}(\mathbf{k}_4+\mathbf{k}_5-\mathbf{k})\times$$
$$\times Y^*_{\ell_2 m_2}(\widehat{\mathbf{k}})j_{\ell_2}(kr_L)\Theta(k_c-k_4)\Theta(k_c-k_5)\delta^{(3)}(\mathbf{k}_1+\mathbf{k}_4)\delta^{(3)}(\mathbf{k}_2+\mathbf{k}_5)P_\zeta(k_1)P_\zeta(k_2). \quad (5.18)$$

It may seem that we have been a bit sloppy in leaving (5.18) with such a long expression, full of integration and Dirac deltas. However, taking a second more careful look, one can soon realize that it would not have made much sense to proceed further. The two deltas $\delta^{(3)}(\mathbf{k}_1+\mathbf{k}_4)$ and $\delta^{(3)}(\mathbf{k}_2+\mathbf{k}_5)$, in fact, force the large wavevectors of the $\mu$ distortions $\mathbf{k}_1$ and $\mathbf{k}_2$ to be equal to the small ones of the temperature anisotropies $\mathbf{k}_4$ and $\mathbf{k}_5$, but the latter two $\mathbf{k}$'s are filtered by, respectively, the two Theta functions $\Theta(k_c-k_4)$ and $\Theta(k_c-k_5)$.

Therefore, integrations in $\mathrm{d}^3\mathbf{k}_4$ and $\mathrm{d}^3\mathbf{k}_5$ are not null only if also $k_1, k_2 < k_c$, a thing which is clearly not possible as $\mu$-type spectral distortions arise on small scales, i.e. large $k$'s, so it must necessarily be $k_1, k_2 \gg k_c$.

This stark contrast would then give a $\mu$T cross correlation $\langle a^{\mu}_{\ell_1 m_1} a^{T,(2)}_{\ell_2 m_2}\rangle = 0$ identically. It goes without saying that such result is forced by our assumption (5.16), which represents an extremely strong constraint on the behavior of the curvature perturbation $\zeta_{\mathbf{k}}$. Even though this approach is perhaps a bit too ventured and rushed, it made us realize that transfer functions play a fundamental role when one tries to estimate a cross correlation between $\mu$ spectral distortions and temperature anisotropies, two quantities arising in completely different and independent ways but that can open a new window into the physics of inflation if put together.

This is the reason why, in order to come as close as we can to a conclusive answer to the question if second order temperature anisotropies do contaminate the primordial NG signal, we want to devote our last efforts on focusing once again on the issue of transfer functions, but, this time, taking a step back. In particular, in the next and last section we are going to develop a formula which represents the basis for a full numerical computation of the second-order contamination to the $\mu$T cross-correlation. Such a numerical evaluation could then be done by employing a numerical code, developed recently, known with the acronym *SONG*. This would hopefully provide the most complete computation of the second-order contamination.

## 5.3 The Second Order Non-Gaussianity (SONG) code

As extensively described by authors of [5] and [56], SONG is a numerical code to compute the effect of the non-linear dynamics on the CMB observables. More precisely, SONG is a second-order Boltzmann code, as it solves the Einstein and Boltzmann equations up to second order in the cosmological perturbations. The reason for writing SONG was not to provide a more accurate version of the already existing first-order Boltzmann codes, such as CAMB (Code for Anisotropies in the Microwave Background) [68] or CLASS (Cosmic Linear Anisotropy Solving System) [69]. Rather, SONG is built to provide, given a cosmological model, predictions for 'new' observables or probes that do not exist at first order, such as

- the intrinsic bispectrum of the CMB;
- the angular power spectrum of the spectral distortions;
- the power spectrum of the magnetic fields generated at recombination;
- the angular power spectrum of the B-mode polarization;
- the Fourier bispectrum of the cold dark matter density fluctuations.

SONG's structure is based on that of CLASS. In particular, SONG, just like CLASS, provides an interface built on a modular and flexible internal structure with an intuitive mode of operation. For instance, there are no unknown variables buried deep into the code, but the physical and numerical parameters are controlled through two separate input files by the user, who needs to set only those parameters of interest, the others taking default values. SONG was written following the principle of encapsulation, so that to modify or add a feature to SONG, one has just to edit the code in few localised portions, well described by more than 10,000 lines of comments. Other remarkable features of SONG are that it is an open-source project written in C using only freely distributed libraries, it fully includes CMB polarization at second order, it implements a Fisher matrix module to quantify the observability of any primordial bispectrum and it is extremely fast as it takes about an hour on a modern laptop to compute the primordial bispectrum at 10% precision.

Notice, however, that so far SONG only computes the primordial bispectrum, but is going to include the other effects in the near future because all the observables above can be built starting from the second-order transfer functions. As far as our goals are concerned, it is precisely the feature that SONG is able to compute the radiation second-order transfer function that turns out to be very useful for us. In fact, in the two-point correlation function between CMB temperature anisotropies and $\mu$-type distortions we are studying, on one side we need the second order SW temperature anisotropy and on the other we are now going to see that $\mu$-type spectral distortions can be rewritten in the very same formalism, thanks to the fact that such distortions are born already at second order in the curvature perturbation $\zeta$.

In this section, we will try to follow the steps indicated in [5] as much as possible. We start by defining the *brightness fluctuation* $\Delta$, an alternative parameter for the temperature anisotropy which is related to the parameter we know, $T = T_0(1+\Theta)$, by

$$(1+\Theta)^4 = 1+\Delta,$$

which, up to second-order, it explicitly becomes

$$\Delta = 4\Theta + 6\Theta\Theta,$$
$$\Theta = \frac{1}{4}\Delta - \frac{3}{32}\Delta\Delta.$$

Spatial and directional dependence of $\Delta$ are better characterized after an expansion on spherical harmonics basis and a Fourier transform, both yielding to

$$\Delta_{\ell m}(\tau,\mathbf{k}) = i^\ell\sqrt{\frac{2\ell+1}{4\pi}}\int \mathrm{d}^3\mathbf{x}\mathrm{d}\Omega e^{-i\mathbf{k}\cdot\mathbf{x}}Y^*_{\ell m}(\widehat{\mathbf{n}})\Delta(\tau,\mathbf{x},\widehat{\mathbf{n}}).$$

To compute the anisotropies of the CMB, one need to first solve the brightness-projected Boltzmann equation up to second-order for $\Delta^{(2)}$, and then relate it to the $\Theta$ through the above equation.

The concept of transfer function is then introduce in order to separate the stochastic part of the perturbations from their deterministic evolution. In fact, quoting directly author of [5] (see also [70]): "the transfer function of a given cosmological field is an operator that maps a realization of the field in the early Universe to its state today. The stochastic process is relegated to the initial realization, which is drawn from the probability distribution of whatever physics took place in the early Universe. The transfer function, instead, is completely deterministic as it describes the subsequent physical processes, which are dictated by the Einstein and Boltzmann equations."

Therefore, we shall express the brightness perturbation in terms of its linear and second order transfer functions, $\mathcal{T}^{(1)}$ and $\mathcal{T}^{(2)}$ respectively, as

$$\begin{aligned}\Delta_{\ell m}(\tau,\mathbf{k}) = {}& \mathcal{T}^{(1)}_{\ell m}(\tau,\mathbf{k})\Phi(\tau_{\rm in},\mathbf{k}) \\ &+ \int\frac{\mathrm{d}^3\mathbf{k}'_1\mathrm{d}^3\mathbf{k}'_2}{(2\pi)^3}\delta^{(3)}(\mathbf{k}'_1+\mathbf{k}'_2-\mathbf{k})\mathcal{T}^{(2)}_{\ell m}(\tau,\mathbf{k}'_1,\mathbf{k}'_2,\mathbf{k})\Phi(\tau_{\rm in},\mathbf{k}'_1)\Phi(\tau_{\rm in},\mathbf{k}'_2), \qquad (5.19)\end{aligned}$$

where $\Phi(\tau_{\rm in},\mathbf{k})$ is the gravitational potential at the initial time $\tau_{\rm in}$, a stochastic quantity which should be chosen deep in the radiation era, where the evolution of the perturbations is known analytically. Of course, the full perturbation is given by an infinite sum of terms of higher- and higher-order in the primordial potential as well as transfer function, but we are interested only in the second-order, so we can truncate the sum at $\mathcal{T}^{(2)}$.

Notice also that the choice of $\Phi$ as the reference field is arbitrary and choosing another perturbation results in a simple rescaling of the transfer functions; in fact, so far we preferred to choose the curvature perturbation $\zeta$ instead. Moreover, contrary to $\Phi$ and $\Delta_{\ell m}$, the linear and non-linear transfer functions are not perturbed quantities and are $\sim \mathcal{O}(1)$; denoting them with a perturbative order represents then a small abuse of notation.

For the remainder of this section, we will focus only on the second line of (5.19) and we will drop the time dependence as we can choose to evaluate this quantity, for instance, at $t = t_0$, i.e. at present times. Thus, we define

$$\Delta^{(2)}_{\ell m}(\mathbf{k}) \equiv \int \frac{d^3\mathbf{q}_1' d^3\mathbf{q}_2'}{(2\pi)^3} \delta^{(3)}(\mathbf{q}_1' + \mathbf{q}_2' - \mathbf{k}) \mathcal{T}^{(2)}_{\ell m}(\mathbf{q}_1', \mathbf{q}_2', \mathbf{k}) \Phi(\mathbf{q}_1') \Phi(\mathbf{q}_2'). \tag{5.20}$$

To make a contact with the formalism we used so far, we can see that the relation assuring consistency between [5] and our work is

$$a^{T,(2)}_{\ell m} \equiv \int \frac{d^3\mathbf{k}}{(2\pi)^3} \Delta^{(2)}_{\ell m}(\mathbf{k}). \tag{5.21}$$

The above formula tells us that the temperature anisotropy coefficient $a^T_{\ell m}$ is obtained by integrating out the $\mathbf{k}$-dependence from $\Delta_{\ell m}(\mathbf{k})$.

Now, we need an expression analogous to (5.20) for the $\mu$-type spectral distortions. This is possible because $\mu$ distortions, as we know very well at this point, are already at second order in the cosmological perturbations and this allows us to employ the formalism for a second order transfer function. Notice also that since we derived an explicit expression for $a^{\mu}_{\ell m}$, it is just a matter of making the correct identifications.

Therefore, from (5.21) written in terms of $\mu$-distortion and (4.5) we have

$$\Delta^{\mu}_{\ell m}(\mathbf{k}) = \int \frac{d^3\mathbf{q}_1 d^3\mathbf{q}_2}{(2\pi)^3} \delta^{(3)}(\mathbf{q}_1 + \mathbf{q}_2 - \mathbf{k}) \mathcal{T}^{\mu}_{\ell m}(\mathbf{q}_1, \mathbf{q}_2, \mathbf{k}) \Phi(\mathbf{q}_1) \Phi(\mathbf{q}_2), \tag{5.22}$$

where we used $\zeta = -5/3\Phi$ and defined

$$\mathcal{T}^{\mu}_{\ell m}(\mathbf{q}_1, \mathbf{q}_2, \mathbf{k}) \equiv 18.4 \frac{25}{9} \pi i^{\ell} j_{\ell}(k_1 r_L) \left[ e^{-(q_1^2+q_2^2)/k_D^2(z)} \right]^{z_{\mu,i}}_{z_{\mu,f}} \langle \cos(q_1 r) \cos(q_2 r) \rangle_p \\ W\left(\frac{k_1}{k_s}\right) Y^*_{\ell m}(\widehat{\mathbf{k}}). \tag{5.23}$$

The $\mu$T cross correlation is in this case

$$\langle a^{\mu}_{\ell m} a^{T,(2)}_{\ell' m'} \rangle = \int \frac{\mathrm{d}^3\mathbf{k}_1 \mathrm{d}^3\mathbf{k}_2}{(2\pi)^6} \langle \Delta^{\mu}_{\ell m}(\mathbf{k}_1) \Delta^{(2)}_{\ell' m'}(\mathbf{k}_2) \rangle$$
$$= \int \frac{\mathrm{d}^3\mathbf{k}_1 \mathrm{d}^3\mathbf{k}_2}{(2\pi)^6} \int \frac{\mathrm{d}^3\mathbf{q}_1 \mathrm{d}^3\mathbf{q}_2}{(2\pi)^3} \delta^{(3)}(\mathbf{q}_1 + \mathbf{q}_2 - \mathbf{k}_1) \mathcal{T}^{\mu}_{\ell m}(\mathbf{q}_1, \mathbf{q}_2, \mathbf{k}_1)$$
$$\int \frac{\mathrm{d}^3\mathbf{q}_1' \mathrm{d}^3\mathbf{q}_2'}{(2\pi)^3} \delta^{(3)}(\mathbf{q}_1' + \mathbf{q}_2' - \mathbf{k}_2) \mathcal{T}^{(2)}_{\ell' m'}(\mathbf{q}_1', \mathbf{q}_2', \mathbf{k}_2) \langle \Phi(\mathbf{q}_1) \Phi(\mathbf{q}_2) \Phi(\mathbf{q}_1') \Phi(\mathbf{q}_2') \rangle.$$

The four-point function $\langle \Phi\Phi\Phi\Phi \rangle$ can again be opened in three terms invoking the Wick Theorem so that, neglecting the first term proportional to an unphysical infinite wavelength mode and considering the symmetry under integration of the other two, we are left with the contribution

$$\langle \Phi(\mathbf{q}_1) \Phi(\mathbf{q}_2) \Phi(\mathbf{q}_1') \Phi(\mathbf{q}_2') \rangle \longrightarrow 2(2\pi)^6 \delta^{(3)}(\mathbf{q}_1 + \mathbf{q}_1') \delta^{(3)}(\mathbf{q}_2 + \mathbf{q}_2') P_{\Phi}(\mathbf{q}_1) P_{\Phi}(\mathbf{q}_2),$$

which yields to

$$\langle a^{\mu}_{\ell m} a^{T,(2)}_{\ell' m'} \rangle = 2 \int \frac{\mathrm{d}^3\mathbf{k}_1}{(2\pi)^3} \int \frac{\mathrm{d}^3\mathbf{q}_1 \mathrm{d}^3\mathbf{q}_2}{(2\pi)^3} \delta^{(3)}(\mathbf{q}_1 + \mathbf{q}_2 + \mathbf{k}_1) \mathcal{T}^{\mu}_{\ell m}(\mathbf{q}_1, \mathbf{q}_2, -\mathbf{k}_1)$$
$$\mathcal{T}^{(2)}_{\ell' m'}(-\mathbf{q}_1, -\mathbf{q}_2, \mathbf{k}_1) P_{\Phi}(\mathbf{q}_1) P_{\Phi}(\mathbf{q}_2), \tag{5.24}$$

where we sent $\mathbf{k}_1 \to -\mathbf{k}_1$ and took advantage of the integrated Dirac delta functions. We shall stress that the expression above actually holds for every two-point correlation function when both quantities are taken at second order in the respective transfer functions $\mathcal{T}_{\ell m}(\mathbf{k}_1, \mathbf{k}_2, \mathbf{k}_3)$.

At the end of §5.2 we said that we would have taken a step back with regard to the second order radiation transfer function and we can better understand such statement now. In fact, $\mathcal{T}^{(2)}_{\ell' m'}(-\mathbf{q}_1, -\mathbf{q}_2, \mathbf{k}_1)$ is a completely general quantity written in no particular reference frame; thus, since SONG computes the second-order transfer functions assuming that the polar axis of the spherical coordinate system is aligned with the $\mathbf{k}_1$ direction, we first have to rotate the coordinate system so that it is parallel to $\mathbf{k}_1$ vector. Statistical isotropy of the Universe ensures, then, that the angular correlation function is invariant under such rotation.

It can be easily seen that the rotation amounts to performing the following substitution:

$$\mathcal{T}^{(2)}_{\ell' m'}(-\mathbf{q}_1, -\mathbf{q}_2, \mathbf{k}_1) \longrightarrow \sqrt{\frac{4\pi}{2\ell' + 1}} \sum_{m_1} Y^{-m_1}_{\ell' m'}(\widehat{\mathbf{k}_1}) \mathcal{T}^{(2)}_{\ell' m_1}, (-\mathbf{q}_1', -\mathbf{q}_2', k_1)$$

where $Y^{-m_1}_{\ell' m'}(\widehat{\mathbf{k}_1})$ is the spin-weighted spherical harmonic of spin $-m_1$ and $\mathbf{q}_1'$ and $\mathbf{q}_2'$ are the rotated axes in Fourier space. Notice that, after the rotation, the second order $\mathcal{T}$ depends only on the magnitude of the third wavevector, $k_1 = k_1'$, and not anymore on its direction.

We should then, in principle, follow the same procedure for the $\mu$-transfer function but there is a subtlety here: we have an explicit expression for $\mathcal{T}^{\mu}_{\ell m}$ which, most importantly, has been obtained in an already rotated coordinate system. So, recalling (5.23), all we have to do is to extract the $\mathbf{k}_1$-direction

dependency as

$$\mathcal{T}^{\mu}_{\ell m}(\mathbf{q}_1, \mathbf{q}_2, -\mathbf{k}_1) \longrightarrow \mathcal{T}^{\mu}_{\ell}(\mathbf{q}'_1, \mathbf{q}'_2, k_1) Y^*_{\ell m}(-\widehat{\mathbf{k}}_1) = (-1)^{\ell} \mathcal{T}^{\mu}_{\ell}(\mathbf{q}'_1, \mathbf{q}'_2, k_1) Y^*_{\ell m}(\widehat{\mathbf{k}}_1),$$

where we defined

$$\mathcal{T}^{\mu}_{\ell}(\mathbf{q}_1, \mathbf{q}_2, \mathbf{k}) \equiv 18.4 \frac{25}{9} \pi i^{\ell} j_{\ell}(k_1 r_L) \left[ e^{-(q_1^2+q_2^2)/k_D^2(z)} \right]^{z_{\mu,i}}_{z_{\mu,f}} \langle \cos(q_1 r) \cos(q_2 r) \rangle_p W\left(\frac{k_1}{k_s}\right). \tag{5.25}$$

Notice that all the $m$-dependence in the $\mu$-distortions transfer function is encapsulated in the spherical harmonic.

Thus, (5.24) becomes

$$\begin{aligned} \langle a^{\mu}_{\ell m} a^{T,(2)}_{\ell' m'} \rangle = 2 \sqrt{\frac{4\pi}{2\ell'+1}} (-1)^{\ell} \sum_{m_1} \int \frac{\mathrm{d}^3\mathbf{q}_1 \mathrm{d}^3\mathbf{q}_2}{(2\pi)^6} \int k_1^2 \mathrm{d}k_1 \delta^{(3)}(\mathbf{q}_1 + \mathbf{q}_2 + \mathbf{k}_1) \\ \mathcal{T}^{\mu}_{\ell}(\mathbf{q}_1, \mathbf{q}_2, k_1) \mathcal{T}^{(2)}_{\ell' m_1}(-\mathbf{q}_1, -\mathbf{q}_2, k_1) P_{\Phi}(q_1) P_{\Phi}(q_2) \\ \int \mathrm{d}\widehat{\mathbf{k}}_1 Y^{\overline{m_1}}_{\ell' m'}(\widehat{\mathbf{k}}_1) Y^*_{\ell m}(\widehat{\mathbf{k}}_1), \end{aligned} \tag{5.26}$$

where we have split the $\mathbf{k}_1$ integral in its radial and angular parts and we have dropped the prime indices for the wavemodes. Note that we have also assumed that the Dirac delta function does not depend on $\widehat{\mathbf{k}}_1$, but we will see in a moment that this is an harmless assumption.

Taking inspiration from [5], the integral on the last line of (5.26) can be immediately solved using the Gaunt relation for the spin weighted spherical harmonics, i.e.

$$\begin{aligned} \int \mathrm{d}\widehat{\mathbf{k}}_1 Y^{\overline{m_1}}_{\ell' m'}(\widehat{\mathbf{k}}_1) Y^*_{\ell m}(\widehat{\mathbf{k}}_1) &= (-1)^m \int \mathrm{d}\widehat{\mathbf{k}}_1 Y^{\overline{m_1}}_{\ell' m'}(\widehat{\mathbf{k}}_1) Y_{\ell -m}(\widehat{\mathbf{k}}_1) = \\ &= (-1)^m \sqrt{(2\ell'+1)(2\ell+1)} \begin{pmatrix} \ell' & \ell & 0 \\ -m_1 & 0 & 0 \end{pmatrix} \begin{pmatrix} \ell' & \ell & 0 \\ m' & -m & 0 \end{pmatrix} \\ &= (-1)^m (2\ell'+1) \delta^{\ell'}_{\ell} \delta^{0}_{m_1} \delta^{m'}_{m}, \end{aligned}$$

where, in writing the three Kronecker deltas, we used the properties of the Wigner 3-j symbols.

We then have

$$\begin{aligned} \langle a^{\mu}_{\ell m} a^{T,(2)}_{\ell' m'} \rangle = 2(-1)^{\ell} (-1)^m \sqrt{4\pi(2\ell'+1)} \int \frac{\mathrm{d}^3\mathbf{q}_1 \mathrm{d}^3\mathbf{q}_2}{(2\pi)^6} \int k_1^2 \mathrm{d}k_1 \delta^{(3)}(\mathbf{q}_1 + \mathbf{q}_2 + \mathbf{k}_1) \\ \mathcal{T}^{\mu}_{\ell}(\mathbf{q}_1, \mathbf{q}_2, k_1) \mathcal{T}^{(2)}_{\ell' 0}(-\mathbf{q}_1, -\mathbf{q}_2, k_1) P_{\Phi}(q_1) P_{\Phi}(q_2) \delta^{\ell'}_{\ell} \delta^{m'}_{m}. \end{aligned} \tag{5.27}$$

We can see that the particular geometrical structure of the correlation, in particular the presence of

$\delta^{\circ}_{m_1}$, force the radiation transfer function to posses only the $m = 0$ mode for a given $\ell'$.

Now, from the explicit expression (5.23) we know that the transfer function for the $\mu$ distortions does not actually depend on directions of vectors $\mathbf{q}_1$ and $\mathbf{q}_2$, so we can write

$$\mathcal{T}^{\mu}_{\ell}(\mathbf{q}_1, \mathbf{q}_2, k_1) = \mathcal{T}^{\mu}_{\ell}(q_1, q_2, k_1).$$

For the radiation transfer function, instead, we shall follow the procedure indicated in [5] which allow us to isolate the azimuthal dependence. This procedure is based on the presence of the Dirac delta function, which ensures that the integral has support only for those configurations where $\mathbf{q}_1 + \mathbf{q}_2 + \mathbf{k}_1 = 0$; however, we are not going to illustrate it step-by-step, but we will just limit to give the final substitution to perform for a generic $\mathcal{T}^{(2)}$:

$$\mathcal{T}^{(2)}_{\ell m}(\mathbf{k}_1, \mathbf{k}_2, k_3) \longrightarrow (-1)^m \sqrt{\frac{4\pi}{2m+1}} \overline{\mathcal{T}}^{(2)}_{\ell m}(k_1, k_2, k_3) Y_{|m|m}(\widehat{\mathbf{k}}_1), \tag{5.28}$$

where $\overline{\mathcal{T}}$ is the *rescaled transfer function*, defined in (6.26) of [5], and is numerically computed in SONG. This is a substantial advancement because the angular part of the transfer function is now completely separated from the radial one, without the need of performing additional multipole expansions.

Nevertheless, notice that in our case the structure of $\mathcal{T}^{(2)}$ is very simplified as $m$ is constrained to be equal to 0. Thus, (5.28) trivially becomes

$$\begin{aligned}\mathcal{T}^{(2)}_{\ell' 0}(-\mathbf{q}_1, -\mathbf{q}_2, k_1) \longrightarrow & \sqrt{4\pi}\overline{\mathcal{T}}^{(2)}_{\ell' 0}(q_1, q_2, k_1) Y_{00}(-\widehat{\mathbf{q}}_1) = \sqrt{4\pi}\overline{\mathcal{T}}^{(2)}_{\ell' 0}(q_1, q_2, k_1)\frac{1}{\sqrt{4\pi}} \\ & = \overline{\mathcal{T}}^{(2)}_{\ell' 0}(q_1, q_2, k_1),\end{aligned} \tag{5.29}$$

which consequently leads to

$$\begin{aligned}\langle a^{\mu}_{\ell m} a^{T,(2)}_{\ell' m'} \rangle = 2(-1)^{\ell+m}\sqrt{4\pi(2\ell'+1)} \int \frac{\mathrm{d}^3\mathbf{q}_1 \mathrm{d}^3\mathbf{q}_2}{(2\pi)^6} \int k_1^2 \mathrm{d}k_1 \delta^{(3)}(\mathbf{q}_1 + \mathbf{q}_2 + \mathbf{k}_1) \\ \mathcal{T}^{\mu}_{\ell}(q_1, q_2, k_1)\overline{\mathcal{T}}^{(2)}_{\ell' 0}(q_1, q_2, k_1) P_{\Phi}(q_1) P_{\Phi}(q_2) \delta^{\ell'}_{\ell}\delta^{m'}_{m}.\end{aligned}$$

At this stage, we choose to follow the usual strategy of expanding the 3D Dirac delta function in spherical harmonics and Bessel functions and then solve the angular integration analytically:

$$\delta^{(3)}(\mathbf{q}_1+\mathbf{q}_2+\mathbf{k}_1) = 8i^{L_1+L_2+L_3}\sqrt{\frac{(2L_1+1)(2L_2+1)(2L_3+1)}{4\pi}}\begin{pmatrix} L_1 & L_2 & L_3 \\ 0 & 0 & 0 \end{pmatrix}$$
$$\begin{pmatrix} L_1 & L_2 & L_3 \\ M_1 & M_2 & M_3 \end{pmatrix} Y_{L_1M_1}(\widehat{\mathbf{q}}_1)Y_{L_2M_2}(\widehat{\mathbf{q}}_2)Y_{L_3M_3}(\widehat{\mathbf{k}}_1)$$
$$\int_0^\infty x^2\,\mathrm{d}x j_{L_1}(q_1x)j_{L_2}(q_2x)j_{L_3}(k_1x),$$

where a sum over $L$ and $M$ indices is understood. The presence of $Y_{L_3M_3}(\widehat{\mathbf{k}}_1)$ may seem troubling, because we have already integrated out the angular dependence of $\mathbf{k}_1$. However, since $\mathbf{k}_1$ is aligned with the polar axis of the spherical coordinate system, we see that the dependence on $\mathbf{k}_1$ is only apparent:

$$Y_{L_3M_3}(\widehat{\mathbf{k}}_1) = Y_{L_3M_3}(\theta=0,\varphi) = \delta^0_{M_3}\sqrt{\frac{2L_3+1}{4\pi}}.$$

This is indeed the reason why we were allowed to take $\delta^{(3)}(\mathbf{q}_1+\mathbf{q}_2+\mathbf{k}_1)$ out of the $\mathrm{d}\Omega$ integral in (5.26). Moreover, we can see that the dependence on directions of vectors $\mathbf{q}_1$ and $\mathbf{q}_2$ is entirely encapsulated in the two respective spherical harmonics $Y_{L_1M_1}(\widehat{\mathbf{q}}_1)$ and $Y_{L_2M_2}(\widehat{\mathbf{q}}_2)$; so, the last two angular integrals are simply

$$\int \mathrm{d}\widehat{\mathbf{q}}_1 Y_{L_1M_1}(\widehat{\mathbf{q}}_1) = \sqrt{4\pi}\delta^0_{L_1}\delta^0_{M_1},$$
$$\int \mathrm{d}\widehat{\mathbf{q}}_2 Y_{L_2M_2}(\widehat{\mathbf{q}}_2) = \sqrt{4\pi}\delta^0_{L_2}\delta^0_{M_2}.$$

where the factor $\sqrt{4\pi}$ comes from the spherical harmonics normalization. The complexity of the calculation is then extremely reduced because the sums over indices $L$ and $M$ of five Kronecker deltas impose $L_1=L_2=M_1=M_2=M_3=0$ and, for the properties of the 3-j symbols, it must necessarily be that also $L_3=0$.

Therefore, by putting it all together, we finally come to

$$\langle a^\mu_{\ell m} a^{T,(2)}_{\ell' m'}\rangle = 2(-1)^{\ell+m}\frac{\sqrt{4\pi(2\ell+1)}}{4\pi(2\pi)^6}8\cdot 4\pi\delta^{\ell'}_{\ell}\delta^{m'}_{m}\int \mathrm{d}q_1\mathrm{d}q_2\mathrm{d}k_1\mathrm{d}x(q_1q_2k_1x)^2$$
$$\mathcal{T}^\mu_\ell(q_1,q_2,k_1)\overline{\mathcal{T}}^{(2)}_{\ell' 0}(q_1,q_2,k_1)P_\Phi(q_1)P_\Phi(q_2)j_0(q_1x)j_0(q_2x)j_0(k_1x). \tag{5.30}$$

Another conclusive step is possible here. In fact, we can plug the explicit expression for $\mathcal{T}^\mu_\ell(q_1,q_2,k_1)$ (5.25) into (5.30) to obtain

$$\langle a^{\mu}_{\ell m} a^{T,(2)}_{\ell' m'} \rangle = 25.6 \frac{(-1)^{\frac{3}{2}\ell+m}}{\pi^4\sqrt{\pi}} \sqrt{(2\ell+1)} \delta^{\ell'}_{\ell} \delta^{m'}_{m} \int \mathrm{d}q_1 \mathrm{d}q_2 \mathrm{d}k_1 \mathrm{d}x (q_1 q_2 k_1 x)^2$$
$$\left[ e^{-(q_1^2+q_2^2)/k_D^2(z)} \right]_{z_{\mu,f}}^{z_{\mu,i}} \langle \cos(q_1 r) \cos(q_2 r) \rangle_p P_\Phi(q_1) P_\Phi(q_2)$$
$$W\left(\frac{k_1}{k_s}\right) j_0(q_1 x) j_0(q_2 x) j_0(k_1 x) j_\ell(k_1 r_L) \overline{\mathcal{T}}^{(2)}_{\ell' 0}(q_1, q_2, k_1), \qquad (5.31)$$

which is the main result of this section. Its main feature is that the angular component has been separated from the radial one and this has been possible thanks to the expansion of the Dirac delta function $\delta^{(3)}(\mathbf{q}_1 + \mathbf{q}_2 + \mathbf{k}_1)$ in spherical harmonics. Such procedure has allowed us to solve the angular integrations analytically but the final result is still a 4D integral that should be tackled numerically.

Equation (5.31) will tell us everything we want to know about the contamination to the cross-correlation $\mu$T coming from the second order effects in the temperature anisotropy. Furthermore, the huge benefit from using SONG is that the radiation transfer function $\overline{\mathcal{T}}^{(2)}_{\ell' 0}(q_1, q_2, k_1)$ computed by the code will include *every* second order effect and not only the second order Sachs-Wolfe. For what we have seen in the previous section §5.2, our hope is that the output is a $\overline{\mathcal{T}}^{(2)}$ that makes the 4D integral tend towards 0 for large $\ell$, i.e. at small scales; this will ensure that the contamination in the $\mu$T cross correlation from *any* second order effect in the temperature anisotropy is, for all practical purposes, negligible.

# 6

# Conclusions

By means of this Thesis we wanted to point out some aspects related to a quite recent subject in Modern Cosmology, i.e. the cross correlation between the $\mu$-type CMB spectral distortions and the temperature anisotropy. It includes physical processes and aspects that go beyond those typically treated within the Standard Cosmological Model and have been studied only in the latest research literature. Their importance lies in the fact that they provide new tools to investigate the primordial Universe physics at small scales, so far unaccessible, and to provide new constraints on the inflationary scenario.

Thus, we decided to commit ourselves to this issue firstly to offer a rigorous derivation for a few results, uncovering every assumption and approximation implied in the literature, and secondly to try to extend what has been done so far, following an analytical approach, and posing the basis, at the the same time, for a full numerical computation.

We focused on the possibility of constraining the primordial local non-Gaussianity (NG) parameter $f_{NL}^{loc}$ through a two-point correlation between the CMB $\mu$-distortion and the temperature anisotropy at first order (in the Sachs-Wolfe regime). We presented a complete derivation for the correlation amplitude $C_\ell^{\mu T}$ both in the scale invariant and weak scale dependent power spectrum case, recovering known results such as, respectively, (16) of [3] and (5.24) of [52]. Notice that, in the latter case, no running for the spectral index $n_s$ was taken into account, so that $\mathrm{d}n_s/\mathrm{d}\ln k = 0$.

Since any kind of non-Gaussianity generally arises from non-linearity in the evolution of cosmological perturbations, we then asked ourselves if second order effects might contaminate the primordial signal; in other words, we wanted to check the bold claim by authors of [3], according to whom a cosmic variance limited experiment could in principle reach $\Delta f_{NL}^{loc} \sim \mathcal{O}(10^{-3})$. So we introduced the second order Sachs-Wolfe effect in the temperature anisotropy and computed, analytically, the correlation

amplitude $C_\ell^{\mu T,(2)}$ due to such term; interestingly, we had reason to believe that the calculation was completely analogous to the derivation of $C_\ell^{\mu T}$ from a local primordial bispectrum. But we discovered a few subtleties that made the estimate much more tricky. In particular, among the contributions to $C_\ell^{\mu T,(2)}$ we found a divergent integral that we treated introducing a cut-off scale $k_c$. Of course, this is a mere formal divergence because the SW effect appears, by definition, only on large scales and must be necessarily damped for $k > k_c$. However, we saw that the outcome of the integral was extremely cut-off dependent, so one had to be just as much confident in choosing a certain value for $k_c$. We checked, for now, that $C_\ell^{\mu T,(2)}$ would rapidly tend to $o$ by choosing a very large-scale cut-off corresponding also to the ISW effect, pretty much at the order of the cosmological horizon today.

The fact that we found a very low contamination from the second-order Sachs-Wolfe effect made sense to us as the two-point correlation takes two quantity, $\mu$-distortion and temperature anisotropy, that, for the second-order Sachs-WOlfe effect, arise at very different scales, as well as very different times in term of redshift.

Nevertheless, we chose to devote our last efforts toward a more promising direction. The presence of $k_c$ gave us the hint that we were underestimating the role played by the radiation transfer function $\mathcal{T}_\ell(k)$. In fact, we started taking $\mathcal{T}_\ell(k)$ in the SW approximation, i.e. as just a geometrical projection of the anisotropies on the Last Scattering Surface, but it is clear that in our case such expression is not accurate enough. Therefore, exploiting the formalism developed to build the SONG code [5] (whose aim is to compute numerically second-order temperature and polarization anisotropies), we took a step back and considered a very general second order radiation transfer function $\mathcal{T}^{(2)}_{\ell m}(\mathbf{k}_1, \mathbf{k}_2, \mathbf{k}_3)$, which could in principle depend also on the directions of the three wavevectors. Following the procedure indicated in [5], we derived the following expression for the second order $\mu$T cross correlation:

$$\begin{aligned}\langle a^{\mu}_{\ell m} a^{T,(2)}_{\ell' m'}\rangle = 25.6\frac{(-1)^{\frac{3}{2}\ell+m}}{\pi^4\sqrt{\pi}}\sqrt{(2\ell+1)}\delta^{\ell'}_{\ell}\delta^{m'}_{m}\int \mathrm{d}q_1\mathrm{d}q_2\mathrm{d}k_1\mathrm{d}x(q_1q_2k_1x)^2 \\ \left[e^{-(q_1^2+q_2^2)/k_D^2(z)}\right]^{z_{\mu,i}}_{z_{\mu,f}}\langle\cos(q_1r)\cos(q_2r)\rangle_p P_\Phi(q_1)P_\Phi(q_2) \\ W\left(\frac{k_1}{k_s}\right) j_o(q_1x)j_o(q_2x)j_o(k_1x)j_\ell(k_1r_L)\overline{\mathcal{T}}^{(2)}_{\ell' o}(q_1,q_2,k_1). \qquad (6.1)\end{aligned}$$

The result above is probably the most important outcome of this work and the reason why is immediate: when one employs the numerical solutions provided by the code SONG into (6.1), this will tell us the level of contamination to the primordial NG signal in the $\mu$T cross-correlation from any source of second order effect and not only the Sachs-Wolfe one.

As a last remark, we want to point out that, in principle, another analytical approach may be investigated. We focused our attention on the contamination coming from second order effects on the temperature side of the $\mu$T cross correlation, but another source of contamination can arise if we consider third order effects in the $\mu$-distortion, while keeping the CMB anisotropy at first order. In order to do so, one should recall the meaning of (3.3) and, taking inspiration from papers such as [71], [59], [60] and [47], try to employ their formalism of small-scale power spectrum modulation from a long-wavelength

perturbation mode to calculate the contamination.

# References


[1] Philippe Andre et al. PRISM (Polarized Radiation Imaging and Spectroscopy Mission): A White Paper on the Ultimate Polarimetric Spectro-Imaging of the Microwave and Far-Infrared Sky. 2013.

[2] A. Kogut, D. J. Fixsen, D. T. Chuss, J. Dotson, E. Dwek, M. Halpern, G. F. Hinshaw, S. M. Meyer, S. H. Moseley, M. D. Seiffert, D. N. Spergel, and E. J. Wollack. The Primordial Inflation Explorer (PIXIE): a nulling polarimeter for cosmic microwave background observations. *JCAP*, 7:025, July 2011. doi: 10.1088/1475-7516/2011/07/025.

[3] Enrico Pajer and Matias Zaldarriaga. A New Window on Primordial non-Gaussianity. *Phys. Rev. Lett.*, 109:021302, 2012. doi: 10.1103/PhysRevLett.109.021302.

[4] P. A. R. Ade et al. Planck 2015 results. XVII. Constraints on primordial non-Gaussianity. 2015.

[5] Guido Walter Pettinari. *The intrinsic bispectrum of the Cosmic Microwave Background*. PhD thesis, Portsmouth U., ICG, 2013-09. URL https://inspirehep.net/record/1295471/files/arXiv:1405.2280.pdf.

[6] Scott Dodelson. *Modern cosmology*. Academic Press, San Diego, CA, 2003. URL https://cds.cern.ch/record/1282338.

[7] P. A. R. Ade et al. Planck 2015 results. XIII. Cosmological parameters. 2015.

[8] Daniel Baumann. Cosmology part III: Mathematical Tripos. Lecture Notes, . http://www.damtp.cam.ac.uk/user/db275/Cosmology/Lectures.pdf.

[9] P.P. Coles and F. Lucchin. *Cosmology: The Origin and Evolution of Cosmic Structure*. Wiley, 2003. ISBN 9780470852996. URL https://books.google.fr/books?id=BGYcivB1EtMC.

[10] Wayne T. Hu. *Wandering in the Background: A CMB Explorer*. PhD thesis, UC, Berkeley, 1995.

[11] Wayne hu's tutorials. URL http://http://background.uchicago.edu/~whu/.

[12] A.R. Liddle and D.H. Lyth. *Cosmological Inflation and Large-Scale Structure*. Cambridge University Press, 2000. ISBN 9780521575980. URL https://books.google.it/books?id=XmWauPZSovMC.

[13] Alan H. Guth. Inflationary universe: A possible solution to the horizon and flatness problems. *Phys. Rev. D*, 23:347–356, Jan 1981. doi: 10.1103/PhysRevD.23.347. URL http://link.aps.org/doi/10.1103/PhysRevD.23.347.

[14] A. A. Starobinskii. Spectrum of relict gravitational radiation and the early state of the universe. *ZhETF Pisma Redaktsiiu*, 30:719–723, December 1979.

[15] A. D. Linde. A new inflationary universe scenario: A possible solution of the horizon, flatness, homogeneity, isotropy and primordial monopole problems. *Physics Letters B*, 108:389–393, February 1982. doi: 10.1016/0370-2693(82)91219-9.

[16] Andreas Albrecht and Paul J. Steinhardt. Cosmology for grand unified theories with radiatively induced symmetry breaking. *Phys. Rev. Lett.*, 48:1220–1223, Apr 1982. doi: 10.1103/PhysRevLett.48.1220. URL http://link.aps.org/doi/10.1103/PhysRevLett.48.1220.

[17] A. D. Linde. Chaotic inflation. *Physics Letters B*, 129:177–181, September 1983. doi: 10.1016/0370-2693(83)90837-7.

[18] David H. Lyth and Antonio Riotto. Particle physics models of inflation and the cosmological density perturbation. *Phys. Rept.*, 314:1–146, 1999. doi: 10.1016/S0370-1573(98)00128-8.

[19] Daniel Baumann. Inflation. In *Physics of the large and the small, TASI 09, proceedings of the Theoretical Advanced Study Institute in Elementary Particle Physics, Boulder, Colorado, USA, 1-26 June 2009*, pages 523–686, 2011. doi: 10.1142/9789814327183_0010. URL https://inspirehep.net/record/827549/files/arXiv:0907.5424.pdf.

[20] N. Bartolo, E. Komatsu, Sabino Matarrese, and A. Riotto. Non-Gaussianity from inflation: Theory and observations. *Phys. Rept.*, 402:103–266, 2004. doi: 10.1016/j.physrep.2004.08.022.

[21] Alexei A. Starobinsky. Multicomponent de Sitter (Inflationary) Stages and the Generation of Perturbations. *JETP Lett.*, 42:152–155, 1985. [Pisma Zh. Eksp. Teor. Fiz.42,124(1985)].

[22] D. S. Salopek and J. R. Bond. Nonlinear evolution of long-wavelength metric fluctuations in inflationary models. *Phys. Rev. D*, 42:3936–3962, Dec 1990. doi: 10.1103/PhysRevD.42.3936. URL http://link.aps.org/doi/10.1103/PhysRevD.42.3936.

[23] Jens Chluba. Science with CMB spectral distortions. In *Proceedings, 49th Rencontres de Moriond on Cosmology: La Thuile, Italy, March 15-22, 2014*, pages 327–334, 2014. URL https://inspirehep.net/record/1298250/files/arXiv:1405.6938.pdf.

[24] J. Chluba, R. Khatri, and R. A. Sunyaev. Cmb at 2 x 2 order: the dissipation of primordial acoustic waves and the observable part of the associated energy release. *Monthly Notices of the Royal Astronomical Society*, 425(2):1129–1169, 2012. doi: 10.1111/j.1365-2966.2012.21474.x. URL http://mnras.oxfordjournals.org/content/425/2/1129.abstract.

[25] Xingang Chen. Primordial Non-Gaussianities from Inflation Models. *Adv. Astron.*, 2010:638979, 2010. doi: 10.1155/2010/638979.

[26] Jonathan Ganc and Eiichiro Komatsu. Scale-dependent bias of galaxies and $\mu$-type distortion of the cosmic microwave background spectrum from single-field inflation with a modified initial state. *Phys. Rev.*, D86:023518, 2012. doi: 10.1103/PhysRevD.86.023518.

[27] Razieh Emami, Emanuela Dimastrogiovanni, Jens Chluba, and Marc Kamionkowski. Probing the scale dependence of non-Gaussianity with spectral distortions of the cosmic microwave background. *Phys. Rev.*, D91(12):123531, 2015. doi: 10.1103/PhysRevD.91.123531.

[28] Nicola Bartolo, Michele Liguori, and Maresuke Shiraishi. Primordial trispectra and CMB spectral distortions. *JCAP*, 1603(03):029, 2016. doi: 10.1088/1475-7516/2016/03/029.

[29] Maresuke Shiraishi, Michele Liguori, Nicola Bartolo, and Sabino Matarrese. Measuring primordial anisotropic correlators with CMB spectral distortions. *Phys. Rev.*, D92:083502, 2015. doi: 10.1103/PhysRevD.92.083502.

[30] J. Chluba and R. M. Thomas. Towards a complete treatment of the cosmological recombination problem. *Monthly Notices of the Royal Astronomical Society*, 412(2):748–764, 2011. doi: 10.1111/j.1365-2966.2010.17940.x. URL http://mnras.oxfordjournals.org/content/412/2/748.abstract.

[31] Jens Chluba and Donghui Jeong. Teasing bits of information out of the cmb energy spectrum. *Monthly Notices of the Royal Astronomical Society*, 438(3):2065–2082, 2014. doi: 10.1093/mnras/stt2327. URL http://mnras.oxfordjournals.org/content/438/3/2065.abstract.

[32] J. Chluba and R. A. Sunyaev. The evolution of cmb spectral distortions in the early universe. *Monthly Notices of the Royal Astronomical Society*, 419(2):1294–1314, 2012. doi: 10.1111/j.1365-2966.2011.19786.x. URL http://mnras.oxfordjournals.org/content/419/2/1294.abstract.

[33] Jens Chluba. Refined approximations for the distortion visibility function and μ-type spectral distortions. *Mon. Not. Roy. Astron. Soc.*, 440(3):2544–2563, 2014. doi: 10.1093/mnras/stu414.

[34] Jens Chluba. *Spectral Distortions of the Cosmic Microwave Background*. PhD thesis, Ludwig-Maximilians-Universität München, 2005.

[35] Emanuela Dimastrogiovanni, Lawrence M. Krauss, and Jens Chluba. Constraints on Gravitino Decay and the Scale of Inflation using CMB spectral distortions. *Phys. Rev.*, D94(2):023518, 2016. doi: 10.1103/PhysRevD.94.023518.

[36] Yacine Ali-Haïmoud, Jens Chluba, and Marc Kamionkowski. Constraints on Dark Matter Interactions with Standard Model Particles from Cosmic Microwave Background Spectral Distortions. *Phys. Rev. Lett.*, 115(7):071304, 2015. doi: 10.1103/PhysRevLett.115.071304.

[37] J. Chluba and R. A. Sunyaev. The evolution of CMB spectral distortions in the early Universe. *Mon. Not. Roy. Astron. Soc.*, 419:1294–1314, 2012. doi: 10.1111/j.1365-2966.2011.19786.x.

[38] Wayne Hu, Douglas Scott, and Joseph Silk. Power spectrum constraints from spectral distortions in the cosmic microwave background. *Astrophys. J.*, 430:L5–L8, 1994. doi: 10.1086/187424.

[39] R. Khatri, R. A. Sunyaev, and J. Chluba. Does Bose-Einstein condensation of CMB photons cancel $\mu$ distortions created by dissipation of sound waves in the early Universe? 540:A124, April 2012. doi: 10.1051/0004-6361/201118194.

[40] Steven Weinberg. *Gravitation and Cosmology: Principles and Applications of the General Theory of Relativity*. Oxford University Press, Oxford, UK, 2008.

[41] L. Verde, L. Wang, A. F. Heavens, and M. Kamionkowski. Large-scale structure, the cosmic microwave background and primordial non-Gaussianity. *MNRAS*, 313:141–147, March 2000. doi: 10.1046/j.1365-8711.2000.03191.x.

[42] Eiichiro Komatsu. Hunting for Primordial Non-Gaussianity in the Cosmic Microwave Background. *Class. Quant. Grav.*, 27:124010, 2010. doi: 10.1088/0264-9381/27/12/124010.

[43] Daniel Baumann. Primordial non-Gaussianity. Lecture Notes, . http://http://www.damtp.cam.ac.uk/user/db275/TEACHING/INFLATION/NG.pdf.

[44] Eiichiro Komatsu and David N. Spergel. Acoustic signatures in the primary microwave background bispectrum. *Phys. Rev.*, D63:063002, 2001. doi: 10.1103/PhysRevD.63.063002.

[45] Paolo Creminelli and Matias Zaldarriaga. Single field consistency relation for the 3-point function. *JCAP*, 0410:006, 2004. doi: 10.1088/1475-7516/2004/10/006.

[46] Juan Martin Maldacena. Non-Gaussian features of primordial fluctuations in single field inflationary models. *JHEP*, 05:013, 2003. doi: 10.1088/1126-6708/2003/05/013.

[47] Paolo Creminelli, Cyril Pitrou, and Filippo Vernizzi. The CMB bispectrum in the squeezed limit. *JCAP*, 1111:025, 2011. doi: 10.1088/1475-7516/2011/11/025.

[48] Paolo Creminelli, Alberto Nicolis, Leonardo Senatore, Max Tegmark, and Matias Zaldarriaga. Limits on non-gaussianities from wmap data. *Journal of Cosmology and Astroparticle Physics*, 2006 (05):004, 2006. URL http://stacks.iop.org/1475-7516/2006/i=05/a=004.

[49] Leonardo Senatore, Kendrick M. Smith, and Matias Zaldarriaga. Non-Gaussianities in Single Field Inflation and their Optimal Limits from the WMAP 5-year Data. *JCAP*, 1001:028, 2010. doi: 10.1088/1475-7516/2010/01/028.

[50] Hayato Shimabukuro, Shintaro Yoshiura, Keitaro Takahashi, Shuichiro Yokoyama, and Kiyotomo Ichiki. 21 cm line bispectrum as a method to probe cosmic dawn and epoch of reionization. *Mon. Not. Roy. Astron. Soc.*, 458(3):3003–3011, 2016. doi: 10.1093/mnras/stw482.

[51] Alvise Raccanelli, Maresuke Shiraishi, Nicola Bartolo, Daniele Bertacca, Michele Liguori, Sabino Matarrese, Ray P. Norris, and David Parkinson. Future Constraints on Angle-Dependent Non-Gaussianity from Large Radio Surveys. 2015.

[52] Rishi Khatri and Rashid Sunyaev. Constraints on $\mu$-distortion fluctuations and primordial non-Gaussianity from Planck data. *JCAP*, 1509(09):026, 2015. doi: 10.1088/1475-7516/2015/9/026, 10.1088/1475-7516/2015/09/026.

[53] R. K. Sachs and A. M. Wolfe. Perturbations of a Cosmological Model and Angular Variations of the Microwave Background. *APJ*, 147:73, January 1967. doi: 10.1086/148982.

[54] Nicola Bartolo, Sabino Matarrese, and Antonio Riotto. The full second-order radiation transfer function for large-scale cmb anisotropies. *JCAP*, 0605:010, 2006. doi: 10.1088/1475-7516/2006/05/010.

[55] Shun Arai, Daisuke Nitta, and Hiroyuki Tashiro. Test of the Einstein equivalence principle with CMB spectral distortions. 2016.

[56] G. W. Pettinari, C. Fidler, R. Crittenden, K. Koyama, and D. Wands. The intrinsic bispectrum of the cosmic microwave background. *J. Cosmology Astropart. Phys.*, 4:003, April 2013. doi: 10.1088/1475-7516/2013/04/003.

[57] Zhiqi Huang and Filippo Vernizzi. Cosmic microwave background bispectrum from recombination. *Phys. Rev. Lett.*, 110:101303, Mar 2013. doi: 10.1103/PhysRevLett.110.101303. URL http://link.aps.org/doi/10.1103/PhysRevLett.110.101303.

[58] Rishi Khatri and Benjamin D. Wandelt. Crinkles in the last scattering surface: Non-gaussianity from inhomogeneous recombination. *Phys. Rev. D*, 79:023501, Jan 2009. doi: 10.1103/PhysRevD.79.023501. URL http://link.aps.org/doi/10.1103/PhysRevD.79.023501.

[59] N. Bartolo, S. Matarrese, and A. Riotto. Non-Gaussianity in the Cosmic Microwave Background Anisotropies at Recombination in the Squeezed limit. *JCAP*, 1202:017, 2012. doi: 10.1088/1475-7516/2012/02/017.

[60] Paolo Creminelli and Matias Zaldarriaga. CMB 3-point functions generated by non-linearities at recombination. *Phys. Rev.*, D70:083532, 2004. doi: 10.1103/PhysRevD.70.083532.

[61] L. Boubekeur, P. Creminelli, G. D'Amico, J. Noreña, and F. Vernizzi. Sachs-Wolfe at second order: the CMB bispectrum on large angular scales. *JCAP*, 8:029, aug 2009. doi: 10.1088/1475-7516/2009/08/029.

[62] Leonardo Senatore, Svetlin Tassev, and Matias Zaldarriaga. Non-gaussianities from perturbing recombination. *Journal of Cosmology and Astroparticle Physics*, 2009(09):038, 2009. URL http://stacks.iop.org/1475-7516/2009/i=09/a=038.

[63] Nicola Bartolo and Antonio Riotto. On the non-gaussianity from recombination. *Journal of Cosmology and Astroparticle Physics*, 2009(03):017, 2009. URL http://stacks.iop.org/1475-7516/2009/i=03/a=017.

[64] S. C. Su, Eugene A. Lim, and E. P. S. Shellard. CMB Bispectrum from Non-linear Effects during Recombination. 2012.

[65] D. Nitta, E. Komatsu, N. Bartolo, S. Matarrese, and A. Riotto. CMB anisotropies at second order III: bispectrum from products of the first-order perturbations. *JCAP*, 5:014, May 2009. doi: 10.1088/1475-7516/2009/05/014.

[66] Wayne Hu. Weak lensing of the CMB: A harmonic approach. *Phys. Rev.*, D62:043007, 2000. doi: 10.1103/PhysRevD.62.043007.

[67] Daniel Babich, Paolo Creminelli, and Matias Zaldarriaga. The Shape of non-Gaussianities. *JCAP*, 0408:009, 2004. doi: 10.1088/1475-7516/2004/08/009.

[68] A. Lewis, A. Challinor, and A. Lasenby. Efficient Computation of Cosmic Microwave Background Anisotropies in Closed Friedmann-Robertson-Walker Models. *APJ*, 538:473–476, August 2000. doi: 10.1086/309179.

[69] J. Lesgourgues. The Cosmic Linear Anisotropy Solving System (CLASS) I: Overview. *ArXiv e-prints*, April 2011.

[70] C.-P. Ma and E. Bertschinger. Cosmological Perturbation Theory in the Synchronous and Conformal Newtonian Gauges. *APJ*, 455:7, December 1995. doi: 10.1086/176550.

[71] Clifford Cheung, A. Liam Fitzpatrick, Jared Kaplan, and Leonardo Senatore. On the consistency relation of the 3-point function in single field inflation. *JCAP*, 0802:021, 2008. doi: 10.1088/1475-7516/2008/02/021.

[72] Wayne Hu and Scott Dodelson. Cosmic microwave background anisotropies. *Ann. Rev. Astron. Astrophys.*, 40:171–216, 2002. doi: 10.1146/annurev.astro.40.060401.093926.